Structure/Function analysis of the interactions of the *Staphylococcus aureus* Extracellular Adherence Protein and the human innate immune system

by

Jordan Lee Woehl

B.S., University of Missouri, 2011
M.S., University of Missouri-Kansas City, 2013

AN ABSTRACT OF A DISSERTATION

submitted in partial fulfillment of the requirements for the degree

DOCTOR OF PHILOSOPHY

Department of Biochemistry and Molecular Biophysics
College of Arts and Sciences

KANSAS STATE UNIVERSITY
Manhattan, Kansas

2017

Abstract

The pathogenic bacterium *Staphylococcus aureus* actively evades many aspects of human innate immunity by expressing a series of secreted inhibitory proteins. A number of these proteins have been shown to specifically bind to and inhibit components of the complement system. Since complement is known to play a significant role in the pathophysiology of human inflammatory diseases, our long-term goal is to understand the structure, function, and mechanism of Staphylococcal immune evasion proteins to develop complement-targeted therapeutics. Since its discovery, the extracellular adherence protein (Eap) has been shown to be a crucial component in the pathogenesis and survival of *S. aureus* through its ability to interact and inhibit multiple aspects of the innate immune system. We have shown that Eap inhibits the classical and lectin pathways of complement by a previously undescribed mechanism. Specifically, Eap binds with nanomolar affinity to complement protein C4b, and thereby blocks binding of the classical and lectin pathway pro-protease C2 to C4b. This effectively eliminates formation of the CP/LP C3 proconvertase, which is required for amplification of downstream complement activity and subsequent inflammatory events. The full-length, mature Eap protein from *S. aureus* strain Mu50 consists of four ~97 residue domains, each of which adopt a similar beta-grasp fold, and are connected to one another through short linker regions that give rise to an elongated, but structured protein. Through multiple structural and functional assays, we have identified the 3rd and 4th domains of Eap as being critical for interacting with C4b and subsequent inhibition of the complement cascade. Alternative approaches to a standard co-crystal structure of Eap34 bound to C4b provided evidence that Eap domains 3 and 4 both contain a low affinity, but saturable binding site for C4b; we were able to map these sites to the α-chain and γ-chain, specifically the metal-ion-dependent adhesion site of the C345c domain, of C4b, both of which

have been previously shown to be required for pro-protease binding. To provide higher resolution information, we took advantage of the abundance of surface exposed lysines in Eap34, and employed a lysine-acetylation foot printing mass spectrometry technique. This identified seven lysines in Eap34 that undergo changes in solvent exposure upon C4b binding and confirmation of these residues was done through site-directed mutagenesis, followed by direct binding and functional assays. Together, these results provide structural and functional insight into one of the many ways that *Staphylococcus aureus* can evade the killing powers of the innate immune system. Future plans are directed at conducting site-specific screens to identify small molecule/peptide compounds that target the Eap34 binding site on C4b. Such molecules would constitute attractive lead compounds in the search for specific inhibitors of the classical and lectin complement pathways.

Structure/Function analysis of the interactions of the *Staphylococcus aureus* Extracellular Adherence Protein and the human innate immune system

by

Jordan Lee Woehl

B.S., University of Missouri, 2011
M.S., University of Missouri-Kansas City, 2013

A DISSERTATION

submitted in partial fulfillment of the requirements for the degree

DOCTOR OF PHILOSOPHY

Department of Biochemistry and Molecular Biophysics
College of Arts and Sciences

KANSAS STATE UNIVERSITY
Manhattan, Kansas

2017

Approved by:

Major Professor
Dr. Brian V. Geisbrecht

Copyright

Abstract

The pathogenic bacterium *Staphylococcus aureus* actively evades many aspects of human innate immunity by expressing a series of secreted inhibitory proteins. A number of these proteins have been shown to specifically bind to and inhibit components of the complement system. Since complement is known to play a significant role in the pathophysiology of human inflammatory diseases, our long-term goal is to understand the structure, function, and mechanism of Staphylococcal immune evasion proteins to develop complement-targeted therapeutics. Since its discovery, the extracellular adherence protein (Eap) has been shown to be a crucial component in the pathogenesis and survival of *S. aureus* through its ability to interact and inhibit multiple aspects of the innate immune system. We have shown that Eap inhibits the classical and lectin pathways of complement by a previously undescribed mechanism. Specifically, Eap binds with nanomolar affinity to complement protein C4b, and thereby blocks binding of the classical and lectin pathway pro-protease C2 to C4b. This effectively eliminates formation of the CP/LP C3 proconvertase, which is required for amplification of downstream complement activity and subsequent inflammatory events. The full-length, mature Eap protein from *S. aureus* strain Mu50 consists of four ~97 residue domains, each of which adopt a similar beta-grasp fold, and are connected to one another through short linker regions that give rise to an elongated, but structured protein. Through multiple structural and functional assays, we have identified the 3rd and 4th domains of Eap as being critical for interacting with C4b and subsequent inhibition of the complement cascade. Alternative approaches to a standard co-crystal structure of Eap34 bound to C4b provided evidence that Eap domains 3 and 4 both contain a low affinity, but saturable binding site for C4b; we were able to map these sites to the α-chain and γ-chain, specifically the metal-ion-dependent adhesion site of the C345c domain, of C4b, both of which

have been previously shown to be required for pro-protease binding. To provide higher resolution information, we took advantage of the abundance of surface exposed lysines in Eap34, and employed a lysine-acetylation foot printing mass spectrometry technique. This identified seven lysines in Eap34 that undergo changes in solvent exposure upon C4b binding and confirmation of these residues was done through site-directed mutagenesis, followed by direct binding and functional assays. Together, these results provide structural and functional insight into one of the many ways that *Staphylococcus aureus* can evade the killing powers of the innate immune system. Future plans are directed at conducting site-specific screens to identify small molecule/peptide compounds that target the Eap34 binding site on C4b. Such molecules would constitute attractive lead compounds in the search for specific inhibitors of the classical and lectin complement pathways.

Table of Contents

List of Figures

List of Tables

Acknowledgements

I would like to thank a number of individuals for their help in the completion of my PhD and growth as a scientist and an individual. First I would like to thank the entire Geisbrecht lab, Dr. Kasra Ramyar, Dr. Brandon Garcia, and Joe McWhorter. Working with all of you has taught me so much the last five years and without your hard work and help throughout my dissertation, this work could not have been accomplished. I would also like to thank Dr. Om Prakash, Dr. Daisuke Takahashi, and Dr. Alvaro Herrera for their help and guidance in completing structural studies using NMR. I would like to acknowledge my advisor, Brian Geisbrecht, for giving me a chance to obtain a PhD in his lab and for his encouragement, guidance, and support in my development as an independent scientist. A special thanks to Nicole Green, Emery Brown, Benjamin Katz, and Chester Mcdowell for taking the time away from their lives to drink a beer (or many beers), reminisce about life, and avoid the everyday struggles and failures of being a scientist. A special thanks also goes to Stephanie Thau for always believing in me, encouraging me, and putting up with me through the stress of obtaining a Phd. Finally, and most importantly, I would like to thank my parents and my older brother for their support, encouragement, and always being there for me throughout my graduate studies, this dissertation is dedicated to you.

Preface

"Well ya see, Norm, it's like this… A herd of buffalo can only move as fast as the slowest buffalo. And when the herd is hunted, it is the slowest and weakest ones at the back that are killed first. This natural selection is good for the herd as a whole, because the general speed and health of the whole group keeps improving by the regular killing of the weakest members. In much the same way, the human brain can only operate as fast as the slowest brain cells. Excessive intake of alcohol, as we know, kills brain cells. But naturally, it attacks the slowest and weakest brain cells first. In this way, regular consumption of beer eliminates the weaker brain cells, making the brain a faster and more efficient machine; which is why you always feel smarter after a few beers."

-Cliff Clavin

Chapter 1 - General Introduction

Project Goal

Upon infection, *Staphylococcus aureus* secretes a series of virulence factors, enabling the bacterium to evade different aspects of our innate and adaptive immune system. Years of co-evolution alongside humans has allowed *S. aureus* to develop extremely potent ways to escape being destroyed by the many layers of defense that the immune system has for getting rid of foreign pathogens. One of the main drawbacks of the innate immune system, specifically the complement cascade, is over-activation or unintended activation, leading to the destruction of host cells, tissues, etc. as well as rejection of surgical implants. Because of this, there is a dire need for drugs and therapeutics to counteract the activation of our immune system. Using *S. aureus* as a type of model system, our lab, as well as others, have identified and characterized many of the secreted virulence factors that act on the human complement system. Through a structural and biochemical approach, we can identify the mechanism of action of the virulence factor and identify the key residues and regions of the proteins that are critical for its inhibitory effects on the complement cascade. After structural characterization of the protein-protein interactions, we can begin screening through antibodies, small molecule compounds, and peptides to identify the early stages of a therapeutic that "mimics" the effects of the *S. aureus* virulence factor and inhibits complement activation.

The main focus of this dissertation is to understand the structural and functional aspects of the *S. aureus* secreted virulence factor, the extracellular adherence protein (Eap). After identification of the protein as a complement inhibitor, the first goal is to pinpoint which step in the complement cascade is being inhibited upon release of this protein during infection. Chapter 2 describes the process by which we identified Eap's mechanism of action on the complement

cascade. Through an ELISA-based approach, using normal human serum and antibodies specific for deposited complement proteins, we were able to determine that Eap acts at the point of the classical (CP) and lectin (LP) pathway C3 convertase. The second portion of chapter 2 describes characterization of the interaction between Eap and its binding partner, complement component C4b, using chromatography, analytical ultracentrifugation, surface plasmon resonance, and AlphaScreen bead-based methods. The final portion of chapter 2 uses a competition-based approach to show that Eap competes directly with complement component C2 for binding to C4b and forming the CP/LP C3 pro-convertase, therefore explaining its direct mechanism of inhibition on the complement cascade.

After identifying the mechanism of complement inhibition and Eap's binding partner, chapter 3 discusses the structural basis for these inhibitory properties. As a follow up to the functional and binding assays in chapter 2, we obtained dose-response curves of C3b and C5b-9 deposition using an ELISA-based approach for full-length Eap as well as each of the domain-deleted variants. In addition, using a similar binding assay, we obtained binding affinities for each of the domain-deleted variants and were able to show that Eap3 and Eap4 were able to elicit 100% inhibition (~50-100 fold weaker than K_D than full-length Eap or Eap34), confirming that these two domains are critical for binding and inhibiting complement activity. Ideally, a co-crystal structure of Eap34 bound to C4b would give us the necessary information for designing Eap mutants and determining specific binding sites on C4b, but the crystals we obtained diffracted poorly. This required us to use a suite of other structural methods to acquire this information, specifically, zero-length cross-linking mass spectrometry between Eap34 and C4b as well as a lysine-acetylation foot printing technique, taking advantage of the abundance of surface exposed lysine residues on Eap. These two methods allowed us to indirectly map the

binding site of Eap on C4b, an overlap of the α-chain and γ-chain, specifically the metal-ion-dependent adhesion site (MIDAS) on the C345c region of the γ-chain. These regions have previously been shown to be important for binding to the pro-protease, C2, providing us with a key structural element to the inhibitory properties of Eap.

Structural characterization of the single domains, full-length Eap, and the related proteins EapH1 and EapH2 has previously been done through X-ray crystallographic methods (1), as well as small-angle X-ray scattering (2). Unfortunately, the structure of domain 4, one of the critical domains, has eluded us using the above techniques. Chapter 4 describes the process of solution-based NMR structure determination of domain 4, using recombinantly expressed ^{15}N- and ^{13}C-labeled protein and backbone resolution through the collection of triple-resonance spectrum.

The *Staphylococcus aureus* bacterium has numerous strains, all consisting of a slightly different genetic makeup as well as a difference in their overall virulence and pathogenesis. Interestingly, the sequence and structure of the extracellular adherence protein varies slightly from strain to strain. Specifically, the above structural and functional studies have been conducted on Eap secreted from *S. aureus* strain Mu50. When compared to *S. aureus* strain Newman, the sequence variation is more dramatic, with strain Newman secreting an Eap protein with five domains as opposed to Mu50 Eap protein with four domains. The focus of chapter 5 will be the structural and functional comparison of Eap from *S. aureus* strain Mu50 and strain Newman. This will be pursued in terms of complement inhibitory activity, binding affinity for C4b, other possible binding partners, and ability of the bacterium to survive when faced with an immune response. In addition, we have also identified and characterized a small-chain variable fragment (scFv) that binds specifically to Eap and shows anti-microbial properties toward *S. aureus*.

Human Innate and Adaptive Immunity

The human immune system can be broken down into two inter-connected branches, innate immunity and adaptive immunity. Innate immunity is evolutionary conserved and encoded in the germ-line, used as a first line of defense for preventing infections and rapid removal of foreign pathogens. Because of evolutionarily conservation, the innate immune system is unchanging and consists of a set of DNA-encoded receptors [also known as pattern recognition receptors (PRRs)] that are able to recognize many of the common structures shared between invading pathogens. The main goal of the system is rapid removal and phagocytosis/destruction of the pathogen. Included in innate immunity is a series of ~30 extracellular/serum proteins, known as the complement system, which will be discussed in more detail below. A main drawback of this system is the overall lack of specificity between foreign antigens and can lead to an uncontrolled or undesired activation and destruction of host components.

The overall goals of the adaptive immune system are similar to that of the innate immune system, removal of the pathogen in the most effective way possible. Adaptive immunity gets its name from its ability to change and "adapt" to repeated challenges from a similar pathogen, through a process known as immunological memory. Beginning with initial exposure to a pathogen, activation of two different lymphocytes, B cells and T cells, occurs. In short, B cells act within germinal centers (sites within lymph nodes), in which they are able to proliferate, differentiate, and mutate their antibody genes. Differentiation of B cells occurs through somatic hypermutation, in which random mutations are introduced into the genetic region coding for their immunoglobulin (surface antibody) (3). Following mutation, B cells are subjected to selection by T_{FH} cells (Follicular B helper T cells), narrowing down the mutated B cells to clones that have mutated and gained high affinity surface antibodies that recognize the specific antigen (3). Once

selected, the mutated B cells have three possible outcomes: (i) differentiate into plasma cells with increased recognition for the specific antigen, (ii) affinity matured memory B cells (production of antibodies with increased affinity for the antigen), or (iii) subjected to another round of mutations, replication, and selection by T_{FH} cells in the germinal center (3, 4).

T cells, or T lymphocytes (a type of white blood cell), on the other hand, are an important aspect of cell-mediated immunity. They can be subdivided into eight classifications: effector, helper, cytotoxic (killer), memory, regulatory (suppressor), natural killer T cells, mucosal associated invariant, and gamma delta T cells. Their functions are described further in **Table 1-1**, below (5-12). Although the adaptive immune system is far more complicated than described above, this is beyond the scope of this dissertation.

Subtype	Function
Effector	Actively responds to stimulus. Includes helper, killer, regulatory, and other T cell types.
Helper	Maturation of B cells into plasma cells and memory B cells, and activation of cytotoxic T cells and macrophages.
Cytotoxic (killer)	Engaging and destroying virus-infected cells and tumor cells. Have been implicated in transplant rejection.
Memory	Antigen-specific T cell, persisting long term after infection. Provide the immune system with "memory" against past infections. Includes three subtypes: central memory T cells, effector memory T cells, and resident memory T cells.
Regulatory (suppressor)	Maintenance of immunological tolerance. Regulate and shut down T cell-mediated immunity following an immune reaction.
Natural killer T cells	Bridge the adaptive immune system with the innate immune system.
Mucosal associated invariant	Contain a T cell receptor and play a regulatory role in immunity.
Gamma delta T cells	Contain a distinct T-cell receptor on their surface. Function and activation is unknown.

Table 1-1. Subtypes and Function of T cells or T lymphocytes. Effector, Helper (8), Cytotoxic (killer) (9), Memory (7), Regulatory (suppressor) (10), Natural killer T Cells, Mucosal associated invariant, and Gamma delta T cells.

A major difference that distinguishes innate immunity from adaptive immunity is the time of activation in response to a foreign pathogen. The initial response of the innate immune system can occur within seconds of recognition of a foreign antigen, while adaptive immunity is activated ~12 hours post recognition and an initial response towards the pathogen occurs 5-6 days after initial exposure (**Fig. 1-1**). Additionally, regardless of the repetiveness of a similar

pathogen invading the immune system, the innate immune system will continue to act through similar mechanisms. On the other hand, adaptive immunity evolves and "remembers" the pathogen through the development and memory of antibodies and T-cells, allowing the adaptive immune system to respond to a second exposure by a similar pathogen in a greater magnitude and in less time. Scientists have used this tactic to their advantage through the development of vaccines for various infectious diseases; administration of a vaccine to an individual elicits an immune response, allowing the adaptive immune system to develop a specific and long-term adaptive response to protect the individual from future challenges from the specific pathogen.

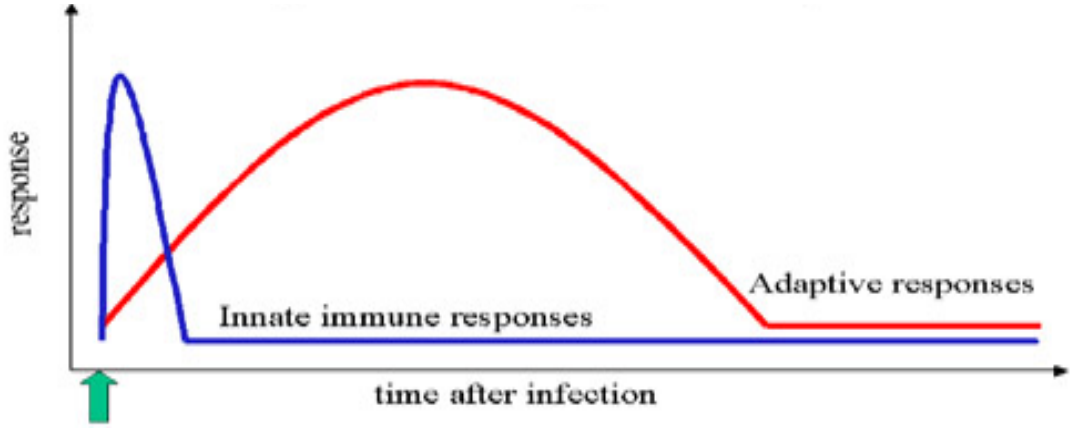

Figure 1-1. Innate immune response vs. adaptive immune response time after initial infection. Innate immunity is activated within seconds of initial recognition of the foreign pathogen to ~12-24 hours recognition, at which time the adaptive immune response is activated and an immune response against the pathogen will occur within 5 to 6 days after initial exposure.

The Human Complement System

The complement cascade is one of the key components of the human innate immune system. This system is critical because it serves as the first line of defense against invading pathogens, including bacteria, viruses, and parasites and acts immediately upon infection or injury (13). In addition, it plays a key role in the acute phase response, a response to infection and injury to eradicate foreign pathogens, limit innate immune-mediated damage to host cells and tissues, and aid in the return to homeostasis (13-16). The overall system consists of ~30 proteins and protein fragments, including serum proteins and cell membrane receptors, synthesized in the liver and circulating in the blood, predominantly as inactive pre-cursors or

pro-proteins. The complement cascade can be activated through three main biochemical pathways, the classical (CP), lectin (LP), and alternative (AP), all with the end goal of stimulation/recruitment of phagocytes, inflammation, and activation of the cell-killing membrane attack complex.

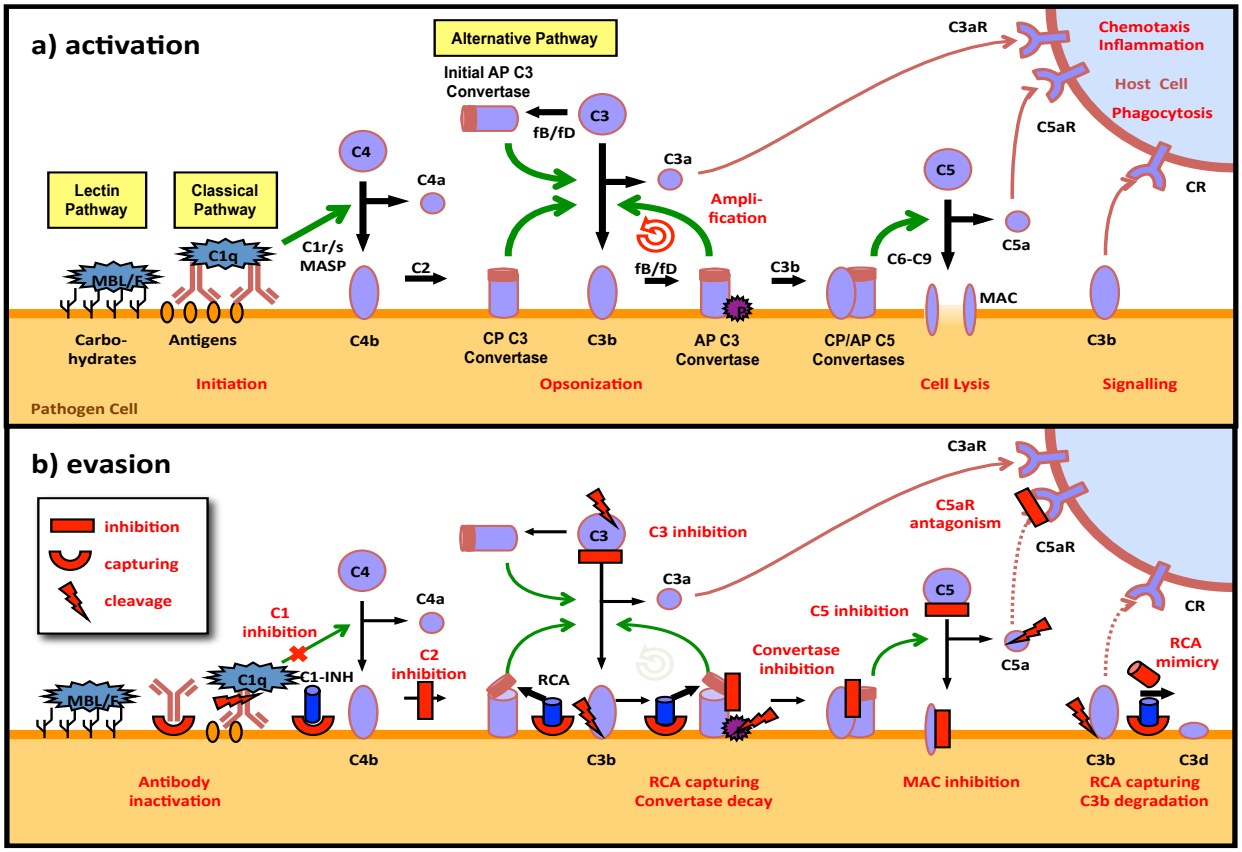

Figure 1-2. Model of the Lectin, Classical, and Alternative Pathways of Complement. (A) Summary of normal complement activation through the lectin, classical, and alternative pathways beginning with initiation and leading to opsonization, cell lysis, and signaling. (B) Complement evasion strategies used by numerous pathogens through inhibition of multiple aspects of the complement cascade. Adapted from Lambris et al. 2008 (83).

The simplest explanation of how each of the three pathways connects in the overall complement cascade can be seen in **Fig. 1-2**, above. In short, the classical pathway is triggered through activation of the C1-complex (consisting of 1 molecule of C1q, 2 molecules of C1r, and 2 molecules of C1s). Activation occurs when C1q binds to IgM or IgG complexed with antigens or bound directly to the surface of a pathogen. This binding causes a conformational change in C1q, activating the two C1r molecules (protease), which are then able to cleave and activate C1s (protease), causing cleavage of complement components C4 and C2 into C4b, C4a, C2b, and

C2a, forming the classical pathway C3-convertase, C4bC2a. Similarly, the lectin pathway is triggered through mannose-binding lectin (MBL) binding to mannose residues on the surface of the pathogen, which in turn activates the MBL-associated serine proteases (MASP-1 and MASP-2). These are then able to cleave C4 and C2, similar to the function of C1s described above. The classical and lectin pathways both converge on the formation of the C3-convertase, C4bC2a.

The alternative pathway is different in the sense that it is always activated a low level due to the spontaneous hydrolysis of complement C3 (the most abundant complement protein in blood), but its main activation is through the CP and LP C3-convertase which cleaves C3 into C3b, the most important opsonin, and C3a, an anaphylatoxin. Once surface bound, C3b can bind to factor B (fB), forming the AP C3-proconvertase, C3bB. In the presence of factor D (fD), fB can be cleaved into Ba, which is released, and Bb, which remains associated with C3b to form the AP C-convertase, C3bBb. This crucial step can begin the feedback and self-amplification loop, because C3bBb can cleave much more C3 to C3b, leading to an increase in opsonization, convertase formation, and C3b generation.

Covalent attachment of a second C3b protein to the AP C3-convertase on the pathogen cell surface forms the C5-convertase, giving it the ability to bind and cleave C5 into C5a, an extremely potent anaphylotoxin, and C5b, which attaches to the surface and recruits C6, C7, C8, and multiple C9 molecules to form the membrane attack complex (MAC). Once formed, the MAC allows free diffusion of molecules in and out of the cell as well as disruption of the cell membrane, leading to cell lysis and death (17, 18). Although MAC formation is the final step in the complement cascade, its effectiveness is only seen in the killing of Gram-negative bacteria, because the thick peptidoglycan layer of Gram-positive bacteria prevents access to the bacterial membrane (19). This leads to the major importance of the anaphylotoxins listed above, C3a, C4a,

and C5a because they have multiple functions for the removal of pathogens, including: mediate chemotaxis, inflammation, generate cytotoxic oxygen radicals, cause smooth muscle contraction, histamine release from mast cells, and enhanced permeability (20-24).

A few of the main drawbacks of the complement system is that it can become overly activated at times when its not needed as well as non-specific interactions with host cells and tissues. Because of this, there are a number of complement control proteins, which help regulate the complement system by distinguishing foreign cells from host cells to avoid damaging host tissue and switch off complement activity when its not needed. The most well studied complement regulators include: complement receptor 1 (CR1 or CD35), membrane cofactor protein (MCP or CD46), C4b-binding protein (C4BP), decay-accelerating factor (DAF or CD55), factor H, and factor I and C1 inhibitor, which do not belong to the same family as the other five regulators. CD35 has multiple functions for regulating complement; it's able to act as a negative regulator of the cascade through inhibition of the classical and alternative pathways as well as process and clear complement opsonized immune complexes (25). CD46 acts as a cofactor for factor I, which inactivates C3b and C4b through cleavage of these components into inactive fragments (26, 27). Similarly, C4BP and factor H act as cofactors for factor I, binding to C4b and C3b, respectively, accelerating the decay of the C3-convertases through cleavage into inactive fragments, shutting down the classical/lectin and alternative pathways, respectively (27, 28). The DAF acts on the fragments created activation of C4 and C3, interfering with the conversion of the pro-proteases C2 and factor B, preventing formation of C3-convertases, the amplification loop, and limiting the downstream formation of the membrane attack complex (29). Finally, the C1 inhibitor acts as a protease inhibitor by irreversibly binding and inactivating the classical and lectin pathway activation proteases, C1r, C1s, MASP-1, and MASP-2, preventing spontaneous

complement activation (30-32). A number of complement-associated diseases are caused through mutations and deficiencies in the complement regulator proteins, allowing spontaneous and over activation of the complement system damaging host cells, tissues, and organs. In addition, mutations and deficiencies in specific complement proteins can lead to a number of diseases because of the suboptimal or absent function of the complement system as a whole (33-35).

Staphylococcus aureus Bacterium and Virulence Factors

Staphylococcus was first identified back in 1880 by surgeon Sir Alexander Ogston and was later amended to *Staphylococcus aureus* by Friedrich Julius Rosenbach in 1884 (36). It's classified as a gram-positive bacterium, meaning it has a thick peptidoglycan layer in the cell wall which retains the stain in the Gram stain test after the decolorization step. Another difference from gram-negative bacterium is that gram-positive are more susceptible to antibiotics because they lack the outer membrane seen in gram-negative bacteria. Recent analysis has shown that upwards of ~30% of the population is currently colonized with a strain of *S. aureus* and of that percentage, ~1% has been characterized as methicillin-resistant *Staphylococcus aureus* or MRSA (37, 38). Because of this increase in percentage of people carrying the bacteria, it can lead to an extremely wide range of illnesses from minor skin infections, abscesses, cellulitis, to life-threatening diseases like pneumonia, meningitis, bacteremia, and sepsis. Upwards of half a million patients in hospitals each year contract a staphylococcal infection, mainly due to *S. aureus*, which leads it to be one of the main causes of infections in hospitals and wound healing following surgeries (39). Numerous amounts of research have begun to explain why *S. aureus* infections are so common, and they have started with the characterization of all the virulence factors produced by this bacterium. Upon infection, *S. aureus* produces a number of virulence factors including: enzymes (coagulase, hyaluronidase, deoxyribonuclease, lipase, etc.), toxins

(superantigens, exfoliatin, and other toxins), small RNA, post-transcriptional regulation by 3'UTRs, protein A, and staphylococcal pigments. Although all of these are critical for the virulence and survival of *S. aureus*, the main focus of this dissertation is virulence factors that affect the innate immune system and specifically, the complement cascade.

Recent reports have displayed numerous *S. aureus* proteins that directly target the complement cascade and block or inhibit a specific aspect of the pathway. The main focus of the following dissertation is an understanding of the mechanism by which the extracellular adherence protein inhibits the classical and lectin pathways of complement. We have shown that Eap's mechanism of action is to bind complement C4b and directly block the interaction between C2 and C4b, inhibiting the formation of the CP/LP C3-proconvertase (40, 41). Although a number of direct inhibitors of the classical pathway of complement have been discovered in other pathogens, highlighted by the recent review from Garcia BL et al. 2016, only Eap and the Cna-like MSCRAMM (microbial surface components recognizing adhesive matrix molecules) secreted by *S. aureus* have been shown to direct inhibit this pathway (40, 42-44). Cna from *S. aureus* acts on the classical pathway by binding directly to C1q, interfering with the interaction between C1r and the collagenous stems of C1q, and blocking the $C1r_2C1s_2$ tetramer from docking with C1q, which inhibits formation of the C1 complex (43). This effect can also be seen on preformed C1 complexes because Cna is able to displace C1r and C1s from the complex, isolating the nonactive C1q (43). Interestingly, this family of Cna-like MSCRAMMs currently includes ~20 members from Gram-positive and Gram-negative pathogens, but only five members have been shown to bind C1q and inhibit the classical pathway as described above (43, 45-53).

The majority of *S. aureus* secreted virulence factors act on the alternative pathway of complement, specifically targeting C3b and the AP C3-convertase. SCIN-A, SCIN-B, and SCIN-C are small, triple helical-bundle proteins secreted by *S. aureus* that bind directly to the C3-convertase (C3bBb), causing formation of a dimer (C3bBb-C3bBb-SCIN-SCIN), and locking the convertase in a stable, inactive conformation, blocking complement activation by inhibiting the production of C3a, C3b, C5a, and C5b (54-60). A second family of proteins, Ehp, the extracellular fibrinogen-binding protein (Efb-C), and its homologue, extracellular complement-binding protein (Ecb), bind to the C3d domain of complement C3, causing an "inhibition from a far" through an allosteric mechanism that alters the solution conformation of C3, blocking cleavage and formation of C3b (61-64). Efb-C also has a secondary mechanism of inhibition that will be discussed more in chapter 5. In short, the C-terminus of this protein binds to C3 as discussed above, but the N-terminus is able to bind fibrinogen, which causes attraction of fibrinogen to the surface of the *S. aureus*, coating the cell and blocking further opsonization by C3b and recognition by phagocytic receptors (65).

Although the formation of the membrane attack complex (MAC) has been shown to be ineffective in the killing of Gram-positive bacteria like *S. aureus*, C5 cleavage into to C5a and C5b is still a critical process because of the release of the power anaphylotoxin, C5a. Because of this, *S. aureus* has evolved a mechanism for inhibiting the cleavage of C5 through the release of the virulence factor superantigen-like 7 (SSL-7). This protein acts specifically at the point of C5 cleavage through direct interaction with C5, and a secondary interaction with the Fc region of immunoglobulin A (IgA) (66, 67). Through the binding of SSL-7 to C5 and IgA, this virulence factor directly inhibits cleavage of C5 to C5a and C5b by interfering with C5 binding to C5-convertases (66, 67). Because SSL-7 interacts so far away from the C5a cleavage site, ~70 Å, it's

thought that the requirement for IgA binding mediates a steric hindrance for C5 recognition and binding by the C5-convertase (66). Additionally, SSL-7 can bind to pre-formed C5b and block the interaction of C5b with C6, C7, C8, and C9, inhibiting formation of the MAC, although this is not crucial because the MAC has been shown to be ineffective against *S. aureus* (66). Identifying the binding partners and mechanisms for all of these virulence factors is an important task in understanding the pathogenesis of *Staphylococcus aureus* and pinpointing potential drug targets to stop this bacteria or mimic the effects of these bacteria in order to develop complement-based inhibitors.

Solution-based NMR

The development of solution-based nuclear magnetic resonance (NMR) has become an important tool in the structural elucidation and dynamics of relatively small proteins and protein complexes. Recent advances in NMR technology and magnetic power have allowed researchers to do away with sensitivity and resolutions limits that were once an issue with this technique. Although there are still limitations to the proteins that can be studied, a major strength of this technique is the sensitivity to a wide range of motions because of ability to probe the dynamics of a protein in times ranging from picoseconds to seconds (68-71). This can prove to be extremely useful in studying conformational transitions involving proteins and nucleic acids, resolving important structural features in each of the different conformers (68, 72-74). Compared to X-ray crystallography, this is very advantageous because the limitation of crystallography is that once a crystal is grown, the protein is packed into a single conformation/snapshot, giving no information on the dynamics of the protein beyond the base structural elements. Although this can be improved upon by growing crystals under different conditions and using possible binding partners to understand the conformation of the unbound vs. bound form of the protein, which can

be extremely useful for proteins that undergo large conformational changes upon binding to a specific ligand or substrate.

In the context of this dissertation, we were unable to use X-ray crystallography to solve the structure of the single Eap4 domain in the full-length protein. Numerous efforts were done using amino acid conjugations, site-directed mutagenesis, buffer conditions, seeding, etc. in order to obtain diffraction quality crystals but none of these techniques proved worthwhile. Solution-based NMR proved to be the correct technique, and chapter 4 of this dissertation discusses the background and methods for identifying to the backbone residues, amino acid sequence, secondary structure elements, and finally a complete structure of the Eap4 protein. Understanding these elements of the structure will be very important for further studies involving neutrophil serine proteases because we can use the backbone identification to perform docking-based experiments to provide insight into the critical residues required for the binding of Eap4 to elastase, cathepsin G, and proteinase 3 (75, 76).

Antibody Screening

The screening of large chemical compound libraries has opened up a new wave in the identification and development of novel therapeutics. Unlike the typical small organic compounds, the emergence of antibody-based drugs has revolutionized the industry. Rather than screening through millions of compounds, looking for hits, re-screening, and repeating this process till you have a compound that you can build upon, antibodies can be developed through multiple approaches like phage display, single B cell culture, single cell amplification from various B cell populations, and single plasma cell interrogation technologies which specifically select for the target that you are screening. In short, the phage display technique displays an antibody or peptide on the filamentous phage coat protein, allowing it to freely bind the target

you are screening. After the phage are bound to the specific target and unbound phage are washed away, a secondary target can be introduced to "compete" out the displayed coat protein/peptide, identifying an antibody or peptide that overlaps the site specific for the protein-protein interaction. Once specific phages are identified, they can be selected for, amplified, and sequenced to obtain the DNA to express recombinantly separate from the filamentous phage. This allows for rapid screening of protein-protein interactions to identify specific inhibitors to block these interactions. This approach has been used in our lab for identifying a series of peptide inhibitors based on the SCIN-C3b interaction that inhibit the alternative pathway of complement, highlighted by Summers et al. 2015 (77).

A new approach to identifying inhibitors can be seen through the development of small-chain variable fragments (scFv), which are fusion proteins of the variable regions of the heavy and light chains of immunoglobulins, connected through a short linker peptide (**Fig. 1-3**) (78). An advantage to screening and using scFvs as opposed to monoclonal antibodies (mAbs) is that they can be screened through a phage display approach and they can often be produced in bacterial cell cultures like *E. coli*, as opposed to producing mAbs in mammalian cell cultures. A comparison between the techniques for identifying mAbs, scFvs, and Fabs can be seen in Colwill et al. 2011 and highlighted in Nollau et al. 2011 (**Fig. 1-4**) (79, 80).

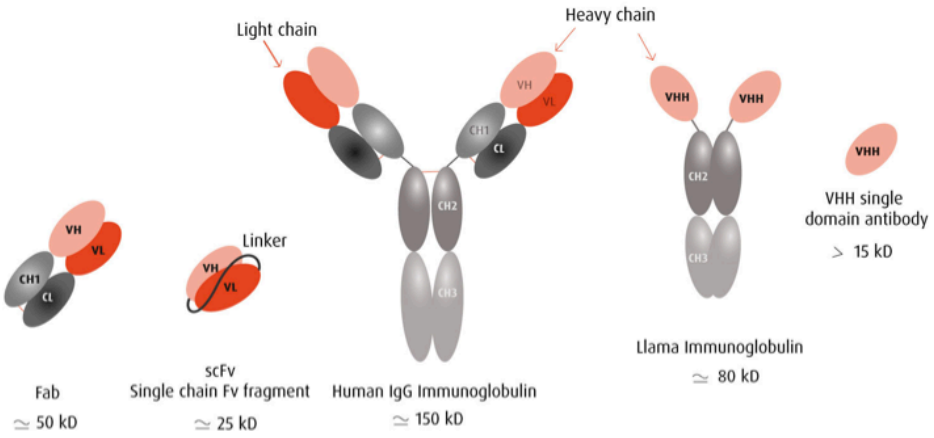

Figure 1-3. Variations and Size of Antibodies that can be screened in order to identify potential binding partners. Fabs and scFvs can be recombinantly expressed in *E. coli*, while IgG must be expressed in mammalian cultures.

Although the speed in which one can identify potential binders using immunization and hybridoma technologies to identify mAbs varies greatly in comparison to phage display for the identification of scFvs and Fabs, the results for the final quality of identified binders is comparable between the two methods. Chapter 5 of this dissertation highlights the large screening approach for the identification of an scFv that interacts specifically with Eap and shows anti-microbial effects toward the killing properties of *S. aureus*.

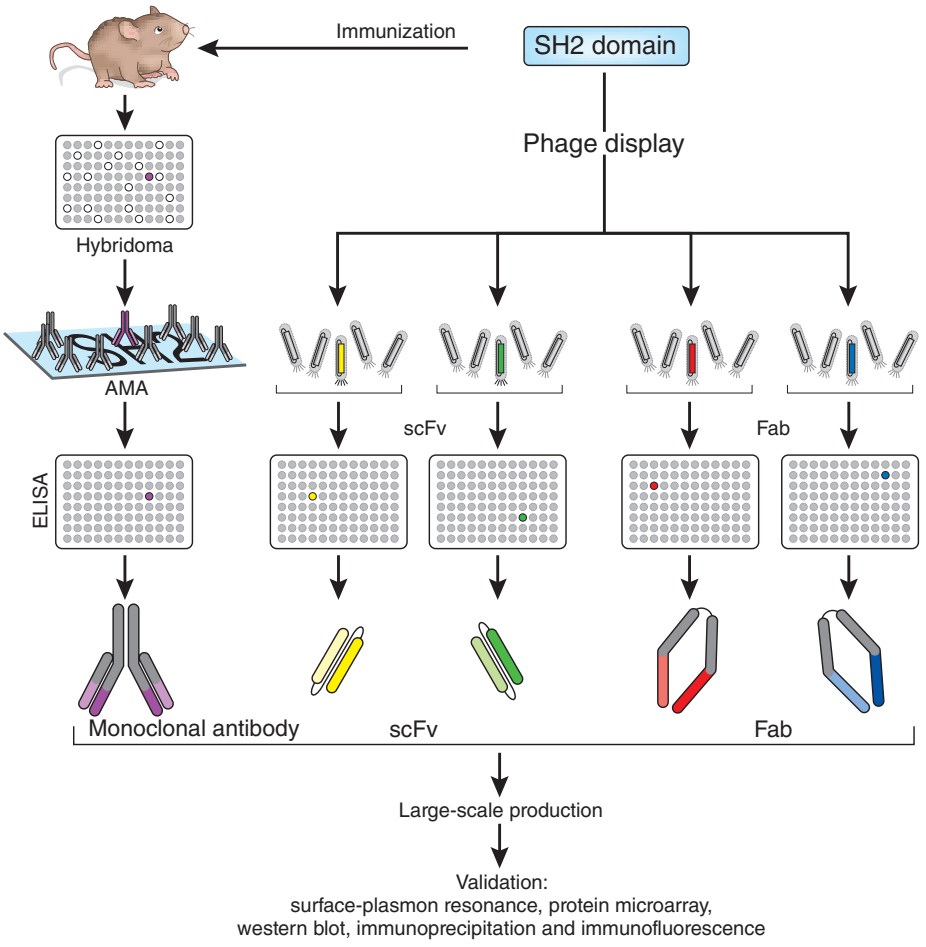

Figure 1-4. Roadmap for the generation of protein binders for SH2 domains (80). Monoclonal antibodies were generated through immunization and hybridoma technology. ScFvs and Fabs were generating by a phage display approach using four different phage libraries.

Chapter 2 - The extracellular adherence protein from *Staphylococcus aureus* inhibits the classical and lectin pathways of complement by blocking formation of the C3 proconvertase

Jordan L. Woehl[1*], Daphne A.C. Stapels[2*], Brandon L. Garcia[1], Kasra X. Ramyar[1], Andrew Keightley[3], Maartje Ruyken[2], Maria Syriga[4], Georgia Sfyroera[4], Alexander B. Weber[3], Michal Zolkiewski[1], Daniel Ricklin[4], John D. Lambris[4], Suzan H.M. Rooijakkers[2#], and Brian V. Geisbrecht[1#]

[1]Deparment of Biochemistry & Molecular Biophysics;
Kansas State University, Manhattan, KS, USA

[2]Medical Microbiology;
University Medical Center Utrecht, Utrecht, The Netherlands

[3]School of Biological Sciences;
University of Missouri-Kansas City, Kansas City, MO, USA

[4]Department of Pathology and Laboratory Medicine;
University of Pennsylvania, Philadelphia, PA, USA

*Equal Contribution
[#]These authors shared supervision of this study

Journal of Immunology (2014). 193(12): 6161-6171

Abstract

The pathogenic bacterium *Staphylococcus aureus* actively evades many aspects of human innate immunity by expressing a series of small inhibitory proteins. A number of these proteins inhibit the complement system, which labels bacteria for phagocytosis and generates pro-inflammatory chemoattractants. While the majority of staphylococcal complement inhibitors act on the alternative pathway (AP) to block the amplification loop, only a few proteins act on the initial recognition cascades that constitute the classical (CP) and lectin (LP) pathways. We screened a collection of recombinant, secreted staphylococcal proteins to determine if *S. aureus* produces other molecules that inhibit either the CP and/or LP. Using this approach, we identified the extracellular adherence protein (Eap) as a potent, specific inhibitor of both the CP and LP. We found that Eap blocked CP/LP-dependent activation of C3, but not C4, and that Eap likewise inhibited deposition of C3b on the surface of *S. aureus* cells. In turn, this significantly diminished the extent of *S. aureus* opsonophagocytosis by neutrophils. This combination of functional properties suggested that Eap acts specifically at the level of the CP/LP C3 convertase (C4b/C2a). Indeed, we demonstrated a direct, nanomolar-affinity interaction of Eap with C4b. Eap binding to C4b inhibited binding of both full-length C2 and its C2b fragment, which indicated that Eap disrupts formation of the CP/LP C3 pro-convertase (C4b/C2). As a whole, our results demonstrate that *S. aureus* inhibits the two initiation routes of complement by expression of the Eap protein, and thereby define a novel mechanism of immune evasion.

Introduction

The complement system serves as a critical hub in the human innate immune and inflammatory system, and fulfills numerous roles in homeostasis, defense, repair, and disease (81). Despite its diverse list of functions, complement remains best known for its ability to

opsonize and eliminate invading microorganisms. To achieve this most efficiently, the microbial surface must first be recognized by one of a series of pattern-recognition proteins (81). These ligand-bound 'sensors' can then trigger one of three canonical activation routes, (the classical (CP), lectin (LP), and alternative (AP) pathways), which all result in cleavage of the abundant plasma protein C3 into its bioactive C3a (chemoattractant) and C3b (covalent opsonin) fragments. Although such activation of C3 may occur at a low level spontaneously, this central process is catalyzed at the bacterial surface through the function of two transiently-stable, multi-subunit proteolytic complexes known as C3 convertases. In the case of the CP or LP, the initiating complexes of surface Ig-bound C1 or carbohydrate-bound MBL/MASPs trigger proteolytic activation of C4 to produce C4b. Surface-bound C4b then binds C2 to form the CP/LP C3 pro-convertase which, when proteolytically-activated by the same initiation complexes named above, gives rise to the fully-active CP/LP C3 convertase, C4b/C2a. C4b/C2a converts native C3 into C3b, and ultimately gives rise to the AP C3 convertase (C3b/Bb). In this scenario surface deposed C3b, along with the pro-enzyme factor B (fB) and factor D (fD), cooperate to generate the C3b/Bb complex. It is this surface-bound AP C3 convertase that activates massive amounts of C3 into C3b, thereby being responsible for the self-amplifying nature of the complement response, and which stimulates massive opsonization of bacteria and production of powerful inflammatory mediators like C3a and C5a (82). Furthermore, deposited C3b molecules also activate the terminal pathway of complement that results in the formation of the terminal complement complex (C5b-9) that can directly kill Gram-negative bacteria.

The pathogenic bacterium *Staphylococcus aureus* has evolved a diverse and multifaceted approach to successfully evade the human innate immune response (19, 83, 84). Central to this global strategy is its ability to manipulate the human complement system to a greater extent than

perhaps any other pathogen studied thus far (19, 58, 83). While studies from the last decade have revealed much on the diverse nature of *S. aureus* complement evasion, the large number of C3 convertase inhibitors that act on the AP suggests that conceptually similar mechanism(s) that affect the CP and/or LP might be manifested by a component of the *S. aureus* immune evasion arsenal. In this regard, the fact that CP and LP share the same C3 convertase, C4b/C2a, raises the intriguing possibility that a single inhibitor might effectively block C3b deposition and downstream anaphylatoxin production via both of these pathways simultaneously. While SCIN proteins have been reported to inhibit the CP and LP at the level of C3b deposition, their activities against these pathways are only partial and are substantially weaker than they are against the AP (85, 86). Thus, we hypothesized that *S. aureus* might express and secrete an as yet unidentified inhibitor of CP and LP C3 convertase formation and/or activity.

To this end, we screened a collection of recombinant secreted *S. aureus* proteins to examine whether any of these molecules had inhibitory activities on the CP/LP. In doing so, we identified the Staphylococcal extracellular adherence protein (Eap) as a potent, specific inhibitor of both the CP and LP. We found that Eap, but not its structural homologs EapH1 and EapH2 (1), inhibits the CP/LP in a dose-dependent manner by forming a nanomolar affinity complex with C4b. This C4b/Eap complex inhibits binding of C2 to C4b, and therefore impedes formation of the CP/LP C3 pro-convertase. From a broader perspective, the studies we present here suggest that the effects of Eap on the CP/LP in many respects mirror those of Efb-C, which inhibits AP C3 pro-convertase formation by binding C3b (64). In sum, this work provides new insight into staphylococcal immune evasion, and also describes an entirely novel mechanism of CP/LP regulation that may hold significant implications for future design of therapeutic CP/LP inhibitors.

Materials and Methods

Preparation of Native and Recombinant Proteins

Human serum proteins C3, C3b, C4, C4b, C1s, C4b-binding protein (C4BP), and factor I (fI) were obtained in purified form from Complement Technologies (Tyler, TX). Recombinant forms of C2 and C2b were expressed and purified from the conditioned culture medium of transiently transfected HEK293 cells according to the general methods described previously (87). All recombinant *S. aureus* proteins were overexpressed and purified according to the general methods described previously (88), with the exception that recombinant, full-length Eap was prepared according to the published protocol of Xie *et al.* (89).

Human Derived Materials

Blood was drawn from healthy adult volunteers after obtaining informed consent and approval of the protocol by the medical-ethical committee of the University Medical Center Utrecht (Utrecht, The Netherlands). Normal human serum (NHS) was isolated as described before (90), and frozen at -80 °C until needed for further use. For neutrophil preparation, heparinized vacutainers (Becton Dickinson) were used and neutrophils were isolated over a ficol/histopaque gradient as described previously (91).

Complement Pathway Activity on an Artificial Surface

Functional activity of the CP, LP and AP was determined essentially as described (92). In short, Nunc-Maxisorb ELISA plates were coated overnight to specifically activate the CP (coated with 3 µg/ml human IgM (Calbiochem)), LP (coated with 20 µg/ml *Saccharomyces cerevisiae* mannan (Sigma)), or AP (coated with 20 µg/ml *Salmonella enteriditis* LPS (Sigma)). Plates were blocked with 1% (w/v) BSA in PBS with 0.05% (v/v) Tween 20 (Merck). The indicated percentages of NHS were preincubated with 1 µM of recombinant *S. aureus* proteins in

the appropriate assay buffers for 15 min at 25 °C (VBS (pH 7.5) with 0.1% (w/v) gelatin, 500 µM $CaCl_2$, and 250 µM $MgCl_2$ for CP and LP; VBS (pH 7.5) with 0.1% (w/v) gelatin, 5 mM $MgCl_2$, and 10 mM EGTA for AP). Deposited C3b, C4b, and C5b-9 were detected with specific antibodies (0.1 µg/ml aC3c WM-1 clone DIG labeled, American Type Culture Collection; 1 µg/ml aC4d, Quidel; 1 µg/ml aC5b-9 aE11, Santa Cruz respectively). Secondary horse-radish peroxidase (HRP) labeled antibodies were detected with 100 µg/ml TMB and 60 µg/ml ureum peroxidase in 100 mM sodium acetate buffer at pH 6.0. The reaction was stopped by adding an equal volume of 1 N H_2SO_4, and the absorbance at 450 nm was measured using a BioRad microplate reader.

Complement Deposition on S. aureus

S. aureus Newman Δ*eap* (MR1811) (75) was grown on a blood-agar plate. Bacteria were resuspended in assay buffer (20 mM HEPES (pH 7.4) with 140 mM NaCl, 0.5 mM $CaCl_2$, 0.25 mM $MgCl_2$, and 0.1% (w/v) BSA). 8 x 10^6 CFU were incubated with the indicated concentrations of NHS in presence or absence of 1 µM Eap in a total volume of 100 µl for 10 min, while shaking at 37 °C. Unbound components were washed away with assay buffer and deposited C3b was quantified by flow cytometry (FACS Verse, BD) by using the specific FITC-conjugated goat $F(ab')_2$ anti-human-C3 (Protos Immunoresearch, Burlingame, CA).

Phagocytosis assays

S. aureus Newman Δ*eap* transformed with pCM29 (93), a vector inducing constitutive expression of sGFP under the *sarA* promotor, was grown in THB until an OD_{600} of 0.5. Bacteria were washed with RPMI-1640 (Invitrogen) supplemented with 0.05% (w/v) human serum albumin (HSA; Sanquin), aliquoted, and stored at -80 °C until use. 2.5 x 10^6 CFU were pre-opsonized with the indicated concentrations of NHS in RPMI/HSA in presence or absence of 1

μM Eap, EapH1 or EapH2. Then, 2.5 x 10^5 isolated PMN were added to obtain a total volume of 250 μl and incubated at 37 °C with shaking at 600 rpm for 15 min. The reaction was stopped by adding 100 μl ice-cold 2% (v/v) paraformaldehyde. Phagocytosis was assessed by flow cytometry (FACS Verse, BD). Graphs show the percentage of GFP-positive neutrophils. The fluorescent signal originated exclusively from intracellular bacteria, as verified by confocal microscopy.

Neutrophil-mediated killing

S. aureus Newman WT or Δ*eap* was grown in Todd-Hewitt broth to OD_{660} of 0.5 (corresponding to 2 X 10^8 CFU/ml). Eap was added in 1 μM, and 10% NHS was added for 15 min at 25°C in RPMI 1640/HSA to allow for opsonization. Opsonized bacteria (5 X 10^4 CFU) were incubated with 9 X 10^4 neutrophils in 100 μl RPMI 1640/HSA. The reaction was stopped at the indicated time points with 900 μl ice-cold 0.1% saponin (w/v). After 15 min, the samples were resuspended via a 25-gauge needle, to assure lysis of the neutrophils (94). Surviving bacteria were enumerated by plating serial dilutions on Luria broth-agar plates.

Eap affinity isolation of human serum proteins

A recombinant form of Eap that harbored a single, N-terminal cysteine was expressed and purified from *Escherichia coli* similarly to WT Eap (89). Eap produced in this manner was site-specifically biotinylated using EZ-link maleimide-polyethylene glycol 2000-biotin reagent according to manufacturer's suggestions (ThermoFisher). Following derivatization, 2 μg Eap biotin was added to samples containing either 20 μl EDTA serum or C4-depleted serum (Complement Technologies), and an appropriate quantity of PBS to give a final volume of 100 μl. The samples were incubated for 1 h at room temperature, after which time 30 μl of 50% (v/v) slurry of magnetic streptavidin-coated Dynabeads was added (Invitrogen). Following an

additional 15-min incubation, the beads were isolated via a magnet and washed three times with 100 µl PBS, and all remaining liquid was removed by aspiration. A total of 15 µl non-reducing Laemmli buffer was added to each sample, and 5 µl of each sample was analyzed by SDS-PAGE, followed by staining with Coomassie brilliant blue.

Stoichiometry and Molecular Weight Estimations

The apparent molecular weight and stoichiometry of the C4b/Eap complex was determined by a combination of size-exclusion chromatography and sedimentation equilibrium analytical ultracentrifugation. For chromatographic analysis, samples consisting of either C4b or C4b/Eap (20 µM final concentration) were prepared and 100 µl were injected at 0.75 ml/min onto a Superdex S200 Increase 10/30 column that had been previously equilibrated at 4 °C in a buffer of PBS. The contents of peak fractions were analyzed by Coomassie-stained SDS-PAGE of samples that had been prepared under non-reducing conditions. For sedimentation equilibrium analysis, all experiments were performed using a Beckman XL-I ultracentrifuge with a four-position AN-Ti rotor. Protein solutions (1.6 µM C4b or C4b/Eap complex in PBS; 110 µl) and dialysate buffer (PBS; 120 µl) were placed in the double-sector centrifuge cells. The samples were equilibrated at 4 °C at 6,000 rpm and the approach to equilibrium was monitored by repetitive absorption scans at 280 nm every 6 h. The apparent equilibrium was reached after ~60 h. After the final data collection, the rotor was accelerated to 42,000 rpm for ~ 2 h and the cells were scanned to obtain the baseline absorption value. Data were analyzed with the software supplied with the instrument (Beckman-Coulter, Inc.). Both the protein partial specific volume and buffer density were calculated using Sednterp software (http://bitcwiki.sr.unh.edu/index.php/Main_Page).

Biotinylation of C4b

Biotinylated C4b was prepared by overnight, room-temperature incubation of native C4 (1 mg/ml final concentration) with C1s (5 µg/ml final concentration) in the presence of EZ-link Maleimide-PEG_2-Biotin reagent according to manufacturer's suggestions (ThermoFisher, Inc.). The reaction mixture (250 µl in PBS (pH 7.0)) was buffer exchanged into 20 mM tris (pH 8.0), applied to a 1 ml Resource Q anion exchange column (GE LifeSciences), and the bound proteins eluted with a gradient to 1 M NaCl over 10 column volumes. Fractions containing biotinylated-C4b were identified and characterized by a combination of SDS-PAGE and western blotting using streptavidin-conjugated HRP (ThermoFisher, Inc.). Purified C4b-biotin was pooled, quantified spectrophotometry, and stored at 4 °C in the existing buffer until further use.

AlphaScreen Binding Assays

An AlphaScreen equilibrium competition assay was used to derive both positional information and apparent dissociation constants for C4b binding to various complement components and staphylococcal inhibitors. This assay system is based upon modification of a previously published protocol (59) and is established via the following principle: a luminescence signal is generated by laser excitation of a streptavidin-coated donor bead, which recognizes C4b-biotin that binds directly to a second target protein (in this case myc-Eap), which itself can be adsorbed to an acceptor bead coated with anti-c-myc monoclonal IgG. C4b/Eap competition binding assays were carried out in a total volume of 25 µl by adding each assay component to the following final concentrations: 50 nM myc-Eap, 5 nM C4b-biotin, 20 µg/µl anti-c-myc AlphaScreen acceptor beads, and 20 µg/µl AlphaScreen donor beads. A dilution series was prepared for each unlabeled competitor protein of interest. Reactions were performed over 2.5 h and were begun by incubating the C4b-biotin, myc-Eap, and a given concentration of each competitor protein for 1 h. Following this, the acceptor beads were added, incubated for an hour,

then the donor beads were added and incubated for an additional 0.5 h. At that point, the donor beads were excited at 680 nm and the evolving AlphaScreen signal (photon counts/sec at 630 nm) for each data point was measured using an EnSpire multimode plate reader (Perkin Elmer Life Sciences). Data analysis and curve fitting was carried out as previously described (59).

Surface Plasmon Resonance Experiments

Interactions between C4b-biotin and the *S. aureus* proteins Eap, EapH1, and EapH2 were measured by SPR using either a BiaCore X or BiaCore 3000 instrument (GE Life Sciences) at room temperature. PBS-T (i.e. PBS (pH 7.0) with 0.005% (v/v) Tween-20) was used as the running buffer throughout the entire set of experiments. C4b-biotin was captured on a streptavidin sensor chip (GE Life Sciences) to a density of approximately 5,000 RU. Ligands were diluted to their working concentrations in PBS-T. For comparison of EAP-domain proteins' binding to C4b, samples were prepared at 1 and 10 μM and injected for 1 min at a flow rate of 20 μl/min, followed by a dissociation phase of 2 min. Signals were normalized to the molecular weight of each respective analyte to allow for a ranking of Eap, EapH1, and EapH2 relative affinities for C4b. Surface regeneration was achieved by injecting a solution of 1 M NaCl. Data analyses were carried out using the BiaEvaluation software suite (GE Life Sciences).

A surface plasmon resonance assay was also used to assess the competition between Eap and C2 for binding to C4b (95). Briefly, a C4b-biotin surface was prepared as described above and a room temperature running buffer of HBS-CMT (20 mM HEPES (pH 7.4), 150 mM NaCl, 5 mM $CaCl_2$, 5 mM $MgCl_2$, and 0.005% (v/v) Tween-20) with a flow rate of 20 μl/min was used for all injections. C2 was injected in triplicate at a concentration of 200 nM to establish a basal level of C2 binding. This concentration was held constant for the competition experiments, which were carried out by varying either the Eap or Eap34 concentration over six points from

5000 nM to 8 nM. To calculate residual C2 binding, the sensorgram of the corresponding Eap/Eap34 injection alone was subtracted from the Eap/Eap34+C2 injection series. The averaged response for the 5 s preceding the injection stop was plotted against the concentration of Eap/Eap34 and fit to a dose-response inhibition curve by non-linear regression as previously described (59). Regeneration of the surface was carried out with 2 M NaCl for 2 min followed by 0.2 M Na Citrate for 2 min.

fI Proteolysis Assay

Sequential fI-dependent proteolysis of C4b to iC4b and C4c was monitored by an SDS-PAGE based method. A sample of C4b (1 μg/μl in PBS) was incubated with purified fI (0.01 μg/μl) either in the presence or absence of C4bBP, and/or various concentrations of Eap, Aliquots reflecting the time-course of proteolysis were withdrawn at 0, 2, 5, 10, and 20 min, and the reaction was quenched by addition of Laemmli sample buffer with β-mercaptoethanol to reduce disulfide bonds. Samples were separated on a 10% (w/v) tris-tricine polyacrylamide gel and stained with Coomassie blue. Individual bands were excised, extracted, and digested by trypsin to allow identification by LC-MS/MS according to the general method of Kinter and Sherman (96). Individual band staining intensities and ratios were quantified by ImageJ (97).

Statistics

All analyses were performed in GraphPad Prism 6.0.

Results

Identification of Eap as an inhibitor of the CP and LP of Complement

We screened a library of ~30 secreted staphylococcal proteins to test whether any of these molecules were capable of inhibiting the CP and LP on the surface of pathway-specific activator/acceptor-coated ELISA plates (92). In doing so, we discovered that a recombinant

form of Eap inhibited both pathways at the level of terminal complement complex (C5b-9) deposition (**Fig. 2-1A**). This effect was specific for the CP and LP, because Eap did not block the AP (data not shown). A gene encoding Eap is found in 98% of all clinical isolates of *S.*

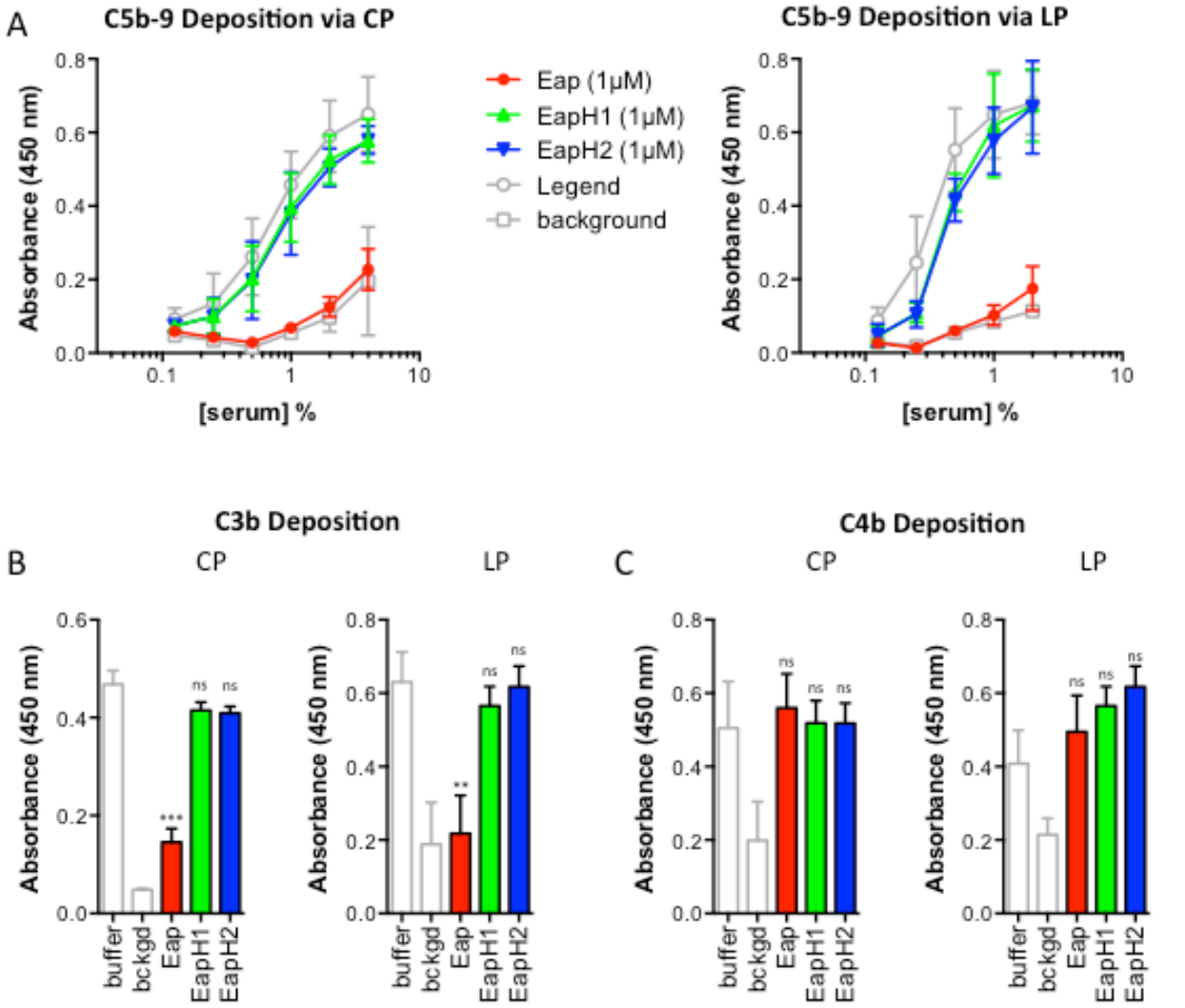

Figure 2-1. Eap inhibits complement activation via the classical and lectin pathways. The effect of Eap on distinct routes of complement activation was assessed via ELISA-based methods. (A) The effect of 1 μM Eap, EapH1, or EapH2 on CP (*left*)- and LP (*right*)-mediated complement activation was measured across a dilution series of NHS. Activation was detected as C5b-9 deposition on an ELISA plate surface. Legend is *inset*. (B) The effect of 1 μM Eap, EapH1, or EapH2 on CP- and LP-mediated complement activation in 1% (v/v) NHS was measured. Activation was detected as C3b deposition on an ELISA plate surface. (C) The same experiment as in (B), except that activation was detected as C4b deposition on an ELISA plate surface. Error bars represent the mean ± SD of three independent experiments. Measures of statistical significance in (B) and (C) were determined by an unpaired *t* test of each experimental series versus buffer control. $^{**}p \leq 0.01$, $^{***}p \leq\leq 0.001$. ns, not significant. Data collected by Suzan H.M. Rooijakkers lab.

aureus (98). Although there is some variability in the molecular mass of Eap from *S. aureus* strain Mu50 (~50 kDa) and Newman (~63kDa) in various assays suggests that these two isoforms retain similar functions (75, 89). Consistent with this, Eap proteins from both *S. aureus*

Mu50 and Newman are equally potent in their ability to inhibit the CP and LP (data not shown). Eap from *S. aureus* strain Mu50 is comprised of four tandem repeats of an ~100 residue motif known as the EAP domain (1). These repeats share between 40 and 80% identity with one another, and show ~25-50% identity to the structurally related *S. aureus* proteins, EapH1 and EapH2, which themselves consist of little more than a single EAP domain (1). Although Eap potently inhibited the CP and LP at the level of C5b-9, neither EapH1 nor EapH2 had any significant impact on either pathway. Thus, the inhibitory effect on the CP and LP is specific to Eap, and not a general feature of EAP domain-containing proteins. To determine the specific steps in the CP and LP that are inhibited by Eap, we investigated whether Eap could block C4b or C3b deposition. We found that Eap inhibited C3b deposition by the CP and LP both in human and mouse serum (**Fig. 2-1B, Supplemental Fig. 2-1A**), but Eap failed to block C4b deposition (**Fig. 2-1C**). Together, these results indicate that Eap blocks activation of C3, but not C4, via both the CP and LP of complement.

Eap inhibits deposition of C3b at the S. aureus surface and blocks phagocytosis and killing

The results described above revealed that Eap specifically inhibits C3 activation via the CP and LP. Nevertheless, one limitation of these experiments is that they employed artificial activator and acceptor surfaces to study the complement response. To test whether Eap could impact an experimental system that more closely reflects the situation found *in vivo*, we examined the effect of Eap on C3b opsonization of the *S. aureus* cell surface. Although Eap is a secreted protein, ~30% of Eap rebinds the bacterial surface after secretion (99). To address the role of surface-bound Eap in complement inhibition, we analyzed C3b deposition and subsequent phagocytosis for both the *S. aureus* Newman WT strain and an isogenic *eap*-mutant strain (Δ*eap*) in parallel (75) (**Supplemental Fig. 2-1B**). Neither assay revealed any difference in the level of

C3b deposition or phagocytosis between the WT and mutant strain in the absence of exogenous Eap, suggesting that surface-retained Eap does not contribute significantly to *S. aureus* complement evasion (**Figs. 2-2A, 2-2B**). However, exogenously added Eap (1 μM) blocked deposition of C3b on both strains by nearly 50% across four different serum concentrations that ranged from 1 to 8% (v/v) (**Fig. 2-2A**). As expected, this diminished level of C3b opsonization in

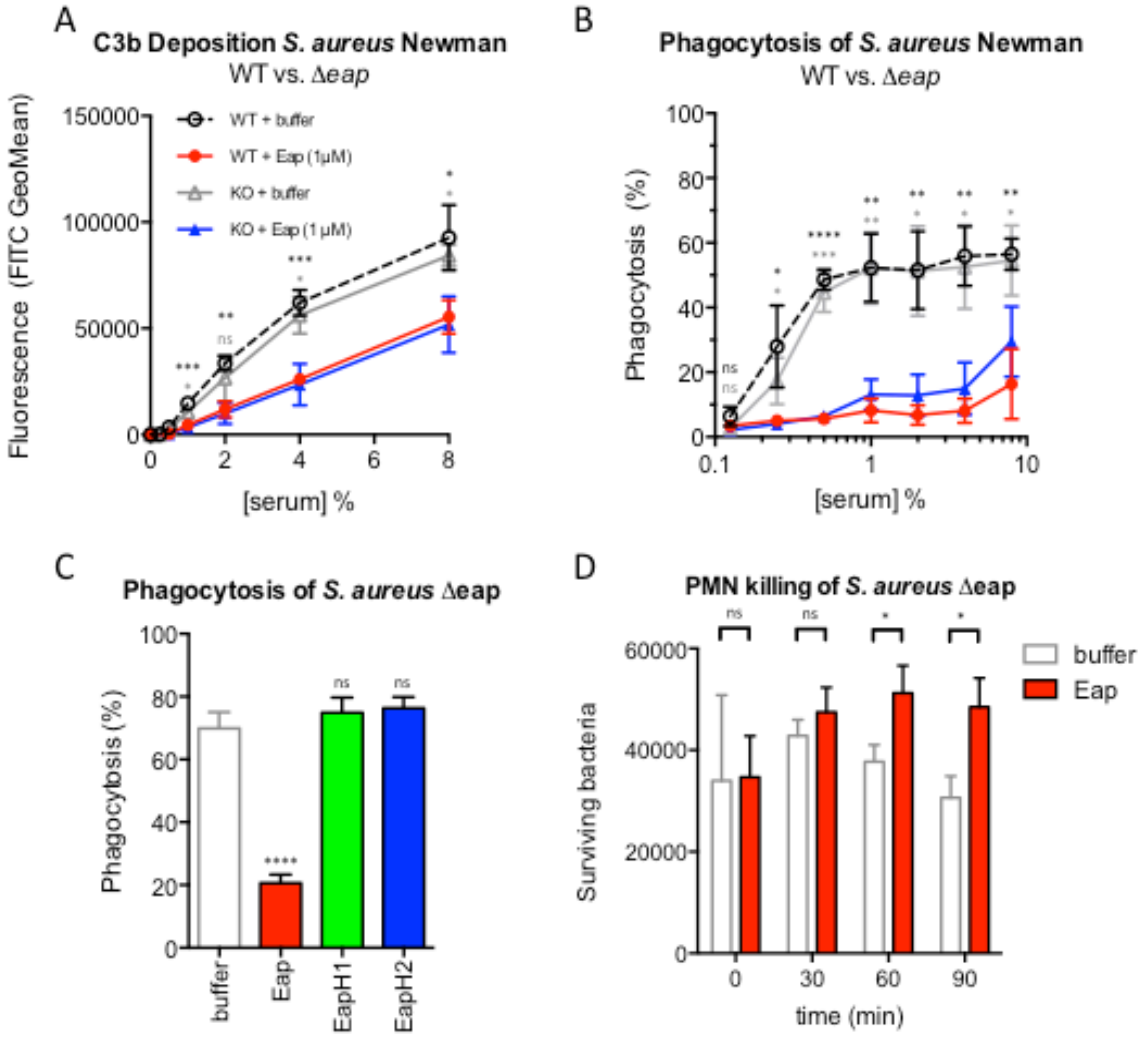

Figure 2-2. Eap inhibits opsonization, phagocytosis, and killing of *S. aureus*. The impact of recombinant Eap on complement deposition and phagocytosis of *S. aureus* Newman strains was assessed using flow cytometry. (A) C3b deposition on the surface of *S. aureus* Newman WT or Δ*eap* in the presence of 1 μM Eap or a buffer control. Legend is inset. (B) Phagocytosis of *S. aureus* Newman WT or Δ*eap* in the presence of 1 μM Eap or a buffer control. Legend is *inset* in the adjacent panel. (C) Extent of phagocytosis of *S. aureus* Newman Δ*eap* using 1% (v/v) NHS in the presence of 1 μM Eap, EapH1, or EapH2, or a buffer control. (D) Neutrophil-mediated killing of *S. aureus* Newman Δ*eap* opsonized in the presence of 1 μM Eap or a buffer control. Error bars represent the mean ± SD of three independent experiments and at least two different donors. Legend is *inset*. Measures of statistical significance were determined by an unpaired *t* test of each experimental series versus the corresponding buffer control for each strain and serum concentration, as appropriate. *$p \leq 0.05$, **$p \leq 0.01$, ***$p \leq 0.001$, ****$p \leq 0.0001$. ns, not significant. Data collected from John D. Lambris lab.

the presence of Eap significantly inhibited the efficiency with which neutrophils phagocytosed both strains (**Fig. 2-2B**).

We then used the Δ*eap* strain to conduct several additional experiments aimed at assessing the significance of Eap's effects on phagocytosis and its impact on bacterial survival. To begin, we found that inhibition of phagocytosis by increasing concentrations of Eap was both dose dependent and saturable (**Supplemental Fig. 2-1C**). Importantly, the concentration of Eap found in stationary liquid cultures of *S. aureus* [up to 10 μg/ml, or ~200 nM (100)] resulted in >50% inhibition of phagocytosis by human neutrophils. Although the concentration of Eap secreted into the human body during *S. aureus* infections remains uncertain, these data suggest that Eap-dependent inhibition of the CP/LP, and subsequently of phagocytosis, is most likely physiologically relevant. Along these lines, and in concordance with the ELISA data presented above, this antiphagocytic effect was not observed when either control protein EapH1 or EapH2 was added at the same exogenous concentration that resulted in potent inhibition of phagocytosis by Eap (**Fig. 2-2C**). Finally, we observed that diminished levels of phagocytosis likewise resulted in significantly diminished killing of *S. aureus* by human neutrophils (Fig. 2D). Together, these results indicate that secreted Eap specifically blocks CP/LP-mediated opsonization of *S. aureus* with C3b and subsequent phagocytosis and killing of *S. aureus* by neutrophils.

Eap binds with nanomolar affinity to complement component C4b

We observed that Eap bound an ~200-kDa protein present in EDTA-treated human serum, but not in C4-depleted serum (**Supplemental Fig. 2-2A**). While this result provided evidence that Eap binds to native C4, the functional studies presented above indicated that Eap inhibits an event within the CP and LP that mediates activation of C3, but leaves C4 activation

intact. We therefore predicted that Eap must act on either the fully assembled CP/LP C3 convertase (C4b2a) or an isolated component thereof. As a first test of this hypothesis, we examined the behavior of purified C4b and a mixture of C4b and Eap by analytical size-exclusion chromatography (**Fig. 2-3A, *left panel***). Inclusion of equimolar amounts of Eap in the C4b sample resulted in a pronounced shift of the peak to a larger apparent molecular mass that eluted as a single species. Indeed, bands corresponding to both Eap and C4b were present when the peak fractions were analyzed by Coomassie-stained SDS-PAGE (**Fig. 2-3A, *right panel***). Due to potential inaccuracy of molecular mass estimates obtained from size-exclusion chromatography, we also used analytical ultracentrifugation to provide further characterization of the C4b/Eap complex. Sedimentation equilibrium data for both C4b/Eap and C4b alone were obtained at one concentration and were well described by a single particle model (**Supplemental Fig. 2-2C**). Whereas the molecular mass for C4b itself was estimated at 268 kDa, the apparent molecular mass of C4b/Eap was estimated at 308 kDa. Because previous sedimentation equilibrium studies of Eap yielded an apparent molecular mass of 51 kDa for this protein (2), these data strongly suggest that Eap forms a 1:1 complex with C4b.

We next used a bead-based AlphaScreen assay to explore both the affinity and specificity of the C4b/Eap interaction in greater detail (59, 60). Whereas untagged Eap itself could diminish the luminescence signal generated by interaction between myc-tagged Eap and C4b biotin in a dose-dependent manner, neither EapH1 nor EapH2 had any competitive effect even at the highest concentrations tested (**Fig. 2-3B**). Nonlinear curve fitting of the C4b/Eap competition data revealed an apparent K_d of 185 ± 14 nM for this complex. Saturable binding of similar affinity was also observed when either native C4 or C4c was used as the competitor, and fit to apparent K_d values of 45 ± 2 and 138 ± 16 nM, respectively (**Supplemental Fig. 2-2B**). To study

the C4b/Eap interaction through an independent approach, we constructed a SPR biosensor wherein C4b biotin was uniformly immobilized on a streptavidin-coated surface similarly to what we have previously reported for C3b biotin (59, 60, 64, 95). Significantly, neither EapH1 nor EapH2 bound the C4b surface even at concentrations 10-fold higher than those that showed clear evidence of C4b binding by Eap (**Fig. 2-3C**). Thus, the ability of Eap to bind C4b and the lack of C4b binding by EapH1 and EapH2 are in agreement with the inhibition of CP/LP function by Eap and the lack thereof by its homologs.

Eap binding to C4b and subsequent inhibition of the CP/LP requires the third domain of Eap

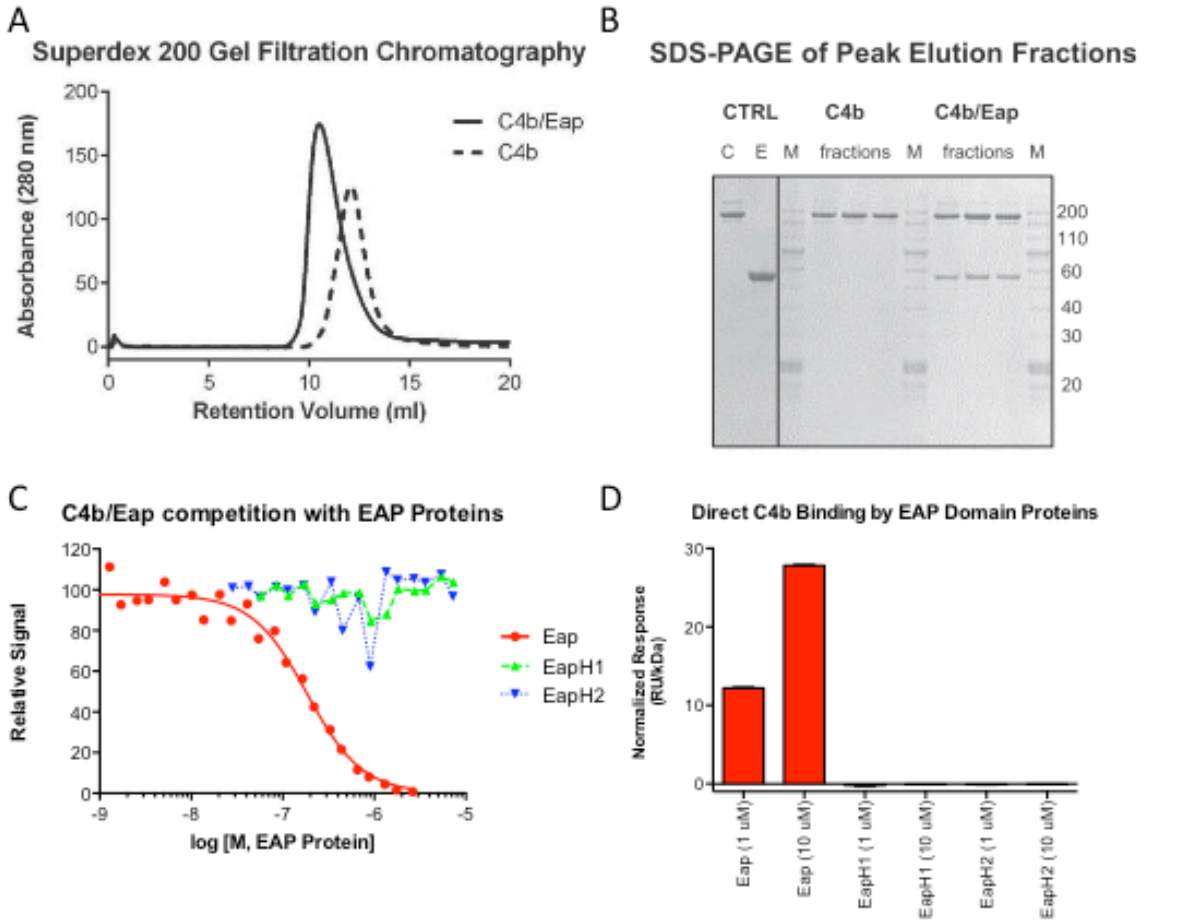

Figure 2-3. Eap forms a nanomolar affinity complex with complement component C4b. (A) Analysis of the C4b/Eap complex by analytical gel-filtration chromatography. Chromatograms for C4b and C4b/Eap are shown in the *left panel*, while Coomassie-stained SDS-PAGE analysis of the peak fractions from each injection is shown in the *right panel*. Control lanes are designated as C, C4b; E, Eap; and M, m.w. marker. (B) The ability of untagged Eap, EapH1, and EapH2 to compete the AlphaScreen signal generated by myc-Eap and C4b biotin was assessed over a logarithmic dilution series. Although three independent trials were carried out, the data presented here are from single representative titrations. The smooth line indicates the outcome of fitting all points to a dose-response curve when competition was observed. Legend is *inset*. (C) Binding of Eap, EapH1, and EapH2 to an oriented C4b-biosensor surface. The peak signals achieved following injection stop for samples at 1 and 10 μM, done in triplicate, were normalized to the m.w. of their respective analyte proteins. Note that error bars are shown, but represent comparatively small variations due to the high precision of the assay system.

The modular architecture of the Eap protein raised questions as to whether a discrete combination of these domains is responsible for binding to C4b and, furthermore, whether that domain drives inhibition of CP/LP activity. To address these issues simultaneously, we overexpressed and purified a series of Eap fragments consisting of adjacent pairs of domains (i.e. Eap12, Eap23, and Eap34) as well as the individual Eap repeats themselves (i.e. Eap1, Eap2, Eap3, and Eap4) (**Fig. 2-4A**). Like EapH1 and EapH2, an equimolar mixture of the individual Eap repeats also did not compete the luminescence signal generated by myc-Eap binding to C4b biotin at concentrations up to 10 μM (**Fig. 2-4B**). Similarly, competition by Eap12 was detected only at the highest concentrations examined. By contrast, saturable binding of nearly equivalent affinity to Eap was observed in the same assay system for both Eap23 (K_d = 293 ± 38 nM) and Eap34 (K_d = 525 ± 65 nM) (**Fig. 2-4B**). Consistent with this, Eap23 and Eap34 both inhibited C5b-9 deposition via the CP and LP, although Eap34 did so at levels closer to Eap in both assays (**Fig. 2-4C**). In summary, the facts that 1) none of the individual Eap domains manifested clear C4b binding or inhibitory properties against either the CP or LP, 2) Eap12 bound C4b nearly 100-fold more weakly than Eap itself and failed to inhibit both the CP and LP on its own, and 3) Eap23 and Eap34 both bind C4b and inhibit the CP and LP indicate that domain Eap3 is necessary, but not sufficient for Eap binding to C4b and inhibition of the CP and LP.

Eap Blocks Binding of C2 to C4b by Interfering with the Initial C2b/C4b Interaction

Formation of the CP/LP C3 convertase is a stepwise process that starts with the deposition of surface-bound C4b. Although C4b has no enzymatic activity of its own, it serves as a molecular platform first for binding of C2 to yield the C4b/C2 proconvertase and then for C1s/MASP-dependent cleavage of C2 to generate a fully-active C4b/C2a convertase (81). We examined whether Eap binding to C4b would inhibit binding of C2 to C4b, and thus disrupt

formation of the C4b2 proconvertase. Indeed, C2 efficiently diminished the luminescence signal in the AlphaScreen assay generated by myc-Eap and C4b-biotin with an apparent IC_{50} of 460 ± 32 nM (**Fig. 2-5A**). The C2 proprotease is comprised of two functionally discrete regions. Whereas the larger C2a region houses its serine protease module, the smaller C2b fragment provides the molecular basis for its initial interaction with C4b (101, 102). We therefore tested whether Eap inhibition of C2 binding to C4b might arise from disrupting the C4b2b interaction using the same AlphaScreen assay system described above. Although C2b bound to C4b with ~7.6-fold lower affinity than full-length C2 (IC_{50} = 3.5 ± 0.6 μM), it still effectively competed with Eap for C4b binding (**Fig. 2-5A**). Together, these data show that Eap shares a common

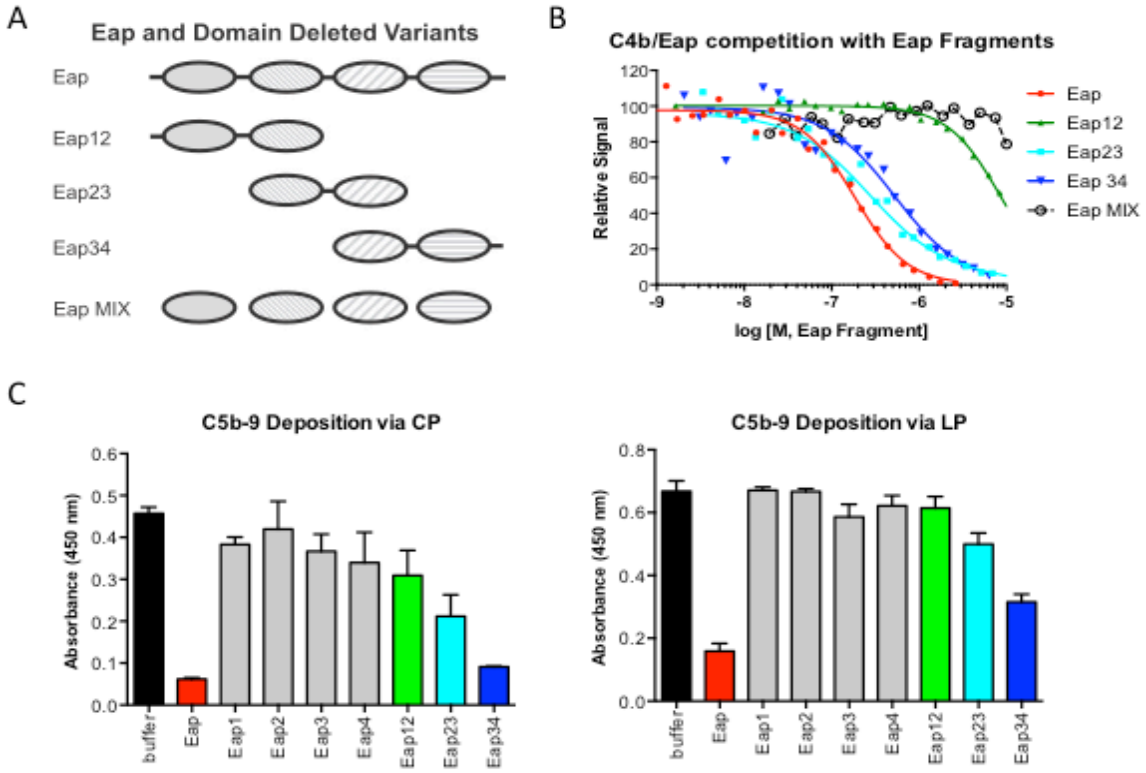

Figure 2-4. The third domain of Eap is necessary for C4b binding and inhibition of the CP/LP. (A) Diagram of full-length and domain deleted forms of Eap used to map functional sites within the Eap protein. (B) The ability of untagged Eap, Eap12, Eap23, Eap34, and an equimolar mixture of individual Eap domains (Eap MIX) to compete the AlphaScreen generated by myc-Eap and C4b biotin was assessed over a logarithmic dilution series. Whereas three independent trials were carried out, the data presented here are from single representative titrations. The smooth line indicates the outcome of fitting all points to a dose-response curve when competition was observed. Legend is *inset*. (C) The effect of including 1 μM Eap, or various truncations thereof, on C5b-9 deposition on ELISA plates coated with either CP (*left panel*)- or LP (*right panel*)-specific activators. 1% (v/v) NHS was used as a source of complement components. Error bars represent the mean ± SD of three independent experiments. Measures of statistical significance were determined by one-way ANOVA for the various Eap truncations versus buffer control alone. *$p \leq 0.05$, **$p \leq 0.01$, ****$p \leq 0.0001$. ns, not significant. Data in (C) and (D) collected from Suzan H.M. Rooijakkers lab.

binding site on C4b with C2 and, further, that this C4b site is also important for forming the initial interaction that gives rise to the CP/LP C3 pro-convertase, C4b/C2.

To test this inhibitory mechanism through an alternative approach, we devised an SPR strategy to investigate the outcome of increasing Eap concentrations on the ability of a C4b biotin surface to bind C2 (**Fig. 2-5B**). In this experiment, if C4b were capable of binding Eap and C2 independently of one another, then the sensorgrams characteristic of the specific concentrations for each analyte alone would be strictly additive. Injection of 200 nM C2 in the presence of Eap resulted in a diminished response from what would be expected from two independent analytes, however. When the residual C2 contribution to the SPR signal from six different observations was fit to a dose-response curve as a function of Eap concentration, we obtained an IC_{50} value of ~50 nM (**Fig. 2-5C**). Because this figure is in reasonably good agreement with the K_d of the C4b/Eap interaction (185 nM, as determined by AlphaScreen [**Fig. 2-3B**]), the outcome from this set of experiments provided an independent confirmation of the results presented in **Fig. 2-5A** above.

The requirement of Eap3 for both C4b binding (**Fig. 2-4B**) and inhibition of CP/LP activity (**Fig. 2-4C**) suggested that the ability to inhibit C4b2 binding should also be intrinsic to a minimal functional region of the Eap protein. To test this hypothesis, we established another AlphaScreen assay system where the ability of various ligands to inhibit the luminescence signal generated by myc-Eap34 binding to C4b biotin could be assessed quantitatively. Using this approach, we determined that full-length C2 likewise competed with Eap34 for a binding site on C4b with an apparent IC_{50} of 180 ± 31 nM (**Fig. 2-5D**). Although this apparent IC_{50} represents somewhat tighter binding than was observed for C2 competing the myc-Eap C4b biotin pair (460 ± 32 nM), the higher noise level inherent to this latter assay may have affected the accuracy of

fitting these data. Nevertheless, a repeat of the SPR competition assay, this time using Eap34 instead of full-length Eap, yielded similar results to those obtained previously (**Fig. 2-5E**). When the residual C2 contribution to the SPR signal from six different observations was fit to a dose-response curve as a function of Eap34 concentration, we obtained an IC_{50} value of ~870 nM (**Fig. 2-5F**). Again, this value is in good agreement with the K_d of the C4b/Eap34 interaction

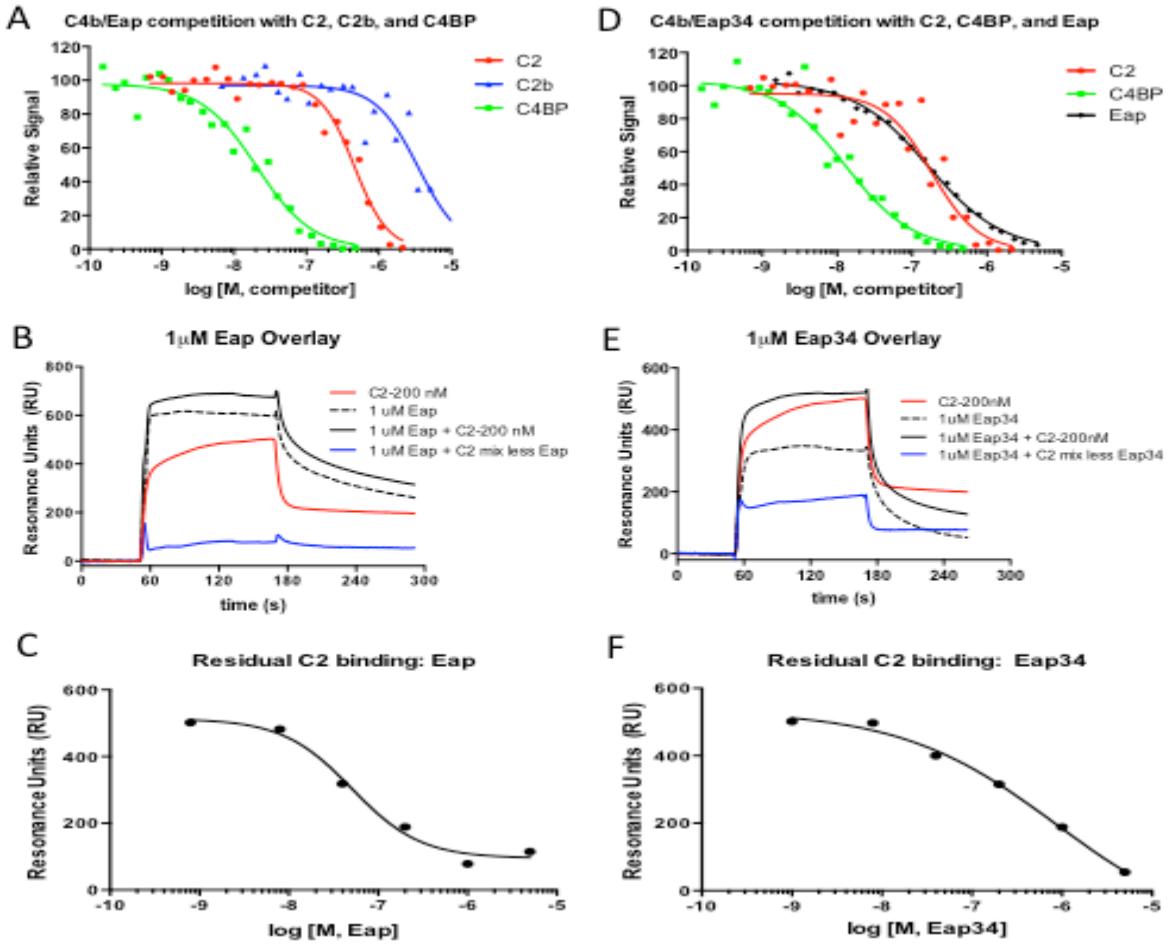

Figure 2-5. Eap binding inhibits the interaction of complement component C2 with C4b. (A) The ability of recombinant human C2, C2b, and C4BP to compete the AlphaScreen signal generated by myc-Eap and C4b biotin was assessed over a logarithmic dilution series. Whereas three independent trials were carried out, the data presented here are from a single representative titration. The smooth line indicates the outcome of fitting all points to a dose-response curve. (B) Representative data from a SPR competition experiment in which the effect of 1 μM Eap on the interaction of 200 nM C2 with a C4b biotin surface was examined. A legend showing the identity of each sensorgram is *inset*. The residual C2 binding in the presence of Eap is shown as a blue line, while the sensorgram for the same concentration of C2 in the absence of any Eap is shown as a red line. (C) Residual C2 binding in the presence of various concentrations of Eap fit to a dose-response curve (IC_{50} = 50 nM). (D) Identical experiment to (A), with the exception that the ability of recombinant human C2, C4BP, and Eap to compete the AlphaScreen signal generated by myc-Eap34 and C4b biotin was assessed. (E) Identical experiment to (B), with the exception that Eap34 was used as the competitor instead of Eap. The residual C2 binding in the presence of Eap34 is shown as a blue, while the sensorgram for the same concentration of C2 is shown as a red line. (F) Residual C2 binding in the presence of various concentrations of Eap34 fit to a dose–response curve (IC_{50} = 870 nM).

(525 nM, as determined by AlphaScreen [**Fig. 2-4B**]). Thus, the observation that Eap34 on its own competes with C2 for C4b binding demonstrates that disruption of the initial proconvertase assembly event is necessary for Eap-mediated inhibition of the CP/LP.

The Eap Binding Site on C4b Represents a Functional Hotspot within the CP/LP

The CP/LP C3 convertase is only transiently stable when formed and decays with a half-life of ~60 s at 37 °C (103). This rate of spontaneous decay is greatly enhanced in the presence C4BP, which irreversibly dissociates C2a from its C4b scaffold and in addition serves as a cofactor for FI-mediated degradation of C4b to iC4b and C4c. Because the results presented in this work demonstrated that Eap effectively inhibits C4b2 binding, we examined whether Eap might also disrupt the interaction of C4BP with C4b. Through use of the AlphaScreen assay, we found that C4BP also competed with Eap for binding to C4b (**Fig. 2-5A**). Non-linear curve fitting of the competition data revealed an apparent IC_{50} of 21 ± 3 nM for the C4b/C4BP interaction, which represents ~9-fold tighter binding when compared with the C4b/Eap interaction (**Fig. 2-3B**). This suggests that Eap would not disrupt the inhibitory function of C4BP when both are present in equimolar concentrations. We obtained a similar result when C4BP was used to compete the luminescence signal generated by myc-Eap34 binding C4b biotin (**Fig. 2-5B**), where non-linear curve fitting revealed an apparent IC_{50} of 13 ± 2 nM. It has to be noted, however, that this IC_{50} value reflects only the apparent affinity, and does not represent that of the individual C4b binding sites present within the polyvalent C4BP assembly (104).

Because Eap binds C4b at a similar site as C4BP, we tested whether Eap itself might display intrinsic cofactor activity to stimulate FI-mediated proteolysis of C4b. When purified C4b was incubated with both C4BP and FI, we were able to show rapid degradation of C4b into iC4b and then C4c, as judged by SDS-PAGE and liquid chromatograpy-coupled tandem mass

spectrometry of tryptic peptides derived from various bands on gel (**Supplemental Fig. 2-3A, *top panel*, *left***). However, substitution of Eap for C4bBP in an otherwise identical assay provided no evidence for proteolysis of C4b by FI (**Supplemental Fig. 2-3A, *top panel*, *right***). Thus, while Eap has no intrinsic FI cofactor activity, it shares a C4b binding site with multiple

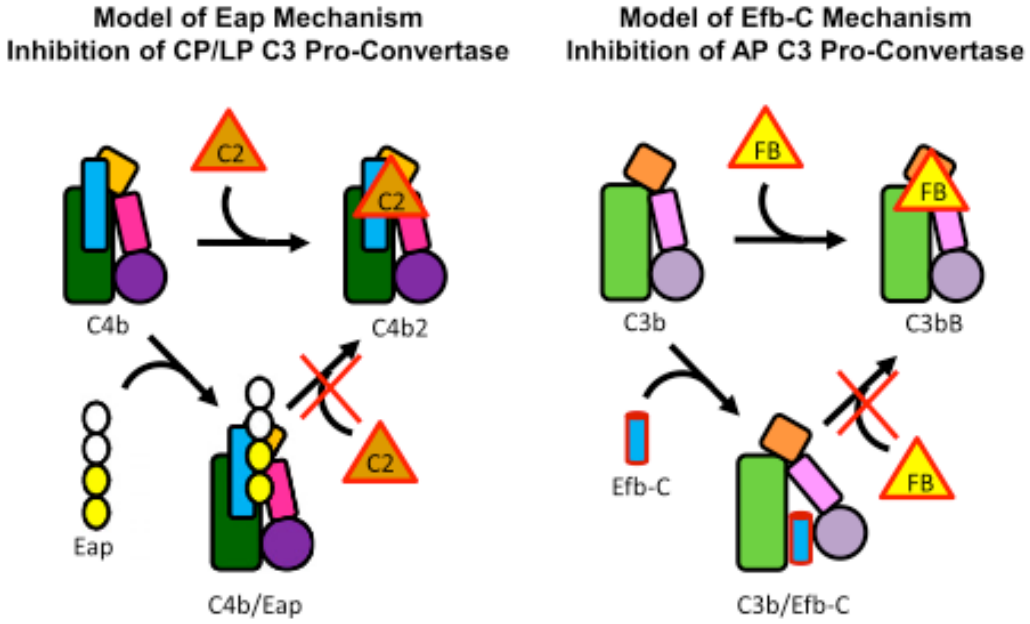

Figure 2-6. Proposed mechanism for Eap-mediated inhibition of the CP/LP and its similarities to the S. aureus AP inhibitor, Efb-C. The overall structural similarities between C4b and C3b are represented by the similar shapes of their cartoon representations. The shaded green rectangle represents the macroglobulin-like core, the orange square the C345C domain, the small pink rectangle the CUB domain, and filled circle the thioester-containing domain (i.e., C4d and C3d). The thin blue rectangle represents the γ-chain unique to C4/b. The inhibitor Eap is shown in the *left panel* with two domains filled in yellow to represent the domains 3 and 4 active sites, as described in Figs. 4 and 5. The inhibitor Efb-C is shown as a blue cylinder in the *right panel*. Efb–C binding to the C3d domain (62) and stabilization of an open, inactive conformation of C3b that is unable to bind factor B (64) are depicted by reorientation of the CUB-TED region relative to the macroglobulin-like core of C3b.

factors critical to the function and regulation of the CP/LP. We therefore propose that the Eap binding site on C4b represents a functional hotspot within the CP/LP, and that this hotspot is analogous to what we previously described for the binding site of the SCIN family of AP inhibitors on C3b (57-59, 95).

Discussion

Although a number of recent studies have described unique mechanisms deployed by *S. aureus* to disrupt and evade human immunity, a large majority of these have focused on strategies that specifically target components within the complement AP (e.g., C3b). In this

study, however, we used a biochemical screening strategy to identify *S. aureus* Eap as an inhibitor of both the CP and LP. Inhibition of the CP/LP is specific to Eap, since this activity is not found in either of its closest structural homologs, EapH1 and EapH2, that also adopt the β-grasp fold characteristic of EAP domains (1, 105). Eap-mediated inhibition of the CP and LP occurs directly, because it arises from Eap forming a nanomolar affinity complex with a shared component of both pathways, C4b. Thus, instead of expressing specific inhibitors for the CP and LP separately, our results show that *S. aureus* simultaneously disrupts the two most potent complement initiation routes via a single protein, Eap. On this basis, we believe that Eap defines both a novel mechanism of staphylococcal immune evasion and a new class of complement-regulatory proteins.

A number of other significant bacterial and fungal pathogens have also been shown to subvert the activity of CP and LP [Reviewed in (83, 106)]. However, nearly all of these organisms evade the CP and LP via adsorption of the naturally occurring CP/LP regulator, C4BP, to their surface via expression of specific C4BP binding proteins. This is conceptually similar to evasion of the AP through cell-surface adsorption of factor H (FH) via FH-binding proteins, which is very likely the single most widely distributed complement evasion strategy among pathogens (83, 106). Interestingly, the fact that Eap functions not by binding to a naturally occurring regulator (i.e., C4BP), but through the altogether distinct mechanism of blocking initial stages of CP/LP C3 pro-convertase assembly, mirrors what we have previously described for *S. aureus* evasion of the AP [Reviewed in (58)]. In this work, expression and secretion of factors such as SCIN-A, SCIN-B/-C, Efb, and Ehp/Ecb has been demonstrated to interfere with one or more of the molecular events required to assemble and/or regulate the fully active AP C3 convertase, C3bBb. For whatever reason, it seems that *S. aureus* has taken a

unique evolutionary path that has led it to produce multiple inhibitors that act by binding directly to either C3b or C4b, which themselves serve as essential scaffolds for assembly of all C3 and C5 convertases. Although the possibility that *S. aureus* also absorbs native host regulators FH (107) and C4bBP (108) cannot be discounted, an overwhelming amount of structural, biochemical, functional, and immunological evidence in the literature strongly suggests that direct inhibition of convertase assembly, dynamics, and function, rather than indirect disruption via adsorption of fluid-phase regulators, is of paramount importance to *S. aureus* pathogenesis.

Our functional data demonstrate that Eap blocks both the CP and LP at the level of C3 activation. This inhibition arises from impaired formation of the CP/LP C3 proconvertase, C4b2, which would subsequently reduce formation of the active CP/LP C3 convertase, C4b2a. The mechanistic basis of CP/LP inhibition by Eap therefore appears very similar to AP inhibition by Efb-C, which itself binds to C3b and reduces formation of the AP C3 proconvertase, C3b/B, by nearly 80% (64) (**Fig. 2-6**). An important distinction between Eap and Efb-C, however, is that the latter has been shown to act in an allosteric manner (64). Our observation of direct competition for C4b binding between Eap and both C2 and C2b seems to favor a purely steric mechanism for Eap inhibition of CP/LP C3 convertase formation, although the possibility of Eap-dependent 'action-at-a-distance' type effects on C4b cannot be dismissed without significantly more structural insight into these interactions. Still, the fact that Eap also blocks the C4b/C4BP interaction strongly suggests that the Eap binding site on C4b constitutes a functional hot spot for CP/LP C3 convertase formation, dynamics, and function. This raises some attractive conceptual analogies between Eap and the SCIN family of C3b-binding AP C3 convertase inhibitors (58, 59, 95). Furthermore, it also suggests that effective targeting of these functional

hot spots that exist in various host response pathways might be a central theme behind pathogen-specific evolution of innate immune evasion mechanisms.

Given its potent effects on the CP and LP, it is perhaps not surprising that Eap has been shown to promote staphylococcal virulence in rodent models of both acute peritonitis (109), as well as chronic arthritis, osteomyelitis, and abscess formation (110). Although the precise contributions of the CP and LP remain to be fully evaluated in each of these experimental systems, the consistent requirement of Eap for maximal levels of staphylococcal virulence in such studies is difficult to ignore. Moreover, the discovery that patients with demonstrated *S. aureus* infections present with high titers of anti-Eap Abs (111), and that their titers of anti-Eap IgG correlate with the severity of infection (111), strongly suggests that Eap inhibition of the CP/LP is relevant to human disease as well. Along these lines, we have recently made the unexpected observation that all staphylococcal EAP domain-containing proteins (i.e., Eap, EapH1, and EapH2) are capable of high-affinity, noncovalent inhibition the innate immune serine proteases neutrophil elastase, cathepsin G, and proteinase-3 (75). These so-called neutrophil serine proteases (NSPs), which are stored in azurophilic granules and released upon neutrophil activation, serve a number of crucial roles in both neutrophil effector functions and in the innate cellular response against invading microorganisms such as *S. aureus* (112). The fact that complement activity is based upon a series of site-specific proteolyses seems to suggest that EAP domain-mediated inhibition of NSPs must share basic molecular-level features with inhibition of the CP/LP by Eap. However, our observations that 1) CP/LP inhibition is specific to Eap, and not intrinsic to all EAP domains [**Figs. 2-1, 2-2**], 2) this inhibition is based upon the unique ability of Eap to bind C4b [**Figs. 2-3, 2-4**], and 3) Eap blocks, rather than promotes recruitment of the C2 proprotease to C4b [**Fig. 2-5**], as might otherwise be expected for a high-

affinity protease inhibitor (75), argue that the structural basis for Eap's effects on the CP/LP must be altogether distinct from EAP domain inhibition of NSPs. Understanding the nature of these distinctions at the structural level should therefore prove to be a very informative endeavor.

Although much remains to be learned in that regard, it is already abundantly clear that a number of debilitating and potentially lethal human diseases have been linked to either acute or chronic overactivation of the complement CP and/or LP (113-115). Among these are ischemia/reperfusion injuries, rheumatoid arthritis, systemic lupus erythematosus, multiple sclerosis, and even Alzheimer's disease. Since many of these diseases are only poorly managed by current therapeutic regimens, our discovery of Eap as a potent CP/LP inhibitor raises the possibility that improved treatment of these conditions might come through further detailed study of Eap, its molecular interactions, and its ability to specifically attenuate CP/LP activity in vivo. Because high levels of anti-Eap Abs are found in even healthy persons (111), direct use of Eap as a therapeutic is unlikely, due to greatly increased risk of immune complex disease. Thus, future work aimed at discovering either non-immunogenic peptides, peptidomimetics, or even small molecules that retain Eap-like inhibitory activities on the CP/LP will be necessary to exploit Eap's promise within these areas.

Acknowledgements

We thank Dr. Edimara S. Reis, Dr. Apostolia Tzekou and Ms. Antigonia Ulndreaj for their assistance in the functional analysis of Eap.

This work was supported by U.S. National Institutes of Health grants AI071028 to B.V.G., and AI068730, AI030040, and AI097805 to J.D.L, and by a Vidi grant from the Netherlands Organization for Scientific Research (NWO-Vidi, #91711379) to S.H.M.R.

Supplemental Figures

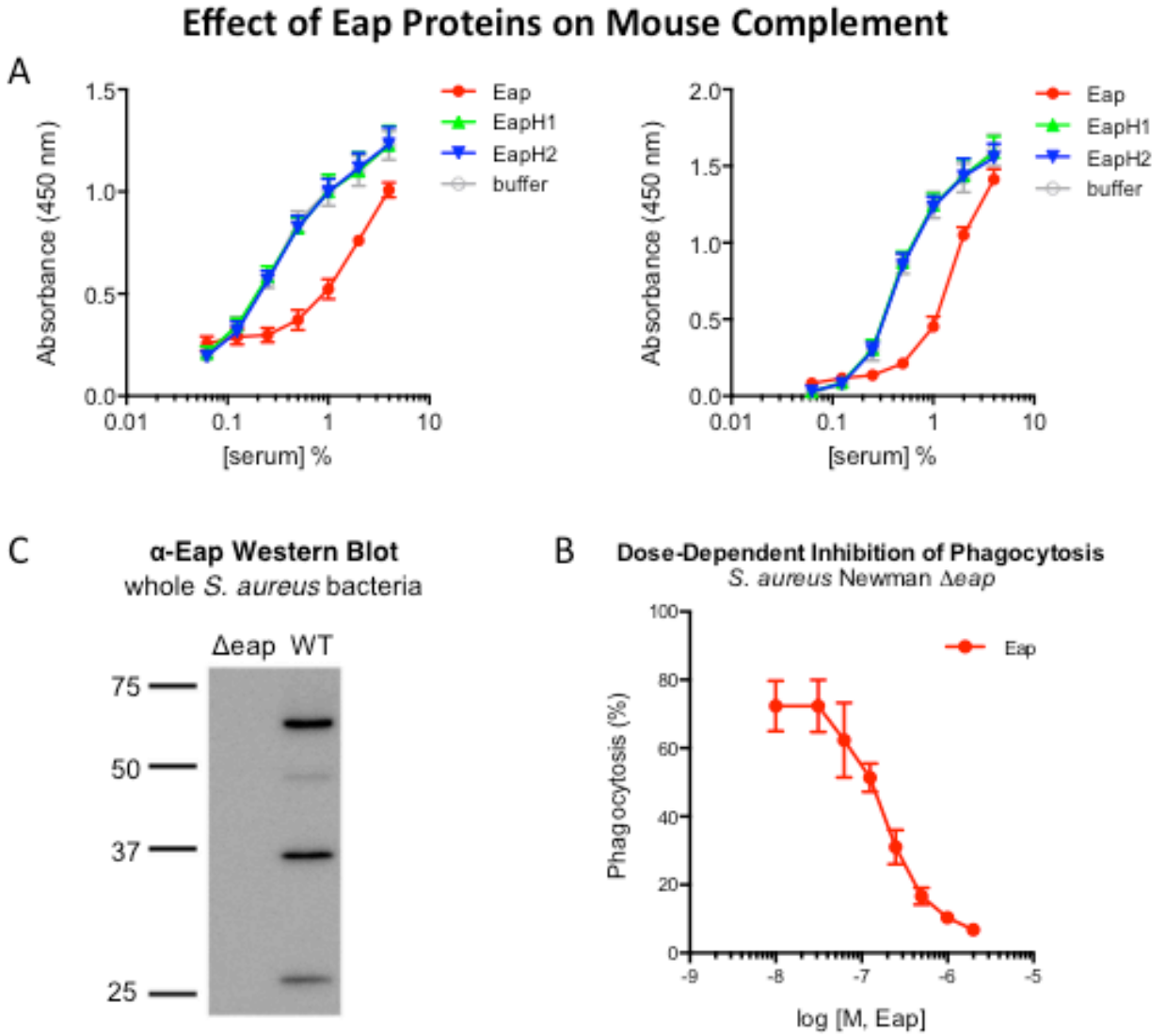

Supplemental Figure 2-1. Supporting Information on Eap Inhibition of CP/LP and Phagocytosis. (A) Eap inhibits the murine CP and LP. The effect of 1 μM Eap, EapH1, or EapH2 on CP (*left*) and LP-mediated (*right*) complement activation was measured across a dilution series of serum concentrations. Activation was detected as C3b deposition on an ELISA plate surface. Legends are *inset*. (B) Eap is present on the surface of cells of a WT but not a Δ*eap S. aureus* strain. Bacteria were grown to stationary phase in liquid culture and harvested by centrifugation. After washing, Laemmli sample buffer with DTT was added to an equal volume of cell suspension and the samples were analyzed on a 12.5% (w/v) glycine polyacrylamide gel. Eap was detected by Western blot with 1:20.000 diluted rabbit-α-Eap serum and an HRP-labeled secondary antibody. A control experiment was performed to ensure that the same amount of bacteria were present in each sample by plating serial dilutions of each sample immediately prior to adding the Laemmli buffer. Note that proteolytic degradation of Eap into various combinations of adjacent subdomains has been reporter elsewhere, and is due to protease sensitivity of the interdomain linkers (27). (C) Phagocytosis of *S. aureus* Newman Δ*eap* using 1% (v/v) NHS as a source of complement components and the indicated concentrations of Eap. Data collected from John D. Lambris lab.

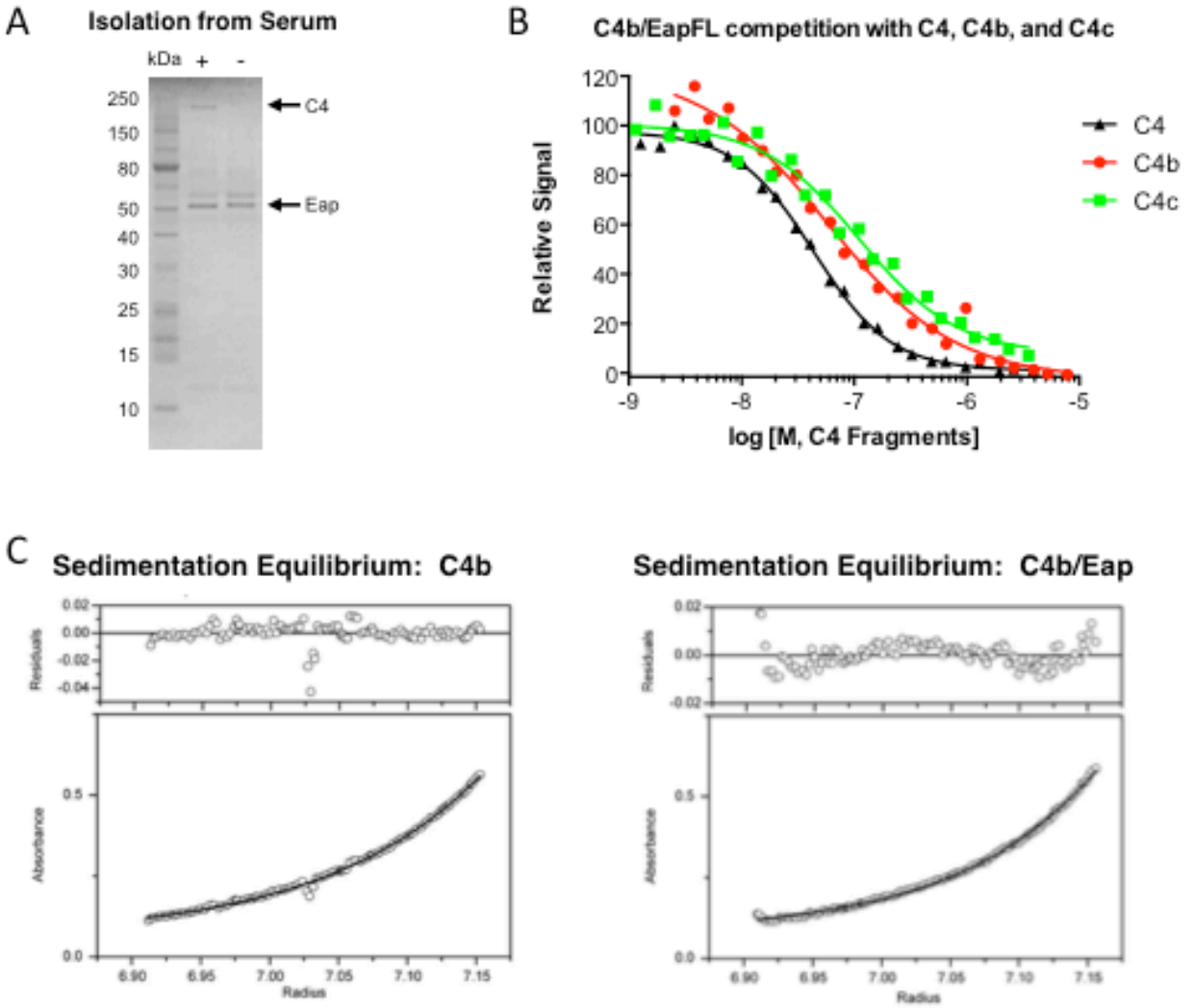

Supplemental Figure 2-2. Supporting Information on Eap Binding to C4 and its Derivatives. (A) Affinity isolation of C4 from human serum. Biotinylated Eap was used as an affinity reagent to identify potential binding partners in both normal and C4-depleted human serum. Following capture of Eap-biotin by magnetic streptavidin beads and a series of washes, the bound proteins in both samples were separated by SDS- PAGE under non-reducing conditions. A band of approximately 200 kDa was found in the lane corresponding to normal but no C4-depeleted serum, strongly suggesting that Eap binds to native C4. (B) The ability of C4, C4b, and C4c to compete the AlphaScreen signal generated by myc-Eap and C4b-biotin was assessed over a logarithmic dilution series. While three independent trials were carried out, the data presented here are from a single representative titration. The smooth line indicates the outcome of fitting all points to a dose-response curve. (C) Sedimentation equilibrium analytical ultracentrifugation analysis of C4b and C4b/Eap. Experimental data were obtained as described in *Materials & Methods* for C4b (*left panel*) and an equimolar mixture of C4b/Eap (*right panel*). Equilibrium profiles were fit to a single particle model to yield the observed molecular weight for both C4b (268 kDa) and C4b/Eap (308 kDa). The top plots in both panels show the random residuals for the respective fits. Analytical ultracentrifugation experiments [(C) and (D)] done with contributions from Michal Zolkiewski.

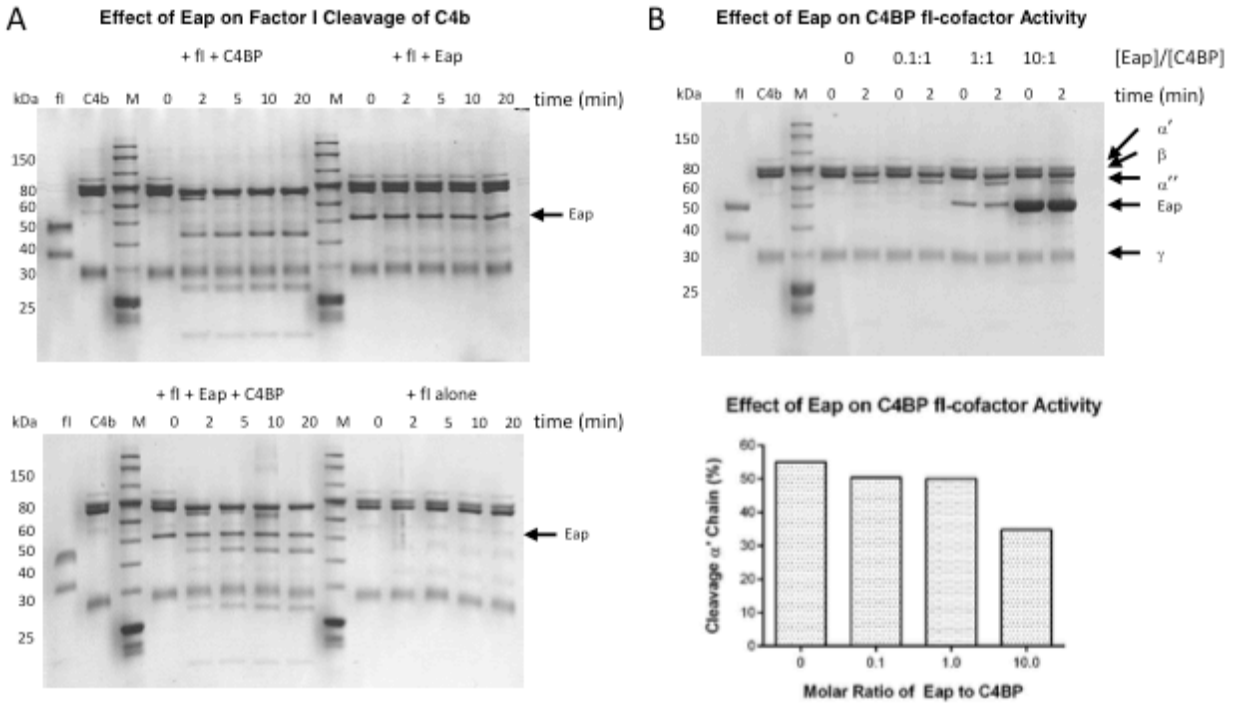

Supplemental Figure 2-3. Eap Lacks FI-cofactor Activity and Only Weakly Impacts C4BP Cofactor Activity. (A) The effect(s) of including Eap, C4BP, both, or neither on FI-mediated proteolysis of C4b was investigated. Aliquots of each reaction series (indicated) were withdrawn over the course of 20 min and the proteins were analyzed by SDS-PAGE. (B) The effect of varying the molar ratio of Eap to C4BP on FI-mediated proteolysis of C4b was investigated. Aliquots of each reaction series (indicated) were withdrawn at 0 and 2 min, and the proteins were analyzed by SDS-PAGE. The identity of various bands, as determined by mass-spectrometry, is indicated. The ability of Eap to inhibit C4BP-dependent cleavage of C4b by FI was quantified by densitometry of the α' chain bands before and after the reaction. Addition of equimolar concentrations of both C4BP and Eap to this assay appeared to slow the rate of FI proteolysis (A, *bottom panel left*). This likely resulted from competition between Eap and C4BP for the same binding site on C4b, which consequently reduced the effective concentration of substrate available to FI since Eap does not have intrinsic cofactor activity (A, *top panel right*). To explore the functional consequences of Eap competition with C4BP in more detail, we carried out a set of studies wherein the molar ratio of Eap to C4BP was varied between 0, 0.1, 1.0, and 10 (B, *top panel*). Significant inhibition of FI-mediated proteolysis appeared to occur only when Eap was present at 10-fold higher concentration than C4BP (B, *bottom panel*). The requirement of such a high level of Eap to disrupt C4BP activity was most likely due to the weaker affinity of Eap for C4b and its lack of polyvalency, as it forms equimolar complexes with C4b. Thus, while Eap competes with C4BP for the same recognition site on C4b, it has no cofactor activity of its own, nor does competition with C4BP appear to be essential to its effects on the CP/LP of complement.

Chapter 3 - The structural basis for inhibition of the classical and lectin complement pathways by *S. aureus* extracellular adherence protein

Jordan L. Woehl[1], Kasra X. Ramyar[1], Benjamin B. Katz[1], John K. Walker[2], and Brian V. Geisbrecht

[1]Department of Biochemistry & Molecular Biophysics;
Kansas State University, Manhattan, KS, USA
[2]Department of Pharmacology and Physiology;
St. Louis University School of Medicine, St. Louis, MO, USA

Manuscript submitted to *Protein Science*

Abstract

The extracellular adherence protein (Eap) plays a crucial role in pathogenesis and survival of *Staphylococcus aureus* by inhibiting the classical and lectin pathways of complement. We have previously shown that Eap binds with nanomolar affinity to complement C4b and disrupts the initial interaction between C4b and C2, thereby inhibiting formation of the classical and lectin pathway C3 pro-convertase. Although an underlying mechanism has been identified, the structural basis for Eap binding to C4b is poorly understood. Here, we show that Eap domains 3 and 4 each contain a low-affinity, but saturable binding site for C4b. Taking advantage of the high lysine content of Eap, we used a zero-length crosslinking approach to map the Eap binding site to both the α'- and γ-chains of C4b. We also probed the C4b/Eap interface through a chemical footprinting approach involving lysine modification, proteolytic digestion, and mass spectrometry. This identified seven lysines in Eap that undergo changes in solvent exposure upon C4b binding. We found that simultaneous mutation of these lysines to either alanine or glutamate diminished C4b binding and complement inhibition by Eap. Together, our results provide insight into Eap recognition of C4b, and suggest that the repeating domains that comprise Eap are capable of multiple ligand-binding modes.

Introduction

The complement system fulfills an essential role in initiating the inflammatory response, and in clearance of foreign, diseased, or damaged cells (Reviewed in (81)). Though it is comprised of nearly 30 proteins, the complement system can be divided conceptually into two distinct stages that consist of (i) initiation, amplification, and opsonization followed by (ii) assembly of the terminal complement complex and effector function. The initial stage of complement activity begins with ligand binding by a series of pattern recognition receptors and

leads to assembly of multi-subunit, surface-associated serine proteases known as C3 convertases. Depending upon the specific biochemical stimuli, which initiate complement activation, the surface-bound C3 convertases that result may exist in two different isoforms. The so-called Classical (CP) and Lectin (LP) Pathway C3 convertase is comprised of the activated fragment of complement C4 (i.e. C4b) bound to the activated form of complement C2 (i.e. C4b2a). Proteolysis of the central complement component C3 by C4b2a leads to generation of C3b; this surface-linked product triggers assembly of the alternative pathway (AP) C3 convertase, which is comprised of C3b bound to the activated form of fB (i.e. C3bBb). The self-amplifying effect of the AP C3 convertase fosters extensive opsonization of target surfaces with C3b, leads to activation of complement component C5, and drives downstream events that contribute to the effector functions of complement. Chief among these are assembly of the terminal complement complex (i.e. C5b-9) and recruitment of inflammatory cells such as neutrophils to the site of complement activation.

Many successful pathogenic and/or parasitic species are capable of disrupting or escaping the immune response of their hosts. Though these so-called immune evasion strategies are highly diversified, their specific modes of action and overall functional outcome are ultimately dictated by the route of infection and tissue tropism of the invading organism in question. As a prototypic endovascular pathogen, the Gram-positive bacterium *Staphylococcus aureus* secretes multiple inhibitory proteins that act on the central innate immune events of opsonization, recruitment of neutrophils, and phagocytosis (19, 83, 116). Because the complement system plays a vital role in each of these processes, there appears to have been heavy selective pressure on *S. aureus* to evolve efficient means for interfering with complement activity. Indeed, studies from throughout the last decade have identified and characterized over a dozen individual complement evasion

proteins from *S. aureus*. On balance, this work suggests that the complement evasion arsenal of *S. aureus* is likely the most diverse of any pathogen examined.

While the number of complement inhibitors expressed by *S. aureus* is noteworthy, the unique mechanisms of action employed by these proteins have also garnered attention. In this regard, *S. aureus* heavily targets formation, function, and stability of the surface-bound, multi-subunit C3 and C5 convertases, which drive amplification of the complement response and opsonization of the bacterial cell (40, 64, 85, 86). We recently characterized the *S. aureus* Extracellular Adherence Protein (Eap) as a novel inhibitor of both the classical (CP) and lectin (LP) complement pathways (40). Eap binds to complement component C4b and thereby prevents binding of the pro-protease C2 to C4b. Since formation of the CP/LP C3 pro-convertase complex (i.e. C4b2) is required for forming the fully-active C3 convertase (i.e. C4b2a) that the CP and LP share, Eap is capable of simultaneously disrupting the two most potent routes for initiating complement activity. In doing so, Eap not only prevents opsonization of the *S. aureus* cell by C3b, it also blocks both phagocytosis and killing of *S. aureus* by neutrophils.

Eap is secreted by nearly all strains of *S. aureus*, though it is found in isoforms that vary in the number of ~100 residue EAP repeats contained within the polypeptide (1, 98). Domain deletion studies on the four-domain isoform of Eap from *S. aureus* strain Mu50 have demonstrated that the C4b-binding and the CP/LP inhibitory activity of Eap lie within its two C terminal-most repeats (40). Whereas full-length Eap binds C4b with low-nanomolar affinity (K_D=185 nM), a truncated form of the protein consisting of domains 3 and 4 (Eap34) binds only ~2.8-fold more weakly (K_D=525 nM). Importantly, inclusion of 1 μM Eap34 in either a CP or LP-specific ELISA assay inhibits formation of the terminal complement complex similarly to full-length Eap. By contrast, Eap domains 1 and 2 (Eap12) bind C4b weakly (K_D ~10 μM) and

inhibit CP and LP activity to only a minor extent (40). While these results strongly suggest that there is specificity for C4b binding within the individual domains of the Eap protein, the structural basis for this specificity remains undefined.

The genome of *S. aureus* strain Mu50 contains three unique coding sequences (*eap*, *eaph1*, and *eaph2*) for proteins that adopt the EAP fold. Eap itself is comprised of a tandem array of four non-identical EAP domains, while both EapH1 and EapH2 consist of a single domain, giving rise to a total of six unique EAP domains expressed by *S. aureus* Mu50 (1, 75). Although EAP domains share a significant level of structural identity as a group (1) they are much more divergent at the sequence level when compared to one another (26-83% pairwise identity among the six). Despite this diversity, we recently discovered that recombinant forms of each individual EAP domain in isolation can act as a potent and selective inhibitor of neutrophil serine proteases (NSPs), as typified by neutrophil elastase (NE) (75). Our subsequent crystal structure of NE bound to EapH1 revealed that the inhibitory site in EapH1 is comprised of a pentagon-shaped surface in the EapH1 tertiary structure (75), and which is formed from two separate stretches of amino acids that are separated by more than 20 residues in the EapH1 sequence. The regions of EapH1 that comprise its NE-binding site are not highly conserved among other EAP domains (**Fig. 3-1A**). This not only raised questions as to how the remaining EAP domains interact with NSPs, it also implied that the NE/EapH1 structure on its own would provide little insight into C4b binding by Eap. Furthermore, these observations led to the hypothesis that EAP domains as a whole may be capable of interacting with their ligands through multiple distinct binding modes.

To investigate these issues in greater detail, we developed a combinatorial strategy of zero-length crosslinking, foot-printing by mass spectrometry, site directed mutagenesis, and

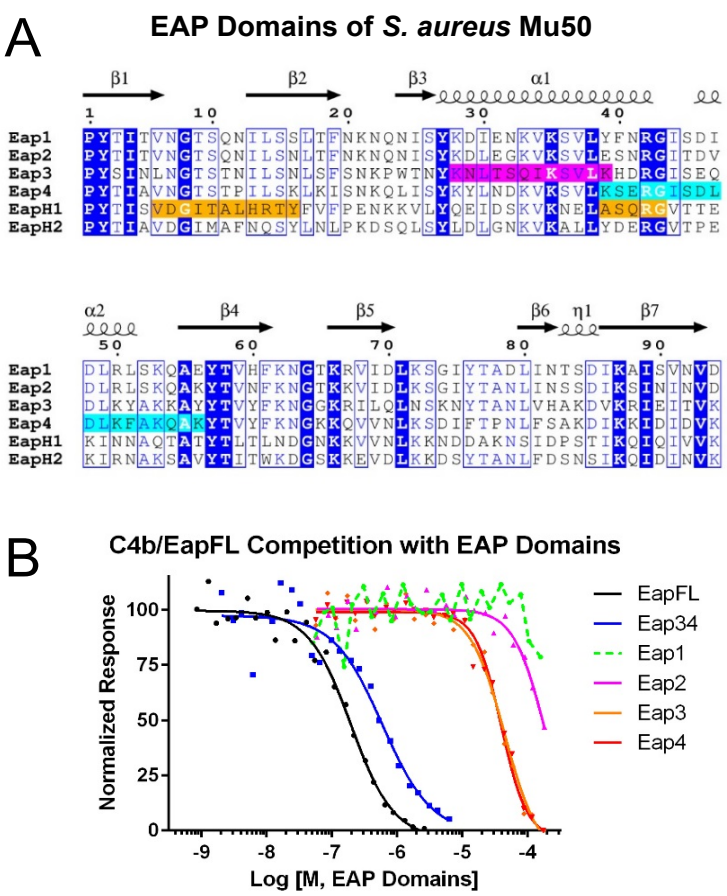

Figure 3-1. Domains Eap3 and Eap4 of the Extracellular Adherence Protein from *S. aureus* Mu50 Each Contain a C4b-binding Site. (A) Sequence alignment of the four EAP repeats from *S. aureus* Mu50, along with the single-domain EAP proteins, EapH1 and EapH2. Invariant positions are depicted in inverse blue typeface, while positions conserved in at least 4 of 6 sequences are drawn inside blue boxes. The secondary structure elements for a canonical EAP domain are shown above the sequence, and are derived from the 1.35 Å resolution structure of Eap2 (PDB Accession Code 1YN3 (1)). EapH1 positions that comprise the NE-binding site in the NE/EapH1 co-crystal structure (PDB Accession Code 4NZL (75)) are shaded orange. Regions in Eap3 and Eap4 spanning the lysines which exhibit a >50% change in solvent accessibility in the presence of C4b are shaded magenta and cyan, respectively. (B) The ability of untagged Eap full-length (EapFL), Eap34, and individual Eap repeats to compete the AlphaScreen signal generated by myc-EapFL and C4b-biotin was assessed over a logarithmic dilution series. Data presented here are taken from a representative trial of at least three independent experiments. Legend is inset.

functional assays to obtain structural insights into C4b/Eap binding. In this manuscript, we present the outcome of this series of experiments which demonstrate the importance of key lysine residues in Eap domains 3 and 4 in mediating an interaction with the C4b α'- and γ-chains. We also present a model for the C4b/Eap34 complex that is consistent with the experimental restraints identified during this work, as well as a recently published solution analysis of the C4b2 complex (117). Together, these data provide a physical basis for understanding the previously described competition between Eap and C2 for binding to C4b (40). This study not only expands our understanding of Eap's impact on formation of the CP/LP C3 pro-convertase, it broadens our appreciation of the structure/function relationships of EAP domains as well.

Results

The Eap3 and Eap4 Domains Each Contain a Complement Component C4b Binding Site and Inhibit the Classical and Lectin Pathways – We have previously shown that both full-length Eap and Eap34 display dose-dependent competition of a luminescence signal generated via site-specifically biotinylated C4b binding to c-myc epitope-tagged Eap (40). In that same study, we observed that an equimolar mixture of the four individual domains from *S. aureus* Mu50 Eap failed to compete in a similar fashion even at concentrations up to 10 μM (i.e. 2.5 μM each domain). Because linking two weakly binding individual ligands into a single larger molecule can provide an increase in apparent affinity, we decided to quantitatively assess the C4b-binding affinities of the individual domains of Eap in isolation. Using the competition-based binding assay described above (**Fig. 3-1B**), we found that both Eap3 and Eap4 bound C4b with a K_D value of ~40 μM. While this value is nearly two orders of magnitude weaker than that of Eap34 (K_D=525 nM) (40), both Eap3 and Eap4 were nevertheless able to compete with full length-Eap for C4b binding, in a dose-dependent, and saturable manner. Furthermore, we observed substantially weaker/no competition when either Eap1 or Eap2 were used in this assay, which indicated that the competitive effect was specific for Eap3 and Eap4.

Binding to C4b is necessary for Eap to inhibit formation of the CP/LP pro-C3 convertase and thereby block CP/LP activity (40). Since our previous study examined the activity of various Eap truncations at a fixed concentration of both inhibitor (i.e. 1 μM) and serum (i.e. 1% (v/v) NHS), we decided to test whether domain-deleted forms of Eap also exhibited dose-dependent inhibition of the LP using a fixed concentration of serum. Consistent with our previous results, Eap34 displayed IC_{50} values closest to full-length Eap in ELISA-based assays designed to measure the deposition of either C3b (160 vs 70 nM, respectively) or C5b-9 (225 vs 75 nM,

respectively) under conditions specific for activating the LP (**Fig. 3-2A**). Likewise, we found that the individual domains of Mu50 Eap inhibited the activity of the LP (**Fig. 3-2B**), albeit at much higher concentrations than required for either the full-length protein or Eap34. Nevertheless, the activity of the individual domains in this assay was consistent with their affinities for C4b (**Fig. 3-1B**), as both Eap3 and Eap4 blocked LP activity with IC_{50} values of ~10 μM. Together, these studies on individual EAP domains demonstrated that both Eap3 and Eap4 contain a specific C4b-binding site that is capable of mediating inhibition of the LP.

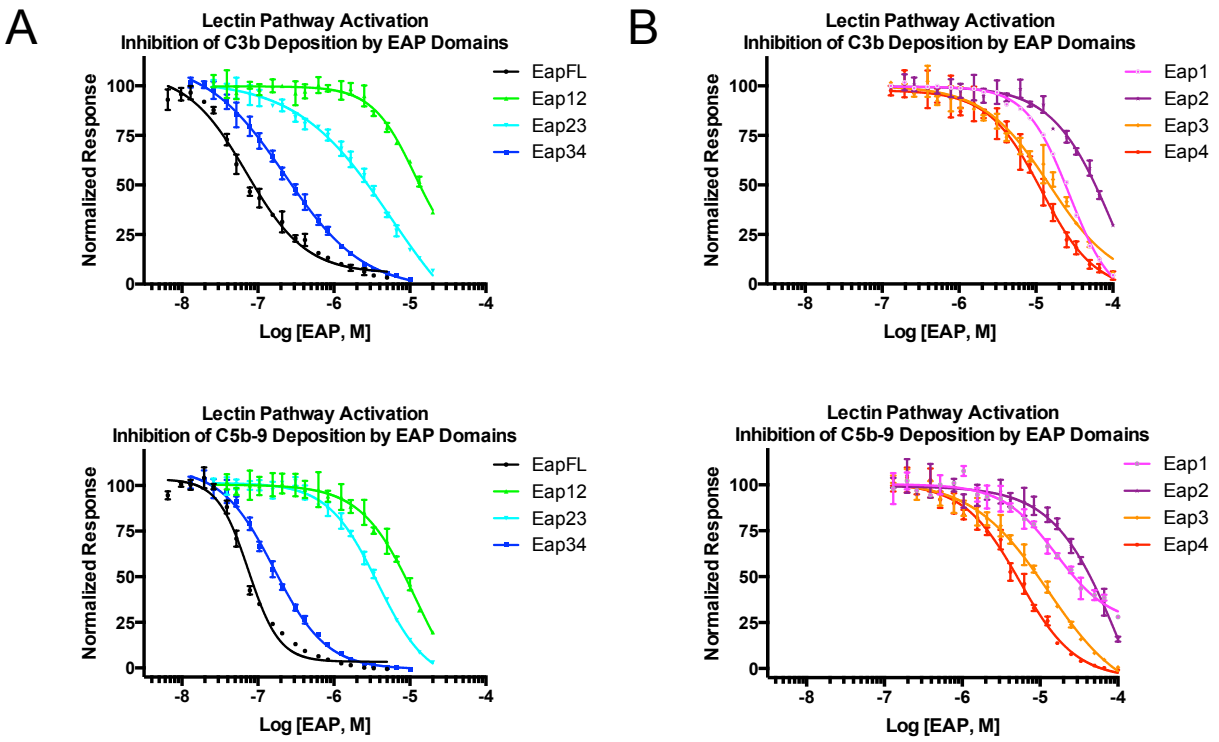

Figure 3-2. Domains Eap3 and Eap4 are Sufficient to Inhibit the Lectin Pathway of Complement. Lectin pathway complement activity was assessed over a logarithmic dilution series of various Eap proteins. 1% (v/v) NHS was used as a source of complement components, and each assay point was repeated in triplicate prior to fitting each series to a dose-response curve. Legends are inset. (A) Lectin pathway activity in the presence full-length Eap, Eap12, Eap23, or Eap34 was assessed by ELISA specific for either C3b (top panel) or C5b-9 (bottom panel). (B) Lectin pathway activity in the presence of Eap1, Eap2, Eap3, or Eap4 was assessed by ELISA specific for either C3b (top panel) or C5b-9 (bottom panel).

Eap34 Binds to the α'- and γ-Chains of C4b – While we previously established that both full-length Eap and Eap34 inhibit C2 binding to C4b (40), the structural basis for this activity remains unknown because the Eap binding site on C4b is undefined. C4b is comprised of three distinct polypeptides that assemble into a disulfide-linked heterotrimer. The identities of these chains are α' (75.5 kDa, pI=4.99), β (71.6 kDa, pI=8.69), and γ (33.1 kDa, pI=6.37), and they are readily resolved by SDS-PAGE when samples are prepared under reducing conditions. Furthermore, the amino acid sequence of *S. aureus* Mu50 Eap is noteworthy for its high lysine content (~15%, or 68 of 446 residues in the predicted full-length protein). Since these lysines are distributed roughly equally throughout the Eap protein (**Fig. 3-1A**), we predicted that lysine-specific chemistries might provide a relatively high level of positional accuracy for mapping the Eap binding site on C4b.

To test this idea, we utilized a 'zero-length' crosslinking strategy that is highly selective for amines and carboxylates within contact distance of one another (118). We first used 1-ethyl-3-(3-dimethylaminopropyl)carbodiimide (EDC) and N-hydroxysulfosuccinimide (sulfo-NHS) to convert the carboxylate groups of C4b into amine-reactive esters. Then we added an equimolar concentration of Eap34, and allowed crosslinking to occur over the course of 3 h. Separation of the reaction products by 10% tris-tricine SDS-PAGE under reducing conditions revealed a time-dependent change in the electrophoretic mobility of the γ-chain in the presence of Eap34 when compared to non-crosslinked C4b (**Fig. 3-3A, Supp. Fig. 3-1A**). Notably, the staining intensity of the γ-chain decreased throughout the course of the reaction, while a new species of mobility distinct from either the γ-chain or Eap34 appeared. Although not directly correlated to the addition of mass of Eap34 to the γ-chain, the mobility of this putative Eap34/γ-chain adduct could be explained by a non-uniform charge/mass ratio for this species when compared to other

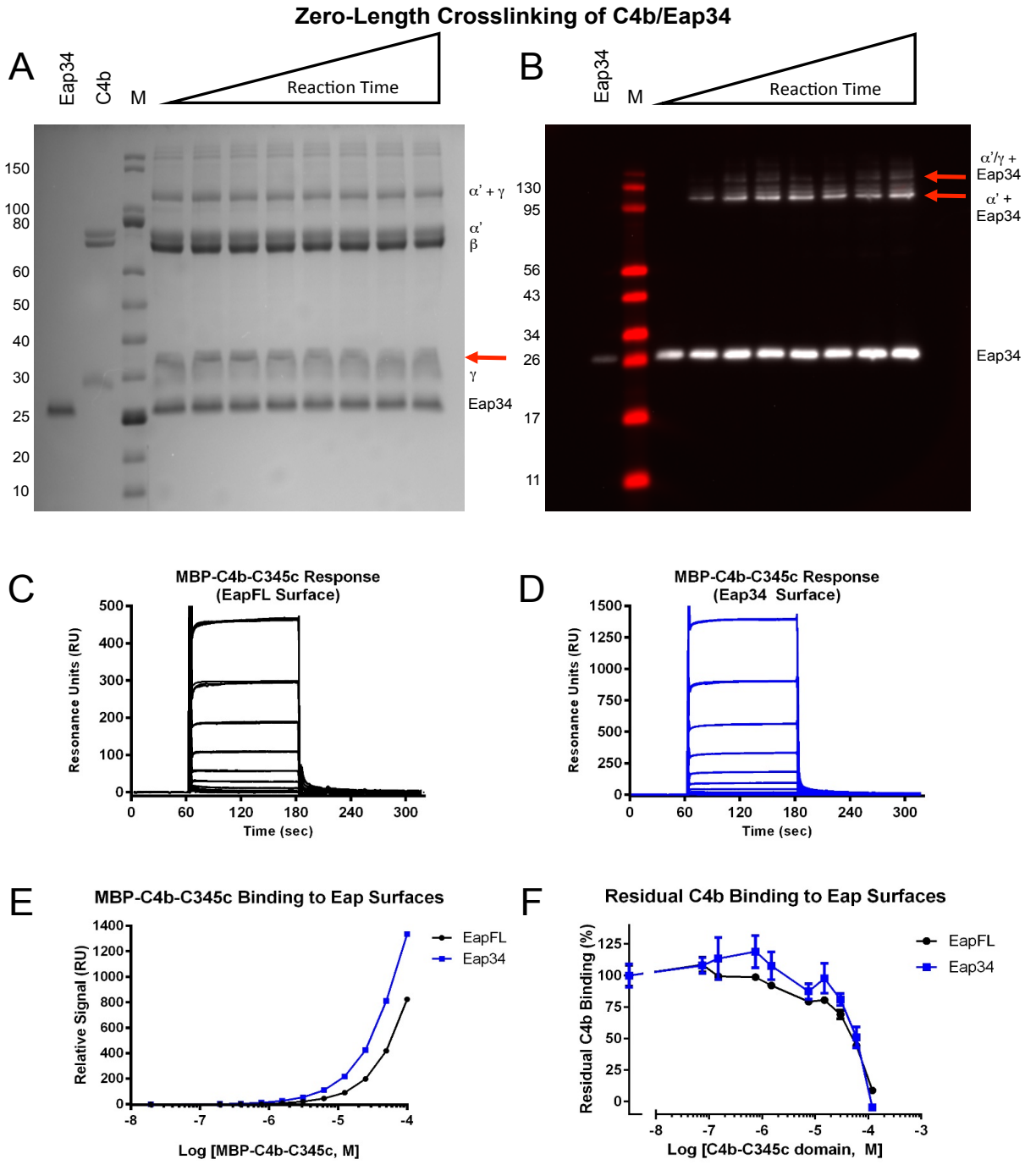

Figure 3-3. The Eap34 Binding Site Involves both the α'- and γ-Chains of C4b. (A) Time-dependent, zero-length crosslinking between free amines of Eap34 and activated carboxylates of C4b. C4b was activated by treatment with EDC and NHS prior to incubation with Eap34. Aliquots were withdrawn over the course of 3 h, and the contents were denatured, reduced, and separated by SDS-PAGE. While no time-dependent changes were visible for either the α' or β-chains of C4b, loss of staining intensity of the γ-chain correlated with the appearance of a band with altered mobility from that of the γ-chain or Eap34 (red arrow). This band contained both Eap34 and γ-chain, as judged by peptide fingerprinting analysis **(Supp. Fig. 3-1)**. (B) An identical reaction series to that shown panel A was prepared, separated by SDS-PAGE (reducing conditions), and transferred to membranes for analysis by immunoblotting. A polyclonal anti-Eap antisera raised in sheep readily detected recombinant Eap34, and additional adduct bands of higher apparent molecular weight corresponding to the α'-chain + Eap34 and the α'/γ-chains + Eap34 (red arrows). Binding of an MBP-C4b-C345c fusion protein to either full-length Eap (C) or Eap34 (D) was investigated by SPR. Injection of a logarithmic concentration series of fusion protein demonstrated clear evidence of binding to both surfaces, although saturation could not be achieved due to limitations of fusion protein solubility. Each injection was performed in triplicate, and all curves are shown. (E) Analysis of the dose-response data shown in panels C and D by a steady-state binding model. (F) Competition binding between recombinant C4b-C345c and native C4b, using the same biosensor surfaces shown in panels C and D. A fixed concentration of C4b was incubated with increasing concentrations of C4b-C345c, and the residual binding of C4b was determined following co-injection in triplicate. Notably, the midpoint of both curves in this study corresponds well to the affinities observed in the MBP-C4b-C345c direct binding studies of panels C-E.

mobility of the γ-chain, we excised the putative adduct band from the 3 h time point, proteolyzed the polypeptides in-gel, and characterized the digestion products by MALDI-TOF mass spectrometry. Peptide fingerprint analysis revealed the presence of both Eap34 and the C4b γ-chain at coverage levels of 94.8 and 54.3%, respectively (**Supp. Fig. 3-1A, B**). Together, these results established the identity of this species as an Eap34/ γ-chain adduct, and strongly suggested that Eap34 recognizes the C4b γ-chain.

To further characterize the products of the crosslinking reaction, we repeated the experiment and processed the samples for Western blotting. We probed the reaction series membrane with a sheep polyclonal anti-Eap antibody followed by detection using an HRP-conjugated secondary antibody. Although this procedure did not reveal anti-Eap immunoreactivity in the region of the membrane corresponding to the Eap34/γ-chain adduct, this could arise from masking or reaction of residues essential for antibody recognition in the cross-linked species (**Fig. 3-3B**). Nevertheless, Western blotting revealed clear anti-Eap immunoreactivity at a molecular weight corresponding to Eap34 coupled to the C4b α'-chain (**Fig. 3-3B, *bottom red arrow***). A species corresponding to Eap34 coupled to the crosslinked α' + γ-chain was also detected, albeit at a far lower abundance (**Fig. 3-3B, *top red arrow***). Analysis of the crosslinking reaction by Western blotting strongly suggested that Eap34 recognizes the C4b α'-chain in addition to the γ-chain, as described above.

The C345c domain lies at the C terminus of the C4b γ-chain and constitutes nearly one-half of the γ-chain molecular weight. To determine if this domain contributes to Eap34 binding, we expressed C4b-C345c as a fusion with *E. coli* maltose-binding protein (i.e. MBP-C4b-C345c). We took advantage of the enhanced solubility that this fusion protein provides relative to C4b-C345c alone to achieve sufficient concentrations for direct binding studies. MBP-C4b-

C345c exhibited clear, dose-dependent binding to biosensor surfaces comprised of either full-length Eap or Eap34 (**Fig. 3-3C, D**). Although we could not reach sufficient concentrations of MBP-C4b-C345c to completely saturate either surface, both sensorgram series fit to nearly identical K_D values of 63 and 69 μM when analyzed by a steady-state model (**Fig. 3-3E**). In an alternative approach, we also tested whether excess C4b-C345c protein inhibited binding of saturating levels of C4b to either full-length Eap or Eap34 biosensor surfaces. Increasing levels of C4b-C345c in the presence of a fixed concentration of C4b led to a gradual loss of C4b binding by both surfaces (**Fig. 3-3F**). Importantly, the midpoint of both competition series matched well with the K_D values obtained for MBP-C4b-C345c binding to full-length Eap and Eap34 (**Fig. 3-3E**). In summary, our results suggest that the C4b γ-chain and more specifically, the C4b-C345c domain, as the binding site of a single domain for Eap34. This interpretation is consistent with the affinities of single EAP domains for C4b (**Fig. 3-1B**) and the relative affinity of the C4b-C345c domain for Eap34 (**Fig. 3-3C-F**). Additional contributions are also made through a single domain of Eap34 binding to the C4b α'-chain (**Fig. 3-3B**). This multipartite interaction with distinct region of C4b explains the enhanced affinity of Eap34 relative to the individual domains (**Fig. 3-1B and** (40)).

Specific Lysine Residues Mediate Eap34 Binding to C4b and Inhibition of the Classical and Lectin Pathways – Our discovery that Eap3 and Eap4 bind C4b and inhibit the LP (**Figs. 3-1B and 3-2B**) indicated that both of these domains contain a specific C4b binding site. Furthermore, the detection of zero-length crosslinks between Eap34 lysine sidechains and C4b α'- and γ-chain carboxylates strongly suggested that specific lysines in Eap34 were critical to forming the C4b/Eap34 complex (**Fig. 3-3**). To identify the lysine residues of Eap34 that mediated interaction with C4b, we employed a chemical footprinting/protection strategy where

mass spectrometry of chymotryptic peptides was used to assess ligand-dependent changes in sidechain acetylation following exposure to N-acetyl-hydroxysuccinimide (NHS-Ac) (**Fig. 3-4A**) (63). Chymotrypsin digestion of Eap34, followed by characterization of the products by MALDI-TOF MS resulted in identification of approximately 60 peptides that covered ~80% of the Eap34 sequence, including 33 of the 37 lysine residues (**Supp. Fig. 3-2A**); the four C-terminal-most lysine residues were not observed. A repeat of this experiment following exposure to NHS-Ac revealed that all of the observed lysines were acetylated, and therefore surface/solvent-exposed **(Supp. Fig. 3-2A)**.

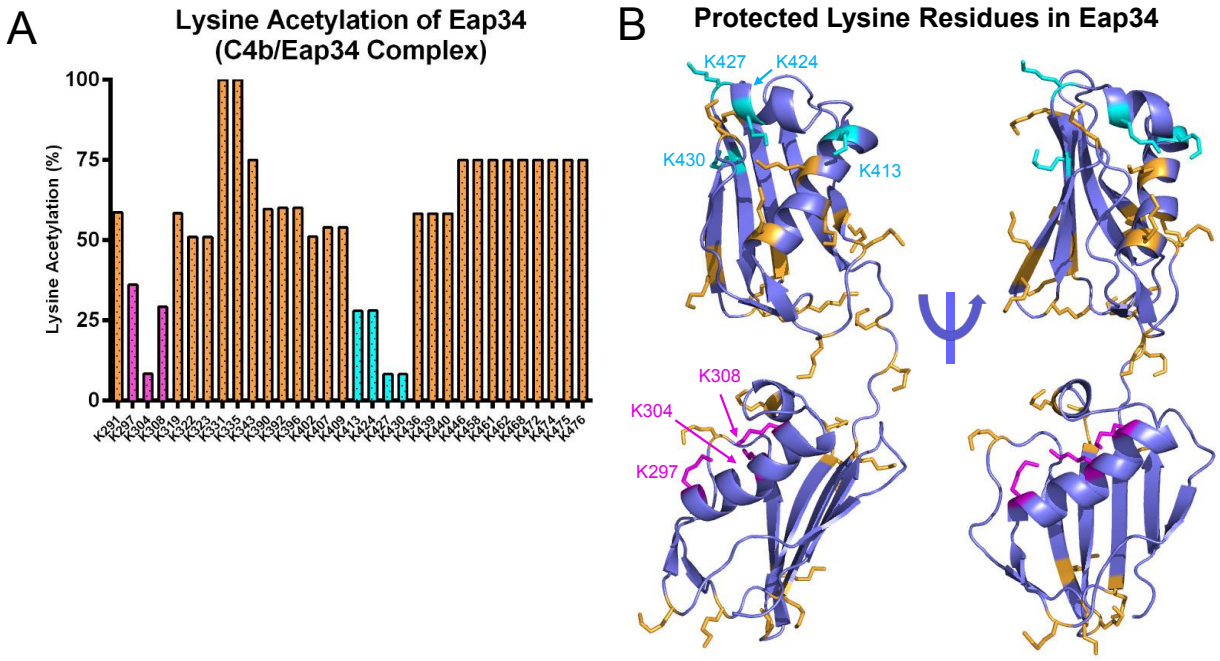

Figure 3-4. Specific Lysine Residues in Eap34 Experience Changes in Solvent Accessibility Upon C4b Binding. The solvent accessibility of Eap34 lysine residues was examined in the absence or presence of C4b through a chemical footprinting approach. A chymotrypsin digestion coverage map was first obtained for Eap34 as described in Materials & Methods, and changes in m/z of various peptides were characterized in an identical sample that had been treated with NHS-Ac. Alterations in these acetylation modification patterns were studied for a pre-formed C4b/Eap34 complex. The results of three independent experiments were merged to arrive at a total number of observations for each individual lysine residue. (A) Relative protection status of each observable Eap34 lysine in samples of C4b/Eap34. Positions K297, K304, and K308 of Eap3 (magenta), and K413, K424, K427, and K430 in Eap4 (cyan) were acetylated in less than 33% of all observations, implying they were less solvent-accessible than other Eap34 lysines (orange) when bound to C4b. (B) Structural context of the lysine residues in Eap34. All lysine sidechains are rendered in ball-and-stick convention. Residues that were readily acetylated in the experiment described above are colored orange, while those identified as protected from acetylation when bound to C4b are colored as magenta (Eap3) and cyan (Eap4), respectively.

We carried out an analogous NHS-Ac labeling experiment on a sample of C4b/Eap34. We used concentrations of each monomer (10 μM C4b and 7 μM Eap34) in sufficient excess of

the K_D for the C4b/Eap34 interaction to ensure nearly 90% occupancy of the complex, but low enough in concentration to avoid generation of non-specific, higher-order aggregates. Analysis of four replicates of Eap34 chymotryptic peptides produced in this manner revealed clear trends in protection differences across the Eap34 sequence (**Figs. 3-4A and Supp. Fig. 3-2**). Whereas twelve lysines (i.e. K330 and K334 in Eap3 and all lysines in Eap4 from K446 to the C terminus) were acetylated in at least 75% of total observations, seven lysines (i.e. K296, K303, and K307 in Eap3, and K412, K424, K427, and K430 in Eap4) were acetylated in fewer than 33% of total observations. Of these, K303, K427, and K430 were acetylated less than 10%. Significantly, we found residues exhibiting high levels of protection from acetylation in both the Eap3 and Eap4 domains. Thus, these chemical footprinting results were consistent with the C4b-binding data presented above **(Fig. 3-1B)**.

Although there are no crystal structures available for Eap3 or Eap4, there do exist high-resolution structures for Eap2, EapH1, and EapH2, which show a high-level of identity to one another (~90% of the residues in each domain align with an r.m.s.d < 1Å) (1). Using these structures as a template, we previously constructed a model for full-length Eap based on small angle x-ray scattering data and energy minimization (2). Inspection of this model revealed that the lysines, which contribute to two C4b contact sites, lie in different regions of their respective domains (**Fig. 3-4B**). While the protected residues of Eap3 are associated with its large α-helix, the key lysines of Eap4 primarily lie near the smaller α-helix and the turn that connects it with the β-strand that follows. Importantly, the locations of these residues within the Eap3 and Eap4 domains differ from those of EapH1 that contact NE in a co-crystal structure (**Fig. 3-1A, *orange highlight* and** (75)). This observation suggests that EAP domains are capable of diverse modes of binding to their respective ligands.

We used site-directed mutagenesis as a strategy for independently assessing the role of these Eap34 lysine residues in C4b binding and complement inhibition. We overexpressed and purified two distinct mutants; the first mutant had all seven of the protected lysine residues identified above changed to alanine (i.e. Eap34-KΔA), while the second mutant had the same residues changed to glutamate (i.e. Eap34-KΔE). Circular Dichroism spectropolarimetry on both mutants revealed no significant structural alterations (**Fig. 3-5A**). However, while both mutants maintained activity in a competition-binding assay, each was diminished in its affinity for C4b (**Fig. 3-5B**). Specifically, the apparent K_D values of 1.53 μM for Eap34-KΔA and 3.75 μM for

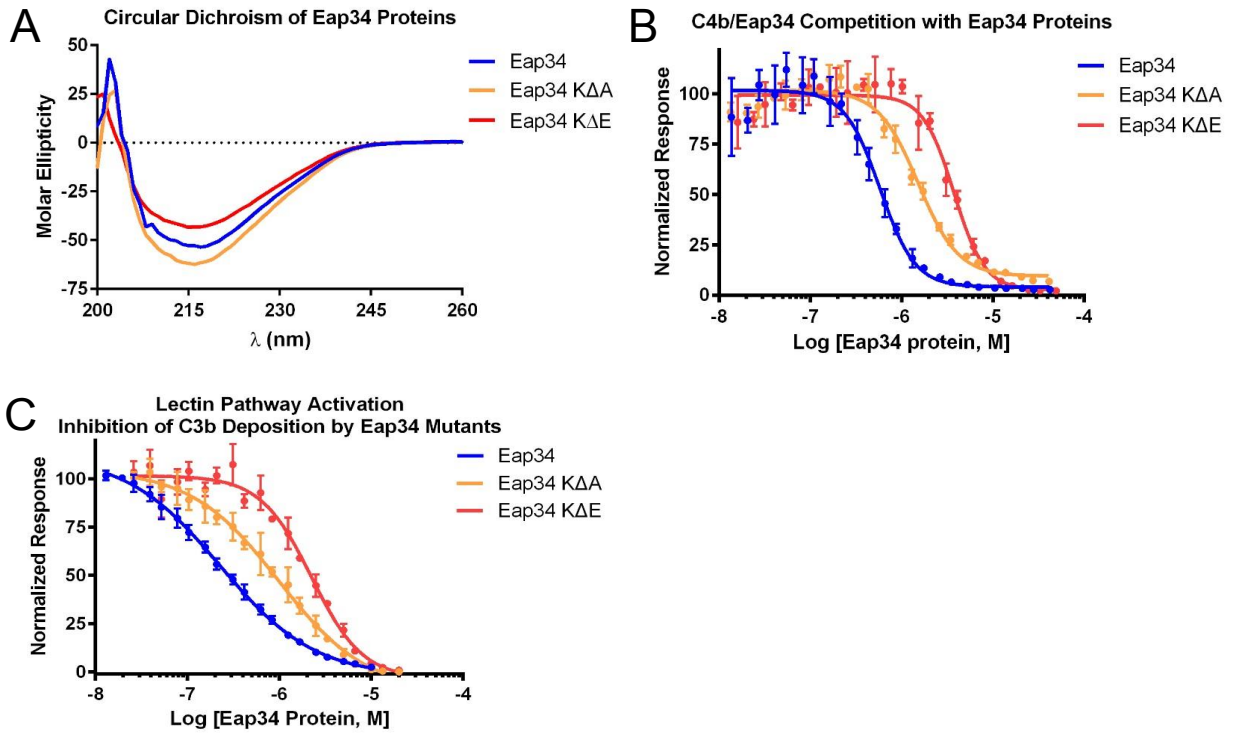

Figure 3-5. Eap34 Lysine Residues Identified by Chemical Footprinting Contribute to C4b Binding. The contribution of Eap34 lysines to C4b binding was explored by site-directed mutagenesis, wherein the seven protected lysines were mutated in concert to either alanine (Eap34-KΔA) or glutamate (Eap34-KΔE). (A) CD Spectropolarimetry was used to assess the secondary structure content of Eap34, as well as the Eap34-KΔA and Eap34-KΔE mutants. (B) The ability of untagged Eap34 and both mutants to compete the AlphaScreen signal generated by myc-Eap34 and C4b-biotin was assessed over a logarithmic dilution series. All assay points were conducted in triplicate prior to fitting to a dose-response curve. (C) Lectin pathway activity in the presence of Eap34 and both mutants was assessed by ELISA specific for either C3b. All assay points were conducted in triplicate prior to fitting to a dose-response curve. Legends are inset.

Eap34-KΔE were decreased by 2.6 and 6.4-fold, respectively, when compared to wild-type Eap34. To investigate the functional consequences of these mutations, we examined the ability

of each protein to inhibit generation of C3b in an ELISA-based assay specific for the LP (**Fig. 3-5C**). Both the Eap34-KΔA (IC_{50}=980 nM) and Eap34-KΔE (IC_{50}=2.2 μM) mutants were less effective inhibitors of the LP when compared to wild-type (IC_{50}=230 nM). Significantly, the magnitude of these changes in inhibitory activity (4.3- and 9.6-fold loss) was consistent with that observed in the C4b-binding studies above. In sum, these results established that specific lysine residues in Eap34 play important roles in mediating binding to C4b and inhibition of complement activity.

Eap Binds C4b at a Different Site than the Group B Streptococcus Complement Inhibitory Protein – We previously determined that C4b/Eap binding impedes assembly of CP/LP C3 pro-convertase (40). More recently, Pietrocola *et al.* identified a novel complement inhibitory protein (i.e. CIP) from Group B Streptococcus that also binds C4b and blocks assembly of the CP/LP C3 pro-convertase (119). Since Eap and CIP appear to share a similar mechanism of action, and since they both act directly on C4b, we hypothesized that Eap and CIP might also share the same C4b binding site. To test this possibility, we investigated whether CIP could compete the luminescence signal generated by biotinylated-C4b binding to either c-myc epitope-tagged full-length Eap or Eap34 (**Fig. 3-6**). Even though the reported K_D for C4b/CIP binding is ~95 nM

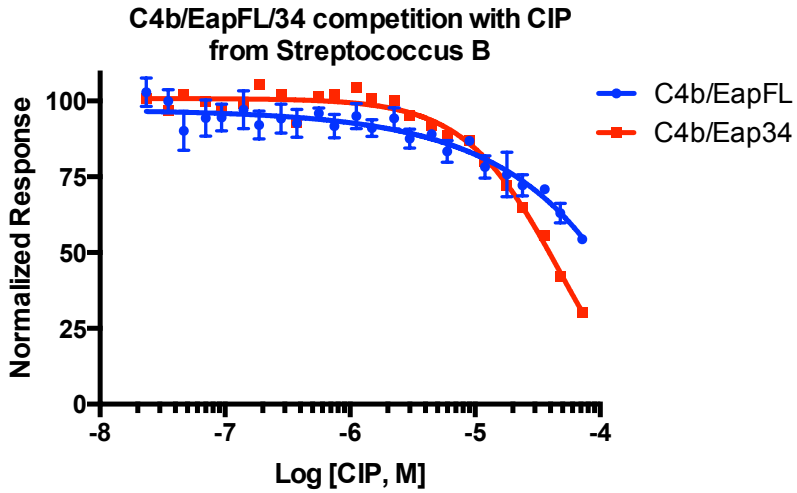

Figure 3-6. CIP from Group B Streptococcus Does Not Compete with *S. aureus* Eap for C4b Binding. The ability of untagged CIP to compete the AlphaScreen signal generated by C4b-biotin and either myc-tagged full-length Eap or Eap34 was assessed over a logarithmic dilution series. All assays points were conducted in triplicate prior to fitting to a dose-response curve. The weak and incomplete competitive effect displayed by CIP at even the highest concentrations tested suggests that the CIP binding site on C4b is distinct from that from Eap.

(119), we observed essentially no competition in either assay at CIP concentrations as high as 10 μM, and only partial competition at the highest levels of CIP attainable. Such weak competition between Eap and CIP strongly suggests that these proteins recognize different binding sites on C4b even though they manifest inhibition of complement activity through an apparently similar mechanism.

Discussion

Since its discovery in the early 1990's, Eap has stood out from other staphylococcal immune evasion proteins by virtue of its reported interactions with multiple host-derived ligands (99, 100, 109, 120-122). This impressive list of binding partners includes large glycoproteins found in the extracellular matrix, such as fibronectin, fibrinogen, vitronectin, and collagen, as well as cell surface receptors, including ICAM-1. More recently, we discovered that Eap binds to complement component C4b (40) as well as to the neutrophil granule proteases elastase (NE), cathepsin-G (CG), and proteinase-3 (PR3) (75). Significantly, these latter interactions have been characterized through direct bio-physical/chemical approaches, such as surface plasmon resonance and isothermal titration calorimetry (ITC). These results have permitted rigorous quantitative validation of both the affinity and specificity of Eap's interactions with C4b and NSPs (40, 75). Such information is essential for understanding the functional consequences of Eap/ligand interactions. It can also help guide structural studies of Eap, the independently folding EAP domains, which comprise it, and the various complexes they form.

A co-crystal structure of the Eap homolog, EapH1, bound to the NSP, NE, has been solved (75). To date, this represents the only structure of an EAP domain-containing protein bound to its target. While the NE/EapH1 co-crystal structure identified a flexible loop region in EapH1 which contributes to the majority of the NE contact site, poor levels of conservation in

this region across various EAP domain sequences suggests that alternative binding modes may be found in other EAP/NSP complexes. Nevertheless, the relatively high-affinity of the NE/EapH1 complex (K_D=20 nM, as judged by ITC (75)) along with its co-crystal structure, provided strong evidence that certain EAP domains can form robust interactions with their respective targets. The case of Eap binding to C4b appears to be somewhat more complex. Not only does C4b bind full-length Eap nearly 10-fold weaker than NE/EapH1 (40, 75), the individual domains that comprise its minimally active fragment (i.e. Eap3 and Eap4) bind C4b with K_D values some 200-fold weaker still (**Fig. 3-1B**). Although the interactions of Eap3 and Eap4 with C4b are saturable, specific, and are sufficient to manifest complement inhibitory activities characteristic of the intact Eap molecule (**Figs. 3-1B and 3-2**), joining the two domains together has a profound effect on their overall affinity and inhibitory activity (**Figs. 3-1 and 3-2 and** (40)). This observation suggests that combinations of adjacent EAP domains may generate composite binding surfaces and synergistically enhance properties that are relatively weak in isolation. Indeed, this sort of structure/function relationship was proposed following solution structural analysis of full-length Eap (2). Collectively, these results suggest that EAP domains can manifest multiple high-affinity protein-protein interaction modes, both as individuals and in combination.

Our understanding of how multiple EAP domains working in tandem can generate a high-affinity ligand would be greatly enhanced by a crystal structure of Eap34 bound to C4b. Although we successfully crystallized a closely related complex (i.e. C4c/Eap34), these crystals ultimately proved unsuitable for X-ray diffraction studies. To circumvent this limitation, we used an acetylation footprinting strategy to identify positions of contact between Eap34 and C4b (**Fig. 3-4**). While a limitation of this approach is that it only reports on free amino groups, the

unusually high percentage of lysines found not only in Eap34, but all EAP domains, makes it particularly suitable for studying these molecules. Indeed, we successfully identified seven lysines in Eap34 that experienced substantial changes in acetylation protection in the presence of C4b (**Fig. 3-4**). Concurrent mutagenesis of these lysine positions to alanine diminished the C4b-binding affinity and complement inhibitory properties of the protein (**Fig. 3-5**). This loss of affinity and inhibitory activity was augmented by changing the same positions to glutamate. On the basis of these results, we conclude that the specific lysine residues identified by acetylation footprinting collectively contribute to C4b binding and complement inhibition by Eap34. Moreover, these data also suggest that the positive charge of the lysine side chain is important at these positions. To further define whether specific chemical features of lysine or positive charge alone was more important, we attempted to prepare a mutant where these seven positions had been concurrently changed to arginine. Unfortunately, this protein could not be produced in a soluble form.

Considerations of specific residues aside, our acetylation protection data have also identified additional interaction sites on EAP domains (**Fig. 3-4B**). In particular, our results show that the C4b-binding site of Eap34 involves the large α-helix in Eap3 and a region including the smaller α-helix in Eap4. While it is noteworthy that these two sites are removed from the prominent loop region of EapH1 that contacts NE in the NE/EapH1 co-crystal structure (**Fig. 3-1A**) (75), it is important to recognize that mutation of these positions diminished, but did not completely abrogate the C4b binding or complement inhibitory activity of Eap34 (**Fig. 3-5**). We believe that this argues for the involvement of additional Eap34 positions in contacting C4b. In this regard, residues nearest the lysines discussed above would be among obvious candidates.

Future work that makes use of complimentary approaches (e.g. scanning mutagenesis) will likely be needed to identify these additional residues and to define their contributions to C4b binding.

The studies described here also help explain how Eap inhibits formation of the CP/LP C3 pro-convertase, since our zero-length crosslinking studies and supporting biochemical data can now be placed in a three-dimensional context (**Figs. 3-3A,B and Supp. Fig. 3-1**). Shortly after our initial characterization of the C4b/Eap interaction and its functional consequences (40), Mortensen *et al.* reported the first crystal structure of C4b (123). More recently, these same authors described an extensive investigation of the CP/LP C3 pro-convertase in solution (117). Together, their work has provided critical insights on the formation of the CP/LP pro-convertase, including description of the domain orientations of C4b bound to both C2 and C2a. Their data, along with our results showing that Eap34 competes with C2 for C4b binding (40) and that Eap34 binds the C4b α' and γ-chains (**Fig. 3-3 and Supp. Fig. 3-1**), has allowed us to construct an experimentally-constrained structural model for the C4b/Eap34 complex (**Fig. 3-7 and Supp. Fig. 3-3**).

We have previously shown that full-length Eap inhibits the initial interaction between the C2b region of C2 and C4b (40). Considering the structural homology between the AP C3 pro-convertase C3bB and the CP/LP C3 pro-convertase C4b2, along with the fact that the smaller fragments of fB (i.e. Bb) and C2 (i.e. C2b) are responsible for the initial association of these pro-proteases with C3b and C4b, respectively (117, 124), our model suggests that the competitive effects of full-length Eap on C2b binding to C4b can be explained by contacts between Eap34 and both the C4b α'- and γ-chains (**Figs. 3-3, 3-7 and Supp. Fig. 3-3**). Specifically, the pocket on C4b that forms between its γ-chain C345c domain and the neighboring macroglobulin-like domain of the C4b α'-chain is too small to accommodate C2b when Eap34 is bound (**Supp. Fig.**

3-3). It is also worth noting that the character of C4b in this region is thought to be influenced by an unusual stretch of 10 residues at the C-terminus of the α'-chain, which consists of 3 sulfated tyrosines along with 7 aspartates and glutamates. Although this sequence is not visible in the C4b crystal structure, SAXS-constrained modeling of this sequence in C4b is consistent with its presence at or near the proposed Eap34 binding site (**Fig. 3-7 and** (123)). Thus, the proposed Eap34 binding site is ideal not only for disturbing interactions between the C4b and its ligand, C2, it may also facilitate recruitment of the highly positively charged Eap molecule (pI=9.96) to this particular binding site on C4b in the first place.

Many powerful complement evasion mechanisms act at the level of C3 convertases (42). Formation of active C3 convertases is predicated upon assembly of their corresponding pro-convertases, however, which has rendered these latter structures very effective points for execution of evasion strategies (42, 58). Indeed, both *S. aureus* Eap and Group B *Streptococcus* CIP (119) share the ability to block initial interaction between C4b and C2, and thereby inhibit formation of the CP/LP C3 pro-convertase (42). Even though Eap and CIP manifest similar activities, CIP surprisingly failed to compete with either Eap or Eap34 for C4b binding (**Fig. 3-6**). This observation suggests the structural basis for CIP function is substantially different than that of Eap. In this regard, the results we present here demonstrate that the Eap binding site lies on the C4b α'- and γ-chains (**Figs. 3-3, 3-7 and Supp. Figs. 3-1, 3-3**), and are broadly consistent with orthosteric inhibition of pro-convertase formation. By contrast, comparatively little is known regarding the structural basis for C4b/CIP binding. Although structural information for CIP is limited, Pietrocola *et al.* suggested that CIP might share structure/function similarity to the *S. aureus* AP inhibitors, Efb-C and Ehp (58, 119). While neither Efb-C nor Ehp bind C4 or its activated fragment C4b, both of these proteins bind a native complement protein (i.e. C3), its

major activation product (i.e. C3b), and inhibit pro-convertase formation through an allosteric mechanism (58, 64). By analogy, these authors' suggestion also predicts that (i) CIP binds C4b in an altogether different site than Eap, and that (ii) occupation of this binding site alters C4b conformational states in a way that disturbs normal C2 binding. While additional structural information is clearly needed to draw accurate conclusions on these matters, the lack of competition between CIP and Eap for C4b binding, which we report here, suggests that an allosteric mechanism is likely for CIP.

Experimental Procedures

Native and Recombinant Proteins – Human serum proteins C4, C4b, C1s, C4b-binding protein (C4BP), and Factor I were obtained in purified form from Complement Technologies (Tyler, TX). Site-specific biotinylation of C4b was carried out using a previously described method (40). All recombinant S. aureus proteins, CIP from Group B Streptococcus, as well as C4-C345c and the MBP fusion MBP-C4-C345c were overexpressed and purified according to previously described methods (88). Site-directed mutagenesis was used to constructed lysine to alanine (KΔA) and lysine to glutamate (KΔE) forms of Eap34 using gBlocks® Gene Fragments (Integrated DNA Technologies) with SalI and NotI restriction sites added at the 5' and 3' end, respectively. Following PCR, the mutagenic product was subcloned into the prokaryotic expression vector, pT7HMT, and sequenced to confirm its integrity (88). Protein expression and purification was carried out as described for the wild-type Eap34 protein (88).

AlphaScreen Binding Assays – An AlphaScreen competition-based binding assay was performed using a previously published protocol (40, 59). In short, C4b/EapFL, C4b/Eap34, and C4b/CIP competition based assays were done using a total volume of 25 μL, in a buffer composed of HBS (pH 7.4), 0.1% (w/v) BSA, 0.01% (v/v) Triton-X 100. Each component was

added to the final concentrations: 50 nM myc-EapFL (50 nM myc-Eap34), 5 nM C4b biotin, 20 μg/μL anti-c-myc AlphaScreen acceptor beads, and 20 μg/μL AlphaScreen donor beads. A two-fold dilution series was prepared for each unlabeled competitor protein and allowed to equilibrate with myc-Eap/myc-Eap34/myc-CIP and C4b biotin for 1 h. Following this, the acceptor beads were added, incubated for 1 h, and then the donor beads were added and incubated for an additional 0.5 h. Reactions were then transferred to ½-Area 96-well plates and measured using an EnSpire multimode plate reader (Perkin Elmer Life Sciences). Data analysis and curve fitting were carried out as previously described (59).

Activity of the Lectin Pathway of Complement on an Artificial Surface – Functional activity of the lectin pathway (LP) was determined using a previously described method (40, 92). In short, 96-well polystyrene high bind microplates (Corning Life Sciences) were coated overnight to specifically activate the LP (coated with 20 μg/ml *Saccharomyces cerevisiae* mannan [Sigma-Aldrich]). Plates were blocked with 1% (w/v) BSA, in PBS (pH 7.4) with 0.05% (v/v) Tween 20 for 1 h at 37 °C. In order to obtain IC_{50} values for each inhibitor, a two-fold dilution series was done by diluting the protein 1:1 in LP buffer [50 mM HEPES (pH 7.5), 140 mM NaCl, 0.1% (w/v) Gelatin, 0.1% (w/v) BSA, 2mM $CaCl_2$, 0.5 mM $MgCl_2$, 1% (v/v) Serum (Pooled Complement Human Serum, Innovative Research Inc.)] before direct application to the coated, blocked ELISA plate and incubated for 1 h at 37 °C. Deposited C3b and C5b-9 were detected with 0.333 μg/mL C3d Antibody (003-05): sc-58928 and 0.2 μg/mL C5b-9 (aE11): sc-58935 (Santa Cruz Biotechnology, Inc.), respectively, diluted in PBS (pH 7.4), 0.1% (w/v) BSA, 0.05% (v/v) Tween-20 and incubated at RT for 0.5 h. Finally, the Goat anti-Mouse IgG, IgM (H+L) Cross Absorbed Secondary Antibody, HRP conjugate (Thermo Scientific) was diluted to 1.6 μg/mL in equivalent dilution buffer and added to each well for 0.5 h at RT. HRP-labeled Abs

were detected with 50 μL of 1-Step Ultra TMB-ELISA (Thermo Scientific), the reaction was stopped by the addition of an equal volume of 2 M H_2SO_4, and the absorbance at 450 nm was measured using a $VERSA_{MAX}$ microplate reader. Data were fit to a four-parameter (variable slope) dose-response – inhibition curve software (GraphPad, La Jolla, CA).

EDC/Sulfo-NHS Zero-length Crosslinking of Eap34 and C4b – A zero-length cross-linking procedure was adapted from a previously described method (118). In short, purified complement C4b (Complement Tech) and recombinant Eap34 were buffer exchanged into 0.05 M MES (pH 6.0), 0.5 M NaCl (reaction buffer) and 0.1 M NaPi (pH 7.5), respectively. C4b was activated by the addition of 2 mM 1-Ethyl-3-(3-dimethylaminopropyl)-carbodiimide (EDC) and 5 mM N-hydroxysulfosuccinimide (sulfo-NHS) at RT for 15 min. The reaction was quenched by quickly desalting the protein using a 30 kDa centrifugal filter. Eap34 was added in 5% excess of a 1:1 molar ratio and reacted for 3 h at RT. After quenching and addition of Eap34, aliquots were removed at time points t=0, 15, 30, 60, 90, 120, 150, and 180 mins, added to reducing Laemmli sample buffer, and separated on a 10% SDS-PAGE gel. Cross-linked gel bands were excised, extracted, digested with 30 ng/μL sequencing grade Trypsin (Promega) and subjected to MALDI-TOF (Bruker Daltonics Ultraflex III) mass spectrometry analysis. Western blot analysis was done using a specific polyclonal sheep anti-Eap antibody (gift from Prof. J.-I. Flock, Karolinska Institute, Sweden) followed by detection with an HRP-conjugated secondary antibody. Eap34 gel bands were visualized on a FluorChem M system (Protein Simple) following reaction with SuperSignal West Pico Chemiluminescent Substrate (Thermo Scientific) according to manufacturer's suggestions.

Surface Plasmon Resonance Experiments – C4b-C345c direct binding and competition studies were done using a Biacore 3000 (GE Healthcare) at 25°C. Experiments were run at a

flow rate of 20 μL min^{-1} in HBS-T (20 mM HEPES (pH 7.4), 140 mM NaCl, 0.005% (v/v) Tween-20) supplemented with 5 mM $NiCl_2$. Although nickel is not a physiologically relevant cation, it has been shown to stabilize complement proteins and C3 convertases for *in vitro* analysis (117, 125, 126). C4b-C345c direct binding and C4b residual binding experiments were carried out by immobilization of full-length Eap (4000-7000 RU) and Eap34 (4400-5900 RU) by amine coupling to a CM-5/CMD-200M sensor chip (GE Healthcare/Xantec). Dose-response experiments were performed using an MBP fusion of C4b-C345c in order to obtain saturating concentrations. MBP-C4-C345c was injected for 2 min with 1 min dissociation, followed by a 1 min regeneration injection of 2 M NaCl. The average response for the 5-15 s preceding the injection stop was plotted versus concentration of MBP-C4b-C345c and fit using a nonlinear regression, log (agonist) vs. response – variable slope curve in GraphPad Prism6.

Using the sensor chip configuration described above, an assay was done to assess competition between C4b-C345c and C4b for binding to Eap. In short, a flow rate of 10 μL min^{-1} in the same buffer described above was used for all injections. C4b was injected in triplicate at a concentration of 500 nM to establish a basal level of C4b binding, and this concentration was held constant for the competition experiments. C4b and subsequent samples of C4b plus C4b-C345c (varying concentrations from 75 nM to 120 μM) were injected for 2 min with 2 min dissociation, and regenerated by two 1 min injections of 2 M NaCl. To calculate residual C4b binding, an injection of C345c alone was subtracted from the [C4b + C345c] injection, normalized to the basal C4b response, and plotted against the concentration of C345c.

Lysine-acetylation Footprinting MALDI-TOF Mass Spectrometry of Eap34 and C4b – The general approach was adapted from Chen et al. (63); Specifically, a 10 μL solution of Eap34 (7 μM) and complement C4b (10 μM) was incubated for 20 min at RT in HBS (pH 7.4). These

concentrations allowed the reaction to be 10-fold above the K_D as well as have excess C4b to eliminate any free-Eap34. 5 μL of a 1:10 dilution of 2 M N-acetyl-hydroxysuccinimide (synthesized as previously described (63)) in acetonitrile (ACN) was added to the incubated proteins and allowed to react for 20 min at RT. The reaction was stopped by the addition of 10 μL of 1 M NH_4HCO_3 (pH 8.0) for 20 min at RT. Eap34 and C4b were separated by SDS-PAGE performed under non-reducing conditions. The gel was zinc-imidazole (0.3 M $ZnCl_2$, 0.2 M imidazole) stained and the Eap34 bands were excised and subjected to in-gel digestion overnight at 37°C by 10 ng/μL sequencing grade Chymotrypsin (Promega). Digested peptides extracted by subsequent additions of 200 μL 0.1% (v/v) TFA and 100 μL ACN, 0.1% TFA and lyophilized. Lyophilized peptides re-suspended in 50 μL of 0.1% (v/v) TFA and purified by C_4-ZipTip (EMD Millipore). Eluted peptides diluted 1:10, mixed 1:1 in matrix buffer (50 mg/mL DHB in 1:1 ACN:0.1% TFA), and subjected to MALDI-TOF (Bruker Daltonics Ultraflex III) mass spectrometry analysis.

Mass spectra were analyzed by mMass Version 5.5.0 (http://www.mmass.org). Spectra were calibrated to known high intensity peptides. Peaks were matched with a tolerance of less than 0.4 Da, with a mass range of 500-3500 Da, and were subjected to envelope fitting to determine the measured versus the computer-generated model. A mass shift of 42.0106 Da was observed for each acetylated lysine residue. Analysis of final, calibrated peptide coverage map was done using a scoring system based on percentage of acetylation for each individual lysine residue. As an example, a peptide containing 4 lysines with a peak shift equating to 3 acetylations (126.0318 Da), was scored by the relationship (# of acetyl groups / # of lysine residues in peptide) x 100 = % acetylation per lysine residue or (3/4) x 100 = 75% acetylation/lysine.

Circular Dichroism (CD) – Far-UV CD spectropolarimetry was used to assess the secondary structure content of Eap34 mutants in comparison to the wild-type protein. Samples were dissolved in 20 mM HEPES (pH 7.4), 140 mM NaCl at a concentration of 1 mg/mL (~40 μM). A buffer control was also collected. Spectra were collected across a 190-260 nm range, at 50 nm min^{-1}, using 0.5 nm pitch, 1 s response, and a 1 nm bandwidth. All data was collected on a Jasco J-815 instrument using a cylindrical small volume quartz cuvette (1 mm path length) (Starna Cells, Inc., Atascadero, CA).

Statistical Analyses – Analysis was performed using GraphPad Prism 6.0 and mMass Version 5.5.0.

Structural Modeling – The ClusPro server (127, 128) was used to construct a structural model for the C4b/Eap34 complex. The structure of human C4b (PDB accession code 4XAM (123)) and a SAXS-derived model of Eap34 (2) were used as inputs. Modeling was restrained with experimentally-derived parameters that restricted docked complexes to include the α' and γ-chains of C4b, and designated Eap34 residues K296, K303, K307, K412, K424, K427, and K430 as participating in intermolecular contacts. The resulting model was compared with that of a C4b2 complex generated by superimposing the individual structures of C4b, C2a (PDB accession code 2I6S (102)) and C2b (PDB accession code 3ERB (129)) onto the structure of the AP C3 pro-convertase, C3bB (PDB accession code 2XWJ (124)). This procedure takes advantage of the global architectural similarity between the C3 pro-convertases of the AP and CP/LP (117). All images of protein structures were rendered using PyMol.

Acknowledgements

This work was supported by the American Heart Association Midwest Affiliate Predoctoral Research Fellowship 15PRE25750013 to J.L.W. and by National Institutes of Health

(NIH) Grants AI111203 and AI113552 to B.V.G. The authors thank Drs. Brandon Garcia, Sofia Mortensen, Gregers Andersen, Daphne Stapels, Suzan Rooijakkers, and Michal Hammel for helpful discussions regarding this project. The authors also acknowledge Dr. Jan-Ingmar Flock for generously providing anti-Eap antiserum.

Supplemental Figures

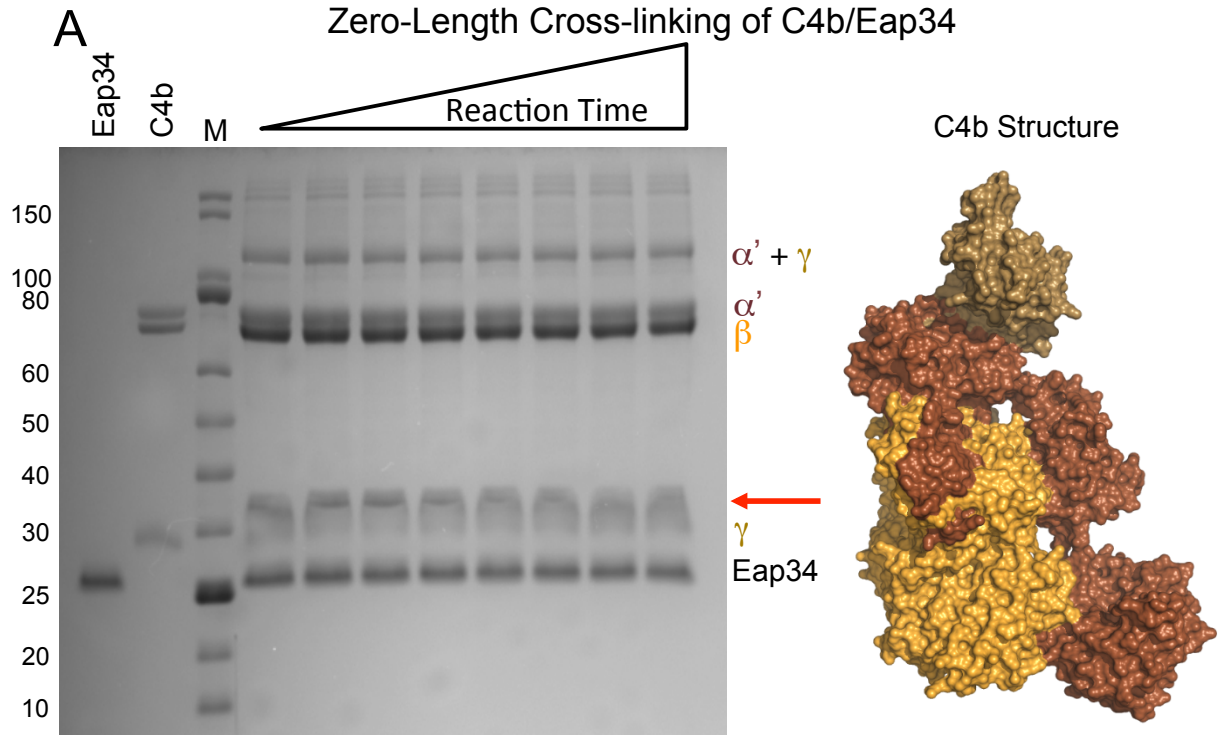

B Composition of Putative C4b + Eap34 Adduct Band (Trypsin Digest)

Sequence	Identity	Coverage (%)
GSTVPYSINL NGTSTNILSN LSFSNKPWTN YKNLTSQIKS VLKHDRGISE QDLKYAKKAY YTVYFKNGGK RILQLNSKNY TANLVHAKDV KRIEITVKTG TKAKADRYVP YTIAVNGTST PILSKLKISN KQLISYKYLN DKVKSVLKSE RGISDLDLKF AKQAKYTVYF KNGKKQVVNL KSDIFTPNLF SAKDIKKIDI DVKQYTKSKK K	Eap34	200/211 (94.8%)
EAPKVVEEQE SRVHYTVCIW RNGKVGLSGM AIADVTLLSG FHALRADLEK LTSLSDRYVS HFETEGPHVL LYFDSVPTSR ECVGFEAVQE VPVGLVQPAS ATLYDYYNPE RRCSVFYGAP SKSRLLATLC SAEVCQCAEG KCPRQRRALE RGLQDEDGYR MKFACYYPRV EYGFQVKVLR EDSRAAFRLF ETKITQVLHF TKDVKAAANQ MRNFLVRASC RLRLEPGKEY LIMGLDGATY DLEGHPQYLL DSNSWIEEMP SERLCRSTRQ RAACAQLNDF LQEYGTQGCQ V	C4b γ-chain	158/291 (54.3%)

Supplemental Figure 3-1. Further Analysis of the Zero-length Crosslinking Reaction Between C4b and Eap34. (A) Time-dependent, zero-length crosslinking between free amines of Eap34 and activated carboxylates of C4b. C4b was activated by treatment with EDC and NHS, prior to incubation with Eap34. Aliquots were withdrawn over the course of 3 h, and the contents were denatured, reduced, and separated by SDS-PAGE. While no time-dependent changes were visible for either the α' or β-chains of C4b, loss of staining intensity of the γ-chain correlated with the appearance of an intermediate mobility band between the γ-chain and Eap34 (red arrow). A representation of the C4b structure is provided for clarity in interpreting the SDS-PAGE image. (B) The adduct band of intermediate molecular weight resulting from the 3 h time point from (A) was further analyzed. In-gel digestion of the excised band by trypsin generated a series of peptides that were mapped to Eap34 and C4b. Observed residues appear in red letters, while unobserved residues appear in black letters. 200 of 211 residues in the recombinant form of Eap34 were observed, for a total coverage of 94.8%, while 158 of 291 residues in the C4b γ-chain were observed, for a total coverage of 54.3%. Interestingly, the Eap34 peptide NLTSQIK, which contains the highly-protected K304 (**Figs. 3-1A and 3-4**), was not observed. This suggests that this particular lysine was not accessible to the protease during the in-gel digestion procedure. Furthermore, a large region of peptide encompassing the C4b γ-chain was not observed, including several residues in the vicinity of the C terminus. These residues contribute a portion of the MIDAS-acceptor site, and are near the proposed binding site of Eap4 in the model of the C4b/Eap34 complex (**Fig. 3-7 and Supp. Fig. 3-3**). One potential explanation for the absence of these peptides is that they represent a location of chemical crosslinks between sidechains of Eap34 and the C4b γ-chain.

A Chymotrypsin Coverage Map of Eap34 in Various Settings

Sequence (Eap34, residues 265-476*)	Sample	Coverage (%)
GSTVPYSINL NGTSTNILSN LSFSNKPWTN YKNLTSQIKS VLKHDRGISE QDLKYAKKAY YTVYFKNGGK RILQLNSKNY TANLVHAKDV KRIEITVKTG TKAKADRYVP YTIAVNGTST PILSKLKISN KQLISYKYLN DKVKSVLKSE RGISDLDLKF AKQAKYTVYF KNGKKQVVNL KSDIFTPNLF SAKDIKKIDI DVKQYTKSKK K	Eap34	175/211 (82.9%)
GSTVPYSINL NGTSTNILSN LSFSNKPWTN YKNLTSQIKS VLKHDRGISE QDLKYAKKAY YTVYFKNGGK RILQLNSKNY TANLVHAKDV KRIEITVKTG TKAKADRYVP YTIAVNGTST PILSKLKISN KQLISYKYLN DKVKSVLKSE RGISDLDLKF AKQAKYTVYF KNGKKQVVNL KSDIFTPNLF SAKDIKKIDI DVKQYTKSKK K	Eap34 + NHS-Ac	178/211 (84.4%)
GSTVPYSINL NGTSTNILSN LSFSNKPWTN YKNLTSQIKS VLKHDRGISE QDLKYAKKAY YTVYFKNGGK RILQLNSKNY TANLVHAKDV KRIEITVKTG TKAKADRYVP YTIAVNGTST PILSKLKISN KQLISYKYLN DKVKSVLKSE RGISDLDLKF AKQAKYTVYF KNGKKQVVNL KSDIFTPNLF SAKDIKKIDI DVKQYTKSKK K	Eap34/C4b + NHS-Ac	168/211 (79.6%)

B Example Changes in Peptides Due to Presence of NHS-Ac/Ligand

M/z	Peptide	Eap34	Eap34 + NHS-Ac	Eap34/C4b + NHS-Ac
1230.7416/1314.7627	^{32}KNLTSQIKSVL^{42}	0	2	-
2197.1975/2365.2398	^{148}KSERGISDLDLKFAKQAKY^{166}	0	4	-
1211.6783/1253.6888	^{157}DLKFAKQAKY^{166}	0	-	1
786.4396/828.4502/ 786.4396	^{134}ISYKYL^{139}	0	1	0

Supplemental Figure 3-2. Supporting Data for Lysine Acetylation/Protection Studies. (A) Chymotrypsin-derived peptide coverage maps from three independent experiments on Eap34, Eap34+NHS-Ac, and C4b/Eap34+NHS-Ac. Coverage maps for Eap34 ranged from 79.6 to 84.4%. Observed residues appear in red letters, while unobserved residues appear in black letters. The asterisk signifies that the first three residues in the recombinant Eap34 protein (i.e. GST) are an artifact of the subcloning procedure, and are not found in the full-length Eap sequence. (B) Example changes in Eap34 chymotryptic peptides in samples of Eap34 alone, Eap34+NHS-Ac, or C4b/Eap34+NHS-Ac. The M/z of the peptide ions is shown along with each peptide identity. The three columns at the right depict the number of acetylations in each peptide that account for the observed increase in M/z. Of note, the third peptide (157-166) contains three lysine residues, but was only found to contain one acetylation in the C4b/Eap34 sample. Thus, the level of protection assigned to each lysine is 1/3 or 33%. A similar analysis was conducted across all observations to arrive at the data presented in **Fig. 3-4A**.

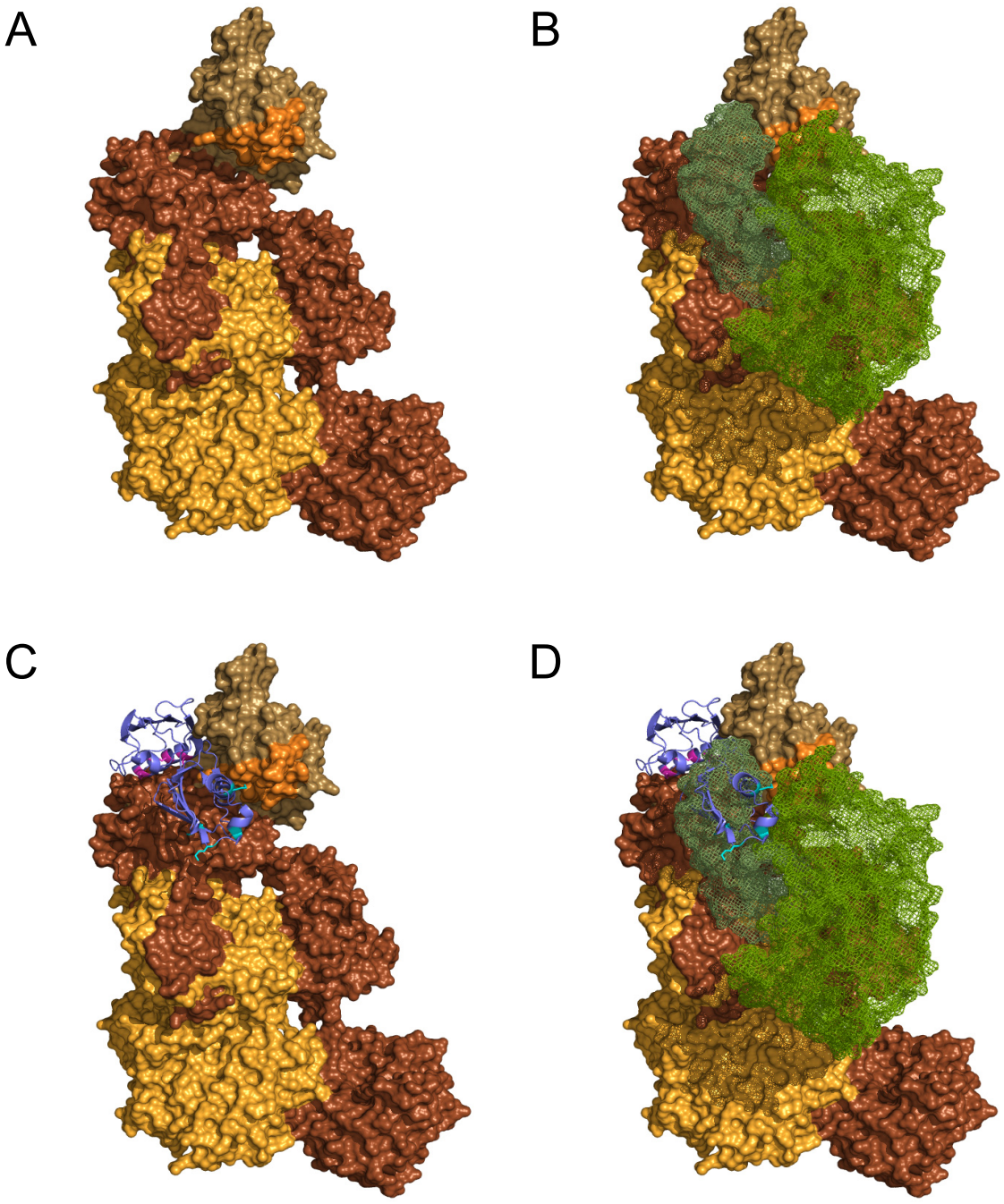

Supplemental Figure 3-3. Supporting Images for the C4b/Eap34 Structural Model Presented in Figure 7. An experimentally-constrained model for the C4b/Eap34 complex was generated by the ClusPro server as described in *Materials & Methods*. (A) Surface rendering of C4b where each distinct polypeptide is shaded as follows: α'-chain in brown, β-chain in yellow-orange, and γ-chain in beige. The MIDAS-acceptor site of the C345c domain, which mediates metal-dependent binding of the vWF domain of C2 to C4b, is shaded orange. (B) Space filling model of the CP/LP C3 pro-convertase, C4b2. C4b is colored as described in panel A, while the two regions of C2 (wire mesh) are colored with C2b in forest green and C2a in light green. (C) C4b/Eap34 structural model where C4b is colored as in panels A and B, while Eap34 is shown as a purple ribbon. The locations of key lysine residues in Eap34 are highlighted in magenta (Eap3) and cyan (Eap4). (D) Superposition of the images from panels B and C. Note the similar locations of the C2b and Eap34 binding sites on C4b, and the potential for extensive steric clash if both proteins were present. This model is therefore in good agreement with the previously described ability of Eap34 to potently compete with C2 for C4b binding.

Unpublished Conclusions

Although discussed briefly in the submitted manuscript, the overlap of the MIDAS motif on the C345c domain of the γ-chain of C4b is instrumental to the inhibitory effects that Eap has on the classical and lectin pathways. Previous work has shown that the MIDAS motif is critical for the formation, stability, and activity of the C3-convertase (102, 130). This has been observed through amino acid residue mutations in this motif completely knocking out hemolytic activity (130). Initial interaction between complement C2 and C4b involves coordination of a divalent metal cation (Mg^{2+}) between the MIDAS motif on the C345c domain of C4b and the von Willebrand factor A-type (vWFA) domain of C2 (131).

Interestingly, during our analysis of the interactions between Eap and the C345c domain of C4b, we observed a few possible conclusions as to how Eap is interacting with the MIDAS motif of the C345c domain. Using the surface plasmon resonance approach, no observable binding could be seen from directly injecting C4b-C345c and C3b-C345c (negative control) over Eap under normal buffer conditions [HBS-T (pH 4.7)]. The addition of specific divalent metal cations (Ni^{2+} and to some extent, Zn^{2+}) coordinated the low affinity interactions between C4b-C345c and Eap, but not C3b-C345c (**UC Figs. 3-1A, 3-1B**). The explanation for this can be that

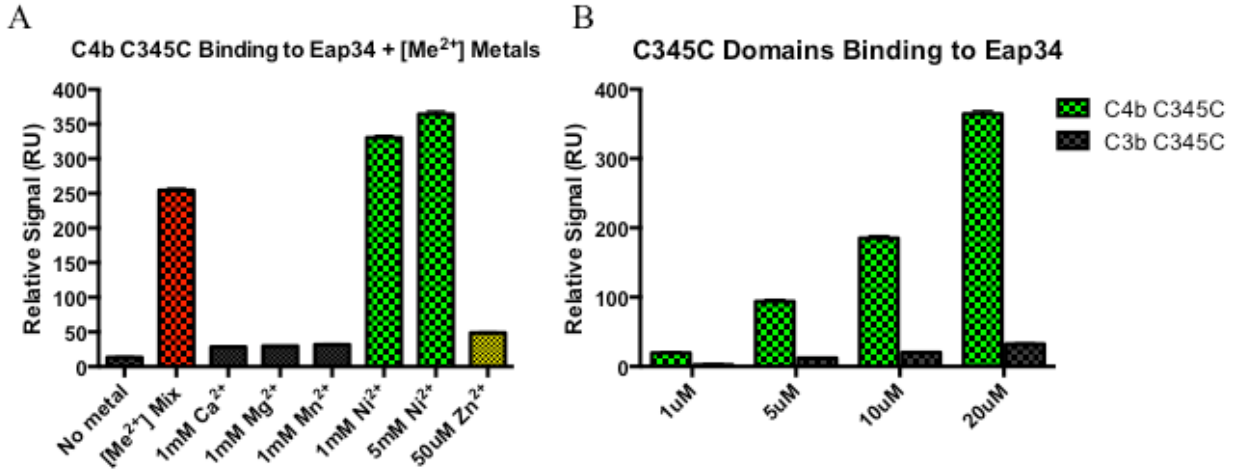

UC Figure 3-1. Eap Binds Specifically to the C345c Domain of Complement C4/C4b. Eap34 was conjugated directly to the SPR chip surface through amine coupling. (A) The C345c was injected at 20 μM over the surface in HBS-T (7.4) buffer with the addition of metal concentrations listed. Observable binding was seen with the addition of a mixture of divalent cations ([Me^{2+}] Mix, *red*), with Ni^{2+} (*green*) at 1 and 5 mM, and with 50 μM Zn^{2+} (*yellow*). (B) The C345c domain from C4b (green) and C3b (grey) was injected at the above concentrations over Eap34 in HBS-T (7.4) + 5 mM $NiCl_2$.

Eap is possibly coordinating a metal with the MIDAS motif of C4b or that a divalent cation is needed to stabilize the C345c domain of C4b in order to initiate an interaction with Eap, as stated above that divalent cations, like Ni^{2+}, have been shown to stabilize complement proteins for *in vitro* analysis (117, 125, 126).

To gain an understanding of these interesting results, we looked to the X-ray structure of Eap domain 3 (domain 4 was not available). Upon resolution of the crystal structure, we noticed that there was coordination of a divalent metal cation (Zn^{2+}) between His^{44} (His^{308} of full Eap sequence) of one Eap3 domain and Thr^{13} (Thr^{277}) and Ser^{14} (Ser^{278}) of a second Eap3 domain (**UC Fig. 3-2**). Although this could be directly related to an artifact of crystallization, we decided to test this hypothesis using a couple of different methods. We began with isothermal titration calorimetry (ITC), testing if there is a direct interaction between Zn^{2+} (syringe) and Eap3 (cell), but saw no evidence of coordination of the metal (*data not shown*). This is not surprising because in many cases, it takes two binding partners to coordinate a metal ion and there is no direct evidence for Eap interacting with itself.

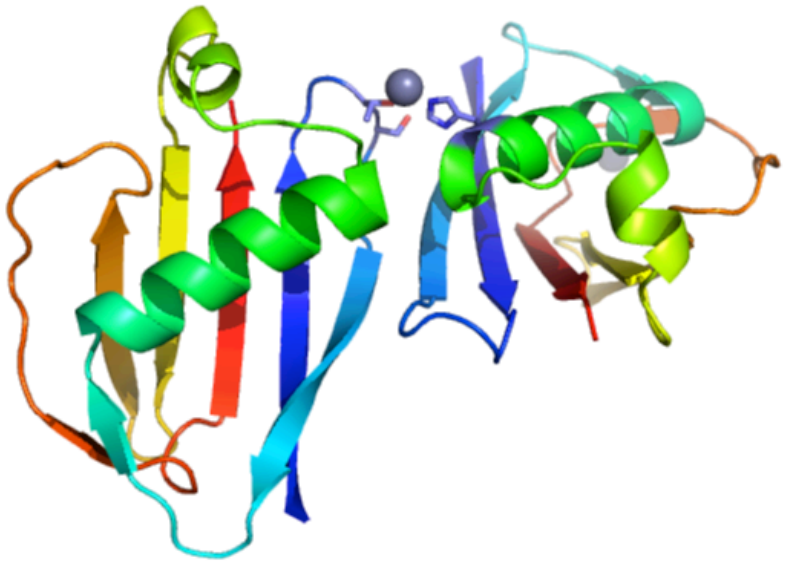

UC Figure 3-2. X-ray Crystal Structure of the Third Domain of Eap. Structure shows two Eap3 domains coordinating a Zinc ion through the His^{308} residue of one domain and the Thr^{277}/Ser^{278} residues of a second domain (*residues shown in stick form, nitrogens colored blue and oxygens colored red*).

Second, using SPR, we can see a direct interaction between C4b (surface) and Eap3 under standard buffer conditions (**UC Fig. 3-3A, *orange line***). With the addition of $ZnCl_2$ into the buffer at 1mM and 2mM, we see an overall increase in Eap3 binding, but with the addition of $NiCl_2$ and $MgCl_2$ at similar concentrations, we do not observe this increase **(UC Figs. 3-3A, 3-3B)**. Finally, using an AlphaScreen with signal generated from C4b-biotin and myc-EapFL, we see complete competition with the addition of unlabeled Eap3 under standard buffer conditions; through the addition of 50 µM $ZnCl_2$ (physiological concentration of Zn^{2+} in blood), we see an

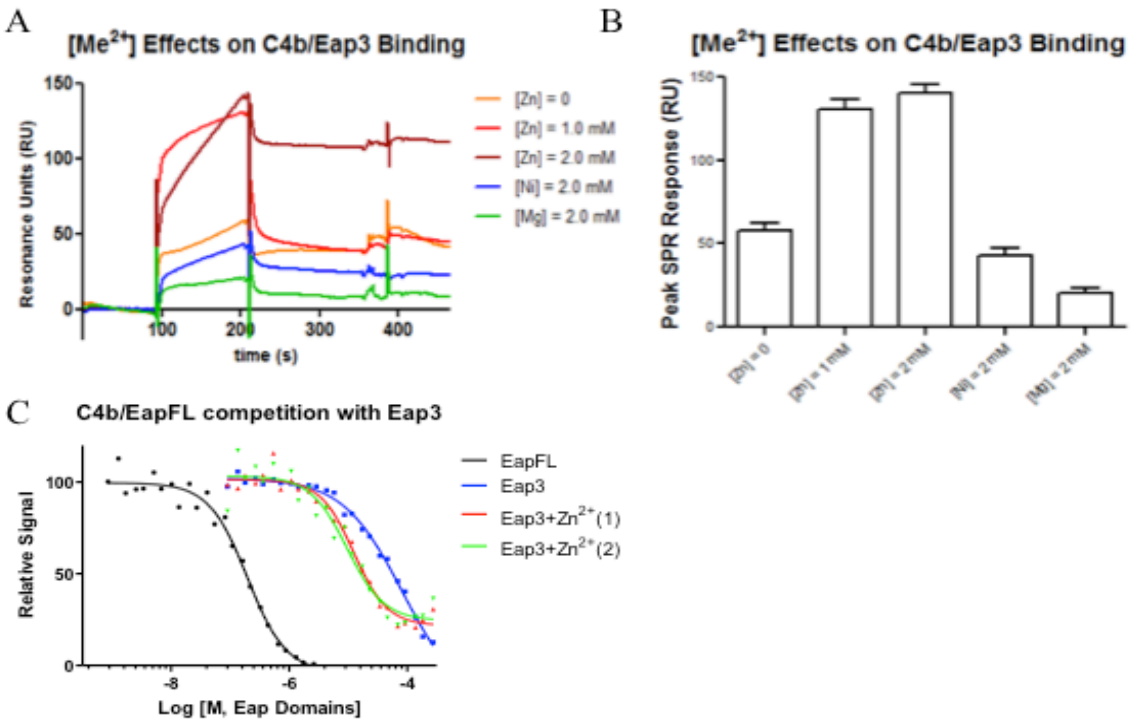

UC Figure 3-3. Zinc-dependent Binding of Eap3 to Complement C4b. C4b was conjugated to the SPR chip surface through biotin-streptavidin. (A) Eap3 was injected directly over the chip surface in triplicate at a concentration of 10 µM in HBS-T (7.4) with or with the addition of metals listed, *legend inset*. (B) Bar graph of the observed binding of Eap3 to C4b taken at the average RU of 5-15 seconds before the injection stop, error bars are the SD of three independent injections. (C) AlphaScreen signal generated with C4b-biotin/myc-EapFL and competed out by untagged Eap3 with and without the addition of 50 µM $ZnCl_2$, *legend inset*.

increase in IC_{50}, from 8.18 x 10^{-5} µM to 1.10 x 10^{-5} µM, a 7.4-fold increase (**UC Fig. 3-3C**). From the above sets of experiments, we can draw the conclusion that Eap domain 3 is able to

coordinate a Zn^{2+} ion upon binding to C4b, and specifically the MIDAS motif of the C345c domain on the γ-chain of C4b. This can be observed in the model described and shown in the manuscript above, as well as a zoomed in model showing the orientation of the His^{308} towards the MIDAS motif (**UC Fig. 3-4**). The minor limitation of the model proposed in the above manuscript is the orientation of the specific EAP domains. In this sense, the proposed structure

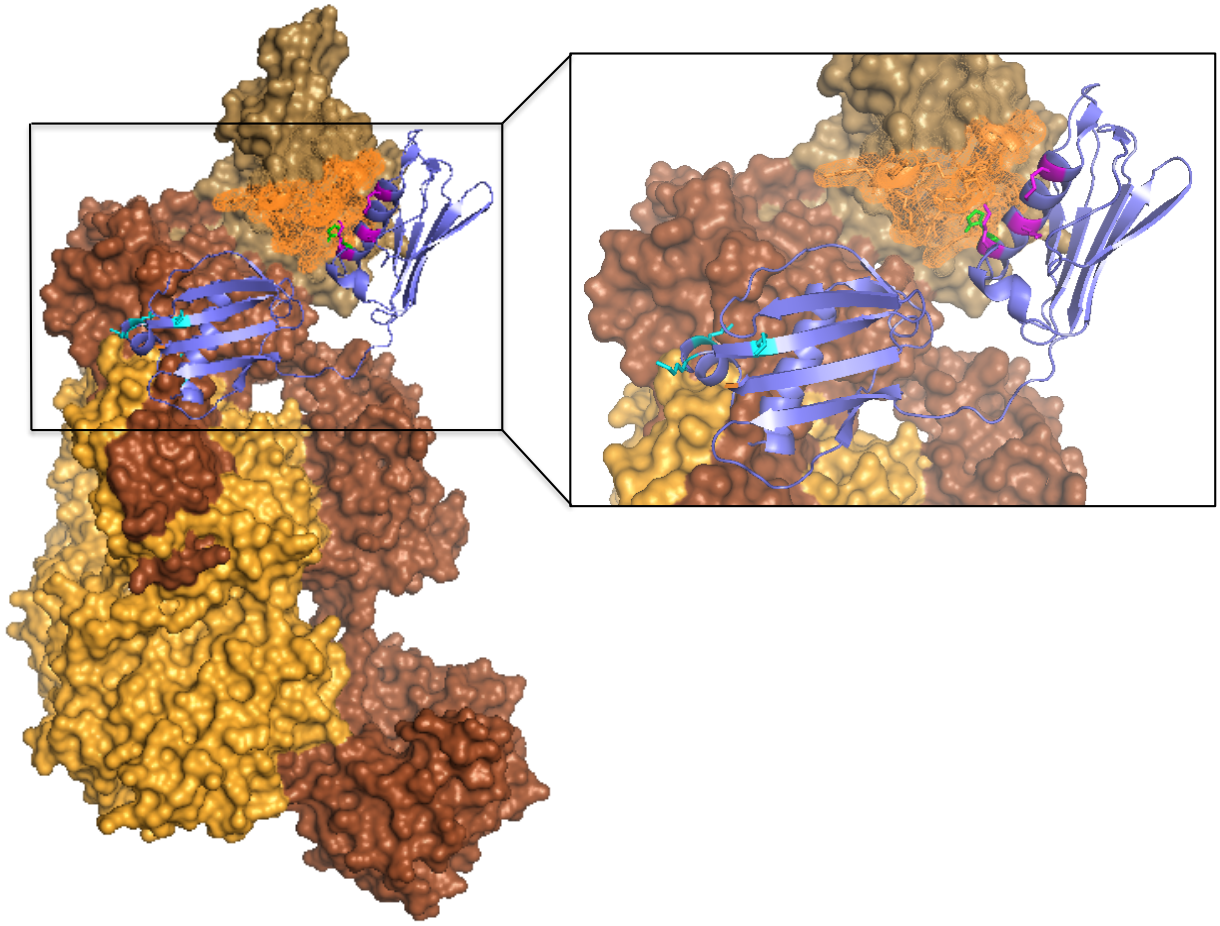

UC Figure 3-4. Model Representation of Eap34 Bound to Complement C4b. Colors represent: Brown = C4b α-chain; Gold = C4b β-chain; Light Brown = C4b γ-chain; Orange = MIDAS motif. Magenta and teal colors on Eap3 and Eap4, respectively, represent identified critical lysine residues observed in the lysine-acetylation foot printing experiments from above manuscript. Zoomed in picture on the right shows the stick orientation of His^{288} (*green*) with respect to the MIDAS motif.

showed Eap4 contacting the C345c domain of the C4b γ-chain, while the Eap3 domain showed contacts with the C4b α'-chain. This is just one of the multiple predictions of this 'complex' using the ClusPro modeling software. Although all the models show similar contact sites between Eap34 and C4b, the orientation of the third and fourth domains are switched in some of

the predicted models. The model shown in **UC Fig. 3-4** shows the domains switched around, and better fits the conclusions drawn after further studies involving metal-coordinated binding of Eap34 to C4b.

A

GSTVPYSINL**NGTSTNIL**SNLSFSNKPWTNYKNLTSQIKSVL**KH**DRGISE
QDLKYAKKAYYTVYFKNGGKRILQLNSKNYTANLVHAKDVKRIEITVK

GSTVPYSINL**AAAAAAAA**SNLSFSNKPWTNYKNLTSQIKSVL**AA**DRGISE
QDLKYAKKAYYTVYFKNGGKRILQLNSKNYTANLVHAKDVKRIEITVK

B

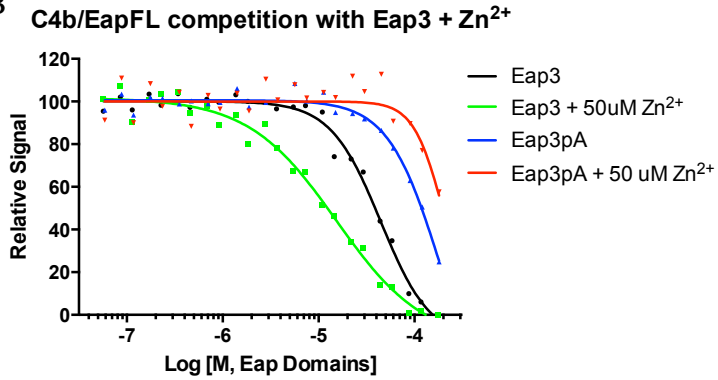

UC Figure 3-5. Site-directed Mutagenesis of Zn^{2+}- Coordinating Residues Observed in the Crystal Structure of Eap3. (A) Sequence of Eap3 with residues that were mutated shown in **bold**. (B) AlphaScreen signal generated by C4b-biotin and myc-EapFL, and competed out with Eap3 and Eap3 with alanine mutations (Eap3pA) with and without the addition of 50 μM Zn^{2+} to the standard buffer.

In order to confirm the observations that we've made using SPR and AlphaScreen, we used site-directed mutagenesis to replace the residues found in the Eap3 metal coordination sites with alanine residues (Eap3pA) (**UC Fig. 3-5A**). Once recombinantly expressed and purified, we set up a similar AlphaScreen using the mutated Eap3 domain with and without the addition of 50 μM Zn^{2+} (**UC Fig. 3-5B**). Results from this showed that with the alanine mutations, there is a decrease in binding to C4b, 4.42 x 10^{-5} μM for Eap3 compared to 1.822 x 10^{-4} μM for Eap3pA, as well as no observable increase in binding after the addition of 50 μM Zn^{2+} (**UC Fig. 3-5B**). Although a structure showing a divalent metal cation being coordinated directly between Eap3 and C4b is needed to confirm the hypothesis stated above, we can conclude that there is an observable difference in binding with the addition of Zn^{2+} to the Eap3/C4b complex.

Appendix – Chapter 3

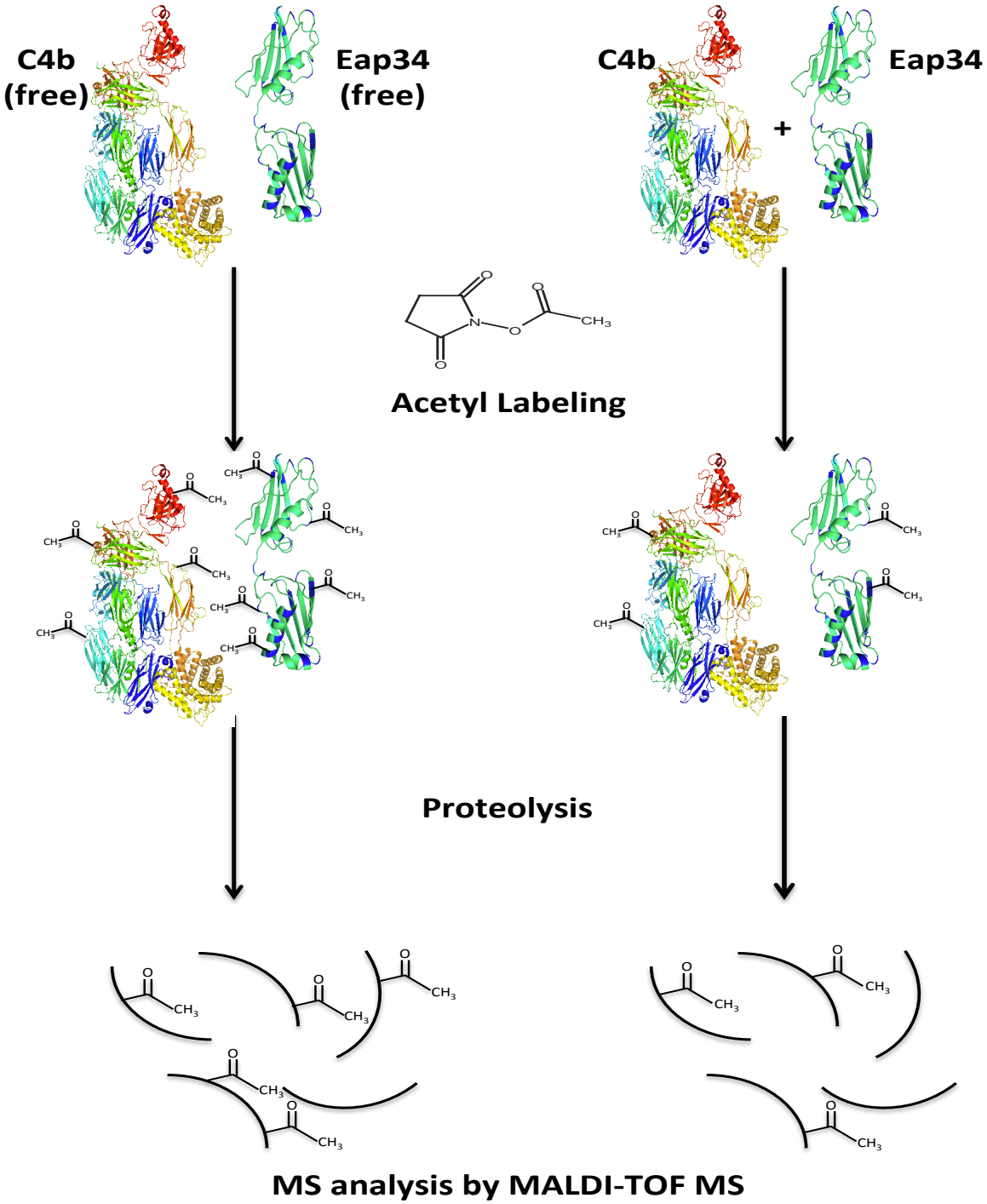

Appendix 3-1. Lysine Acetylation Footprinting of the Interaction Between Eap34 and Complement C4b. Diagram showing the xperimental procedure for lysine footprinting of protein-protein interactions (*top*). The left panel shows the control experiment; all lysine residues in Eap34 are surface exposed when in solution with NHS-Acetyl, and therefore are completely acetylated upon digestion and mass spec analysis (*top, left*). The right panel shows the protection of surface exposed lysine residues upon binding to complement C4b, leading to specific lysine residues missing acetylation upon digestion and mass spec analysis (*top, right*).

Meas. m/z	Calc. m/z	σ (Da)	Rel. Int. (%)	Annotation
609.3080	609.3243	-.0162	100.00	[181-185] KSDIF
786.4217	786.4369	-.0179	10.10	[134-139] ISYKYL
875.5428	875.5197	.0231	6.04	[35-42] TSQIKSVL
908.2521	908.4472	-.1951	6.40	[74-80] QLNSKNY
1523.9233	1523.7781	.1453	91.03	[54-64] KYAKKAYYTVY (3x Acetyl)
1544.8266	1544.8148	.0118	2.46	[54-65] KYAKKAYYTVYF
1545.8440	1545.8523	-.0083	3.38	[109-123] VPYTIAVNGTSTPIL
1563.8119	1563.9105	-.0986	5.47	[124-136] SKLKISNKQLISY (1x Acetyl)
1637.9875	1637.9374	.0501	5.45	[167-180] TVYFKNGKKQVVNL
1639.9766	1639.9418	.0348	2.92	[127-139] KISNKQLISYKYL (1x Acetyl)
1640.9808	1640.8067	.1740	4.24	[22-34] SFSNKPWTNYKNL (1x Acetyl)
1721.0273	1720.9745	.0529	19.52	[62-75] TVYFKNGGKRILQL (2x Acetyl)
1855.0682	1855.0688	-.0005	6.35	[124-138] SKLKISNKQLISYKY (1x Acetyl)
1859.0906	1859.0134	.0772	2.99	[66-80] KNGGKRILQLNSKNY (3x Acetyl)
1888.1208	1888.0498	.0710	4.14	[140-156] NDKVKSVLKSERGISDL
2000.9500	2001.1339	-.1839	1.80	[139-156] LNDKVKSVLKSERGISDL
2674.3140	2674.5026	-.1885	10.43	[191-211] SAKDIKKIDIDVKQYTKSKKK (5x Acetyl)
2697.3067	2697.4822	-.1755	1.36	[134-156] ISYKYLNDKVKSVLKSERGISDL (1x Acetyl)
875.5204	875.5197	.0007	6.86	[35-42] TSQIKSVL
907.4825	9078.4308	.0517	2.56	[22-28] SFSNKPW (1x Acetyl)
1118.4327	1118.5881	-.1554	2.50	[54-61] KYAKKAYY (2x Acetyl)
1253.5704	1253.6565	-.0861	4.09	[56-65] AKKAYYTVYF
1406.5344	1406.7063	-.1719	2.35	[24-34] SNKPWTNYKNL (1x Acetyl)
1523.5880	1523.7781	-.1900	100	[54-64] KYAKKAYYTVY (3x Acetyl)
1598.6233	1598.7962	-.1728	3.89	[22-34] SFSNKPWTNYKNL
1599.6290	1599.7438	-.1148	4.25	[19-31] SNLSFSNKPWTNY (1x Acetyl)
1991.4811	1991.0960	.3850	2.03	[170-185] FKNGKKQVVNLKSDIF (3x Acetyl)
2529.1900	2529.3307	-.1407	1.53	[35-55] TSQIKSVLKHDRGISEQDLKY (2x Acetyl)
2676.1238	2676.3780	-.2543	2.03	[43-64] KHDRGISEQDLKYAKKAYYTVY
2707.1257	2707.4454	-.3197	1.42	[148-170] KSERGISDLDLKFAKQAKYTVYF
2755.3004	2755.3686	-.0682	1.94	[11-34] NGTSTNILSNLSFSNKPWTNYKNL (1x Acetyl)
875.4766	875.5197	-.0431	3.44	[35-42] TSQIKSVL
1523.5078	1523.7781	-.2703	24.69	[54-64] KYAKKAYYTVY (3x Acetyl)
1972.2526	1972.0709	.1816	1.00	[140-156] NDKVKSVLKSERGISDL (2x Acetyl)
2052.4016	2052.1740	.2276	1.48	[124-139] SKLKISNKQLISYKYL (3x Acetyl)
2755.1610	2755.3686	-.2076	2.96	[11-34] NGTSTNILSNLSFSNKPWTNYKNL (1x Acetyl)
2879.9796	2879.5877	.3919	.71	[137-160] KYLNDKVKSVLKSERGISDLDLKF (2x Acetyl)
875.5426	875.5197	.0230	2.87	[35-42] TSQIKSVL
1253.6160	1253.7212	-.1053	3.49	[171-180] KNGKKQVVNL (3x Acetyl)
1253.6160	1253.6888	-.0729	3.49	[157-166] DLKFAKQAKY (1x Acetyl)
1253.6160	1253.6565	-.0405	3.49	[56-65] AKKAYYTVYF
1523.6270	1523.7781	-.1511	23.81	[54-64] KYAKKAYYTVY (3x Acetyl)
1598.6586	1598.7962	-.1376	3.19	[22-34] SFSNKPWTNYKNL
1599.6535	1599.7438	-.0903	3.44	[19-31] SNLSFSNKKOWTNY (1x Acetyl)
1720.5748	1720.9745	-.3997	1.48	[62-75] TVYFKNGGKRILQL (2x Acetyl)
1858.6301	1859.0134	-.3833	23.47	[66-80] KNGGKRILQLNSKNY (3x Acetyl)
2052.5451	2052.1740	.3711	1.98	[124-139] SKLKISNKQLISYKY (3x Acetyl)
2672.1502	2672.4505	-.3003	2.49	[139-160] LNDKVKSVLKSERGISDLDLKF (4x Acetyl)
2674.1657	2674.5026	-.3368	3.52	[191-211] SAKDIKKIDIDVKQYTKSKKK (5x Acetyl)
2676.1834	2676.3780	-.1946	1.67	[43-64] KHDRGISEQDLKYAKKAYYTVY
2707.0954	2707.4454	-.3500	1.03	[148-170] KSERGISDLDLKFAKQAKYTVYF
2755.4142	2755.3686	.0457	1.85	[11-34] NGTSTNILSNLSFSNKPWTNYKNL (1x Acetyl)
2758.4040	2758.5237	-.1197	2.02	[191.211] SAKDIKKIDIDVKQYTKSKKK (7x Acetyl)
2760.3340	2760.3992	-.0651	.63	[43-64] KHDRGISEQDLKYAKKAYYTVY (2x Acetyl)

Appendix Table 3-1. Table of MALDI-TOF mass spectrometry peptides following in-gel digestion. Includes each of the chymotrypsin-digested peptides following SDS-PAGE of lysine foot printing experiments. Changes in background color indicate the four replicates used in determining of lysine acetylation protection upon Eap34 binding to C4b.

Chapter 4 - ^{1}H, ^{15}N, ^{13}C resonance assignments of *Staphylococcus aureus* extracellular adherence protein domain 4

Jordan L. Woehl[1], Daisuke Takahashi[1], Alvaro I. Herrera[1], Brian V. Geisbrecht[1], and Om Prakash[1]

[1]Department of Biochemistry & Molecular Biophysics;
Kansas State University, Manhattan, KS, USA

Biomol. NMR Assign. (2016). 10(2): 301-5

Abstract

The pathogenic bacterium *Staphylococcus aureus* has evolved to actively evade many aspects of the human innate immune system by expressing a series of secreted inhibitory proteins. Among these, the extracellular adherence protein (Eap) has been shown to inhibit the classical and lectin pathways of the complement system. By binding to complement component C4b, Eap is able to inhibit formation of the CP/LP C3 pro-convertase. Secreted full-length, mature Eap consists of four ~7residue domains, all of which adopt a similar beta-grasp fold, and are connected through a short linker region. Through multiple biochemical approaches, it has been determined that the third and fourth domains of Eap are responsible for C4b binding. Here we report the backbone and side-chain NMR resonance assignments of the 11.3 kDa fourth domain of Eap. The assignment data has been deposited in the BMRB database under the accession number 26726.

Biological Context

Staphylococcus aureus is one of the leading causes of health care-associated and community-acquired infections (132). One reason for this trend is the increasing number of drug resistant strains of *Staph* that are insensitive to standard antibiotic treatments, and which have been shown to account for upwards of 50 % of all *S. aureus* strains causing disease within the healthcare system (39). While antibiotic resistance is a significant threat to public health on its own, the enhanced virulence of widespread clinical strains is not simply due to their resistance phenotypes (133, 134). Indeed, the ability of *S. aureus* to thrive in many tissues within its host can be attributed to its array of secreted virulence factors that interfere with the host's immune response. A number of these virulence factors have been shown to specifically bind to and inhibit components of the complement system, which serves as a critical aspect of innate immunity

responsible for opsonizing and killing invading pathogens. Recent reviews have highlighted many of the underlying mechanisms by which these virulence factors are able to inhibit various facets of the innate immune system, including complement (116, 135).

The extracellular adherence protein (Eap) has been shown to affect multiple aspects of the innate immune system, and contributes to the overall virulence of *Staphylococcus aureus* (40, 75). Eap is secreted as a 50- to 70-kDa protein depending upon the specific strain in question, and consists of multiple ~97 residue repeating EAP domains (1). Each EAP domain is characterized by a beta-grasp fold and is connected to the adjacent domain through a short (~10 residue) linker region. Through a multi-disciplinary approach involving analytical ultracentrifugation and small-angle X-ray scattering, Hammel et al. determined that Eap adopts an elongated, but structured conformation in solution (2). Subsequent experimentally-constrained structural modeling on a four-domain isoform of Eap suggested a potential for transient interactions between adjacent pairs of EAP domains, most notably Eap1 with Eap2, and Eap3 with Eap4. Indeed, Raman spectroscopy studies of samples comprised of full-length Eap versus a stoichiometric mixture of all four individual domains revealed that interdomain interactions are detectable, but only in the context of the full-length protein (2). This dependence on the linker regions that connect the domains argues that any interdomain interactions are very low affinity on their own, and EAP domains are unlikely associate with one another at physiologically-relevant concentrations.

Whereas several *S. aureus* complement inhibitors block the alternative complement pathway by binding C3b and disrupting the multi-subunit alternative pathway C3 convertase complex (C3bBb) which processes additional C3 into C3b, Eap instead targets the classical and lectin complement pathways. Though they are initiated by distinct stimuli, the classical and

lectin pathways of complement converge at the point of C4, which is then cleaved to form C4b. C4b binds to complement component C2, forming the C3 pro-convertase (C4bC2). Cleavage of C4b-bound C2 forms the fully active C3 convertase of the classical and lectin pathways (C4bC2a), which is also able to proteolyze C3 into C3b. Eap has been shown to bind with a nanomolar affinity to C4b, and competes out the interaction between C4b and C2. In this manner, Eap blocks activity of the classical and lectin pathways by inhibiting formation of their C3 pro-convertase (40).

Neutrophils also play a critical role in the innate immune response against invading bacterial pathogens. Upon activation, neutrophils release a number of chymotrypsin-like serine proteases into their phagocytic compartment or extracellular environment, including neutrophil elastase, cathepsin G, and proteinase 3 (112). These so-called neutrophil-serine proteases (NSPs) have been shown to degrade outer membrane components of bacteria as well facilitating in the removal of secreted bacterial virulence factors (76). Recently, Eap as well as two homologs comprised of a single EAP repeat, called EapH1 and EapH2, have been shown to bind and inhibit NSPs (75). Mechanistically, Eap, EapH1, and EapH2 bind in a non-covalent manner with nanomolar affinity to each NSP and appear to block substrate access to the protease catalytic cleft (75).

Although the mechanisms of classical and lectin pathway complement inhibition and NSP inhibition have been identified, the structural basis for these diverse activities of EAP domain proteins remain poorly understood. This is particularly intriguing because while all EAP domains appear to be equally potent inhibitors of NSPs, only an Eap fragment containing domains 3 and 4 retained high affinity C4b binding and CP/LP inhibitory activity similar to the full-length Eap protein. Here, we report the backbone ^{1}H, ^{15}N, and ^{13}C resonance assignments for

the fourth domain of the extracellular adherence protein (i.e. Eap 4). These assignments and the structure calculations will be invaluable in identifying specific binding-site interactions between Eap4 and its partners and will promote further NMR-based solution characterization of EAP proteins.

Materials and experiments

A DNA fragment encoding the linker-free Eap4 sequence (residues 374-468 of accession code WP_001557458.1) was subcloned into the *Sal*I and *Not*I sites of the prokaryotic expression vector pT7HMT (88). The recombinant protein expressed from this plasmid retains a "Gly-Ser-Thr" artifact at its N-terminus following digestion by tobacco etch virus (TEV) protease when removing the polyhistidine purification tag. Uniformly ^{15}N- and/or ^{13}C-labeled Eap4 was expressed in *E. coli* BL21(DE3) cells grown in M9 minimal media supplemented with 1 g/L $^{15}NH_4Cl$ and 2 g/L ^{13}C-d-glucose for ^{15}N-labeling and ^{13}C-labeling, respectively. The cells containing the expression plasmid were grown in a starter culture consisting of 30 mL LB media supplemented with kanamycin at 37 °C overnight. The starter was centrifuged and re-suspended twice in sterile PBS to wash out excess LB. The pellet was then re-suspended in M9 minimal media, grown at 37 °C to an OD_{600} value of 0.8–1.0, induced with 1.0 mM isopropyl β-d-thiogalactoside, and further grown at 18 °C overnight. The cells were harvested by centrifugation (7000 RCF for 15 min, 4 °C), and subsequently re-suspended in native binding buffer and lysed using a microfluidizer. After a second centrifugation (30,000 RCF for 35 min, 4 °C), the cell lysate supernatant was purified using a gravity flow Ni–NTA affinity column. Overnight dialysis into native binding buffer and TEV-protease cleavage was performed to remove the hexahistidine and c-myc epitope tags. The protein was re-purified over a reverse Ni–NTA affinity column to remove the cleaved hexahistidine and c-myc epitope tags. Size exclusion

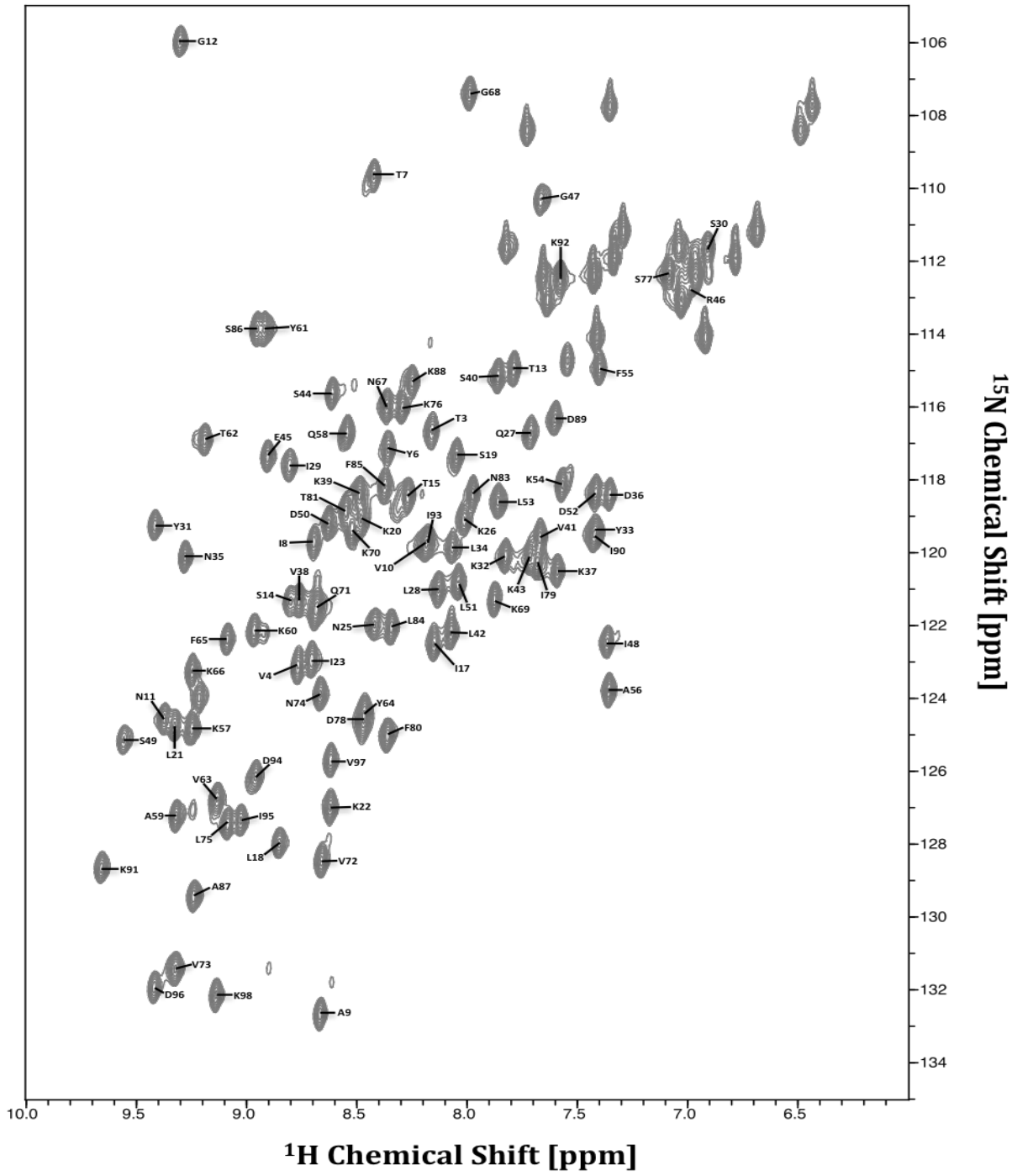

Figure 4-1. 2D $^{1}H–^{15}N$ HSQC spectrum of 0.7 mM $^{13}C/^{15}N$-labeled Eap4. Recorded at 298 K on a Bruker 800 MHz Avance III spectrometer equipped with a TCI cryoprobe. Sequence specific assignments are indicated by single letter residue name and sequence number. Backbone assignments and data collection done with help from Om Prakash lab.

chromatography on a HiLoad 26/600 Superdex 75 prep grade (GE healthcare) was employed as a final purification step. The final protein yield was 7–10 mg from 1 L of growing culture and all

NMR samples contained 0.5–1.0 mM uniformly ^{15}N- or $^{13}C/^{15}N$-labeled Eap4 in NMR buffer (50 mM sodium phosphate pH 6.5 and 0.1 % NaN_3) in 95 % H_2O/5 % D_2O.

NMR measurements were carried out at 25 °C on a Varian 500VNMR System (Agilent Technologies) equipped with a 5 mm triple-resonance inverse detection pulse gradient cold probe operating at 499.84 MHz for ^{1}H frequency, and on a Bruker 800 MHz Avance III spectrometer equipped with a TCI cryo-probe. Backbone resonance assignments were achieved using the following NMR spectra: 2D ^{1}H–^{15}N HSQC and 3D HNCA, HN(CO)CA, HNCACB, CBCA(CO)NH, and HNCO. The following NMR spectra were collected for side chain assignments: 2D ^{13}C HSQC and 3D (H)C(CCO)NH-TOCSY, H(CCCO)NH-TOCSY, HCCH-TOCSY, and ^{15}N-edited NOESY (mixing time 100 ms). Validation of the assignments has also been conducted with the ^{13}C-NOESY-HSQC spectrum. All NMR spectra were processed using NMRPipe (136), and analyzed with CARA (http://www.nmr.ch) and UNIO (http://perso.ens-lyon.fr/torsten.herrmann/Herrmann/Software.html) (137). The ^{1}H chemical shift assignment was referenced by using 2,2-dimethy-2-silapentane-5-sulphonic acid (DSS) at 25 °C as a standard. The ^{13}C and ^{15}N chemical shift were referenced indirectly.

Extent of assignments and data deposition

2D ^{1}H–^{15}N HSQC measurement of Eap4 resulted in a well-dispersed spectrum (**Fig. 4-1**). Amino acid numbering is based upon the authentic Eap4 sequence, excluding the N-terminal His tag, c-myc tag, and TEV-protease cleavage recognition site. A total of 97 % of backbone ^{1}H and ^{15}N resonances of 95 non-proline residues, and 100 % of all $^{13}C_{\alpha}$ resonances, $^{13}C_{\beta}$ resonances, and $^{13}C'$ resonances have been unambiguously assigned based on a standard set of triple resonance spectra described above. The backbone amide residues that could not be assigned include G1, S2, and S24. G1 and S2 lie in a loop region of the artifactual N-terminus as

a result of the subcloning procedure, while S24 lies in the C-terminal region of a short β-strand as judged by comparison to the secondary structure prediction and alignment to the crystal structures of three EAP domains (1). Side chain ^{1}H and ^{13}C resonance assignments were 90 % completed excluding aromatic rings. The secondary structure elements of Eap4 were predicted by the TALOS+ program (138) using the resonance assignments of $^{13}C_{\alpha}$, $^{13}C_{\beta}$, and $^{13}C'$ (**Fig. 4-2**). This prediction is in excellent agreement with the secondary structures observed in EapH1, EapH2, and Eap2, as determined by X-ray crystallography (1). The chemical shift assignments have been deposited in BioMagResBank (http://www.bmrb.wisc.edu) under the accession number 26726.

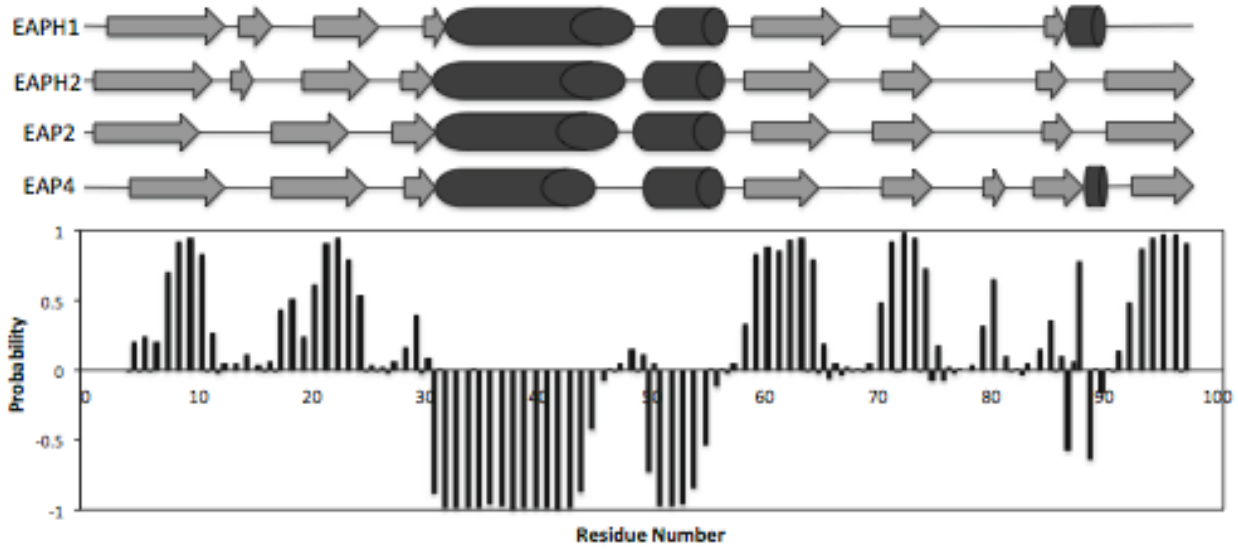

Figure 4-2. Secondary structure prediction for the Eap4 domain based on the TALOS+ program using obtained chemical shift values. β-strand probabilities are given by *positive values*, α-helices are given by *negative values*, and loop regions are given by *values* approximately from -0.3 to 0.3. Shown in the *top portion* are the secondary structure topology obtained from the published crystal structure of EapH1, EapH2, and Eap2 (1) and the TALOS+ prediction of Eap4 with α-helices shown as *cylinders* and β-sheets shown as *arrows*. The predicted secondary structure of Eap4 shows very similar topology to the other three EAP domains whose crystal structures are available. Assignments and data collection done with help from Om Prakash lab.

Acknowledgements

This work was supported by the American Heart Association Midwest Affiliate Pre-doctoral Research Fellowship 15PRE25750013 and by National Institutes of Health (NIH) Grant AI111203.

Unpublished Conclusions

Through the use of the CS-Rosetta program (139, 140), which uses a selection of protein fragments from the PDB database in addition to the chemical shift values obtained from the backbone assignments shown in **Fig. 4-1**, we can determine the three dimensional structure without the use of side chain assignments and structural refinement. Although the obtained structure is just a model based on the chemical shift values and similar, published PDB structures, we know through previous structural studies that Eap domains all have similar secondary structures (1, 2, 75). The obtained structure(s) given through calculations in the CS-Rosetta program show the 10 most likely, energy minimized, structures of Eap4 (**UC Fig. 4-**1). Each of the domains, including EapH1 and EapH2, have been structurally characterized through X-ray crystallography and an overlay of the structures can be seen in **UC Fig. 4-2** (EapH1/H2 structures not shown) (1).

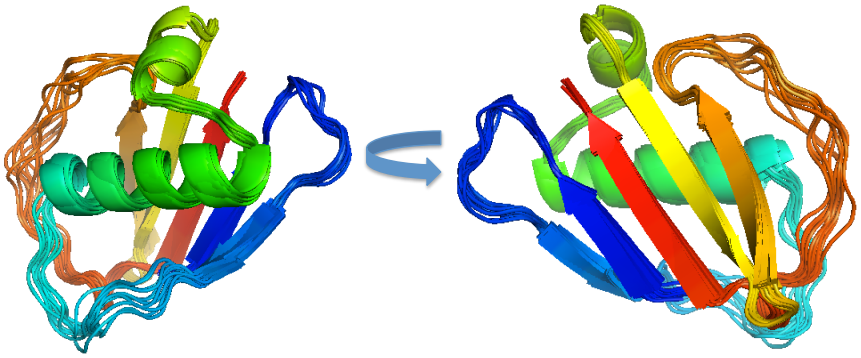

UC Figure 4-1. Overlay of energy minimized structures of Eap4 obtained through CS-Rosetta modeling.

From a direct observation of the four aligned structures, there are no obvious structural differences that would give clarity to the specificity of the different domains for complement C4b as well as neutrophil serine proteases (40, 75, 76). Because of the lack of structural variances, the obvious conclusion would suggest that there is specificity in the sequences of each of the domains for their different targets. To look at this more closely, a direct sequence alignment of the Eap single domains in the regions of Eap3 and Eap4 shown to bind C4b through a lysine acetylation footprinting technique observed in Chapter

3, **Figs. 3-4 and 3-5**, can be seen in **UC Fig. 4-3**. Additionally, a structural alignment with the C4b binding regions shown with stick residues can be seen in **UC Fig. 4-4**. Although there are many conserved residues between the four domains highlighted in red, its obvious that the regions in Eap3 and Eap4 shown to bind C4b show noticeable differences from Eap1 and Eap2. Specifically, residues N30 to I35 of Eap3 only contains a conserved leucine at position 31 when compared to the other three domains. Additionally, as discussed in more detail in Chapter 3, Unpublished Conclusions, there is a histidine at position 41 that shows no conservation in any other known EAP domains. Although the metal-coordinated binding of Eap3 to C4b is not conclusive, the fact that this histidine residue is specific to this EAP domain provides additional evidence that the observed conclusions are significant in understanding the binding properties of this protein.

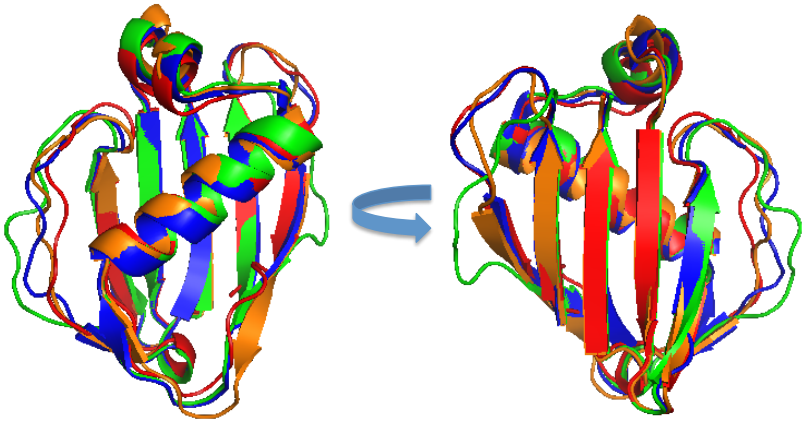

UC Figure 4-2. Overlay of EAP domains 1-4 from *S. aureus* strain Mu50. EAP domains are overlayed through the large alpha helix observed in each of the domains.

In addition to the observations made from Eap's domain specificity for complement C4b, recent publications from Stapels et al. have described domain specificity of EapH1, EapH2, and Eap for binding to neutrophil serine proteases (NSPs) (75, 76). Through structural studies of EapH1 bound to neutrophil elastase (hNE), as well as ClusPro modeling of EapH2 bound to hNE, Stapels et al. was able to show that there are distinct regions in EapH1 and EapH2 that are critical for their interactions with hNE and their inhibitory properties (75, 76). Interestingly, even though EapH1 and H2 show ~45% sequence similarities, the regions required for their binding

and inhibitory activity differ significantly. This can only be explained by the fact that each of the two EAP domains are interacting with hNE using different regions, meaning they both have their own specific mechanisms for inhibiting NSPs.

Eap1	K	D	I	E	N	K	V	K	S	V	L	Y	F	N	R	G	I	S	D	I	D	L	R	L	S	K	Q	A	E
Eap2	K	D	L	E	G	K	V	K	S	V	L	E	S	N	R	G	I	T	D	V	D	L	R	L	S	K	Q	A	K
Eap3	K	N	L	T	S	Q	I	K	S	V	L	K	H	D	R	G	I	S	E	Q	D	L	K	Y	A	K	K	A	Y
Eap4	K	Y	L	N	D	K	V	K	S	V	L	K	S	E	R	G	I	S	D	L	D	L	K	F	A	K	Q	A	K

UC Figure 4-3. Sequence alignment of EAP domains 1-4 from *S. aureus* strain Mu50. Sequence alignment of the Eap3/Eap4 C4b binding regions observed in from the lysine acetylation footprinting experiments. Residues highlighted in red indicate conserved residues found in all four of the EAP domains. Residues highlighted in green and blue indicate the Eap3 and Eap4 regions critical for binding C4b, respectively.

The inhibitory properties of EAP domains inhibiting NSPs can be described further by the fact that Eap from strain Mu50 can bind multiple NSPs, and specifically, one NSP for every EAP domain (Eap from Mu50 interacts with four NSPs) (75, 76). Using a surface plasmon resonance approach, conjugating hNE to the surface of an SPR chip, we were able to show that each of the single EAP domains in Eap-Mu50 are able to independently interact with hNE with similar affinities (**UC Fig. 4-5**). Although there are no structures or ClusPro models of EAP domains from Mu50 bound to hNE, observations of the SPR binding curves give evidence to the fact that each of the domains interacts with hNE differently, similar to what was seen in EapH1 and EapH2. Using a 1:1 kinetic model to fit the observed SPR, dose-response curves, we were able to obtain binding affinitys for each of the single domains bound to hNE. These K_D values are 1.05 nM, 6.7 nM, 0.545 nM, and 0.0179 nM for Eap1, Eap2,

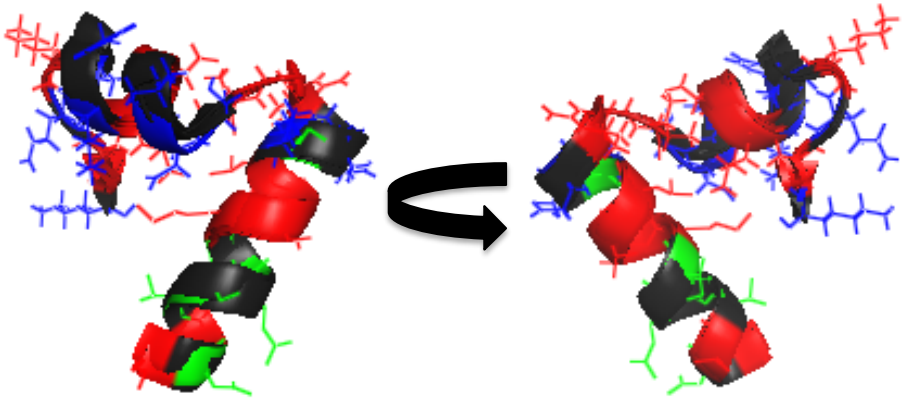

UC Figure 4-4. Structural alignment of the sequence regions shown in UC Figure 4-3. Colors are coordinated with the above color scheme with conserved regions and C4b binding regions shown with stick models.

Eap3, and Eap4, respectively. The shape of the binding curves and the concentration of EAP needed to reach saturation, in addition to the relative affinitys, highlight clear differences in how these proteins interact with hNE. This provides additional evidence that sequence differences between each of the EAP domains are critical for interacting with their specific targets and that each of the EAP domains have a unique mechanism of action for inhibiting NSPs and the complement cascade.

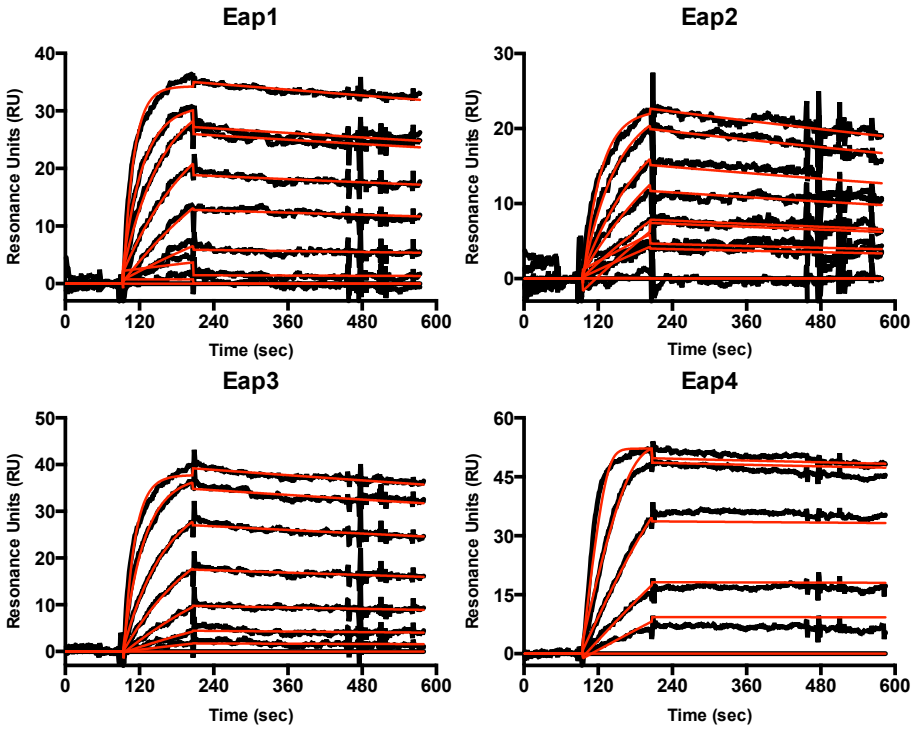

UC Figure 4-5. Surface plasmon resonance dose-response curves of EAP domains binding to human neutrophil elastase. EAP single domains are injected over hNE for 120 seconds in a dose-dependent manner (0-500 nM). Original curves are shown in black and fit using a 1:1 kinetic model, fits shown in red.

Chapter 5 - Structural comparisons of the extracellular adherence protein in *S. aureus* strain Mu50 vs. strain Newman

Jordan L. Woehl[1], Kasra X. Ramyar[1], Dimitrios C. Mastellos[2], and Brian V. Geisbrecht[1]

[1]Department of Biochemistry & Molecular Biophysics;
Kansas State University, Manhattan, KS, USA
[2]National Center for Scientific Research;
Athens, Greece

Manuscript in preparation

Abstract

C-evolution of *Stapyhlococcus aureus* alongside the humans has forced an evolutionary response to ensure pathogenesis of the bacterium and avoid the killing power of the immune system. Throughout this co-evolutionary period, there has been an emergence of new bacterial strains, each with a slightly variant genetic makeup, which allows them to combat the phagocytic effects of the immune response. These slight variations can lead to a change in surface chemistry of the bacteria, allowing it to avoid detection by the innate and adaptive immune response, or it can lead to variable and in some cases, new virulent factors that have mutated in order to block specific a phagocytic response. Interestingly, *S. aureus* strain Mu50 and strain Newman both include the genetic material to produce the secreted virulence factor, the extracellular adherence protein (Eap), but strain Newman releases a protein with five EAP domains as opposed to the four domain version released by strain Mu50. Although there is a change in the structural characteristics of Eap, this didn't amount to a distinguishable difference in the affinity of each protein for its complement target, C4b. We would expect that similar affinities would lead to similar levels of inhibitory activity on the complement cascade but strain Newman was a significantly better inhibitor of complement activity. Without a co-crystal structure to compare the two Eap/C4b complexes, we conclude that the Eap-Newman protein must be occupying a larger surface area on C4b, allowing it to better inhibitor of C2 binding and formation of the CP/LP C3-proconvertase through an increased steric clash. In addition, this effect can be seen on the overall virulence of the bacteria with recombinant Eap from strain Newman increasing the survival of *S. aureus* in a whole blood model as opposed to Eap from strain Mu50.

Introduction

The *Staphylococcus aureus* bacterium has survived and thrived alongside humans for centuries based on its ability to adapt and mutate in order to evade the phagocytic effects of the immune systems. In addition, *S. aureus* is able to thrive in a wide range of sites in the body, including the nose, respiratory tract, and on the skin. This ability can be attributed to the numerous virulence factors, adhesins, nucleases, toxins, and immune evasion proteins that are produced and released upon infection to attack and inhibit specific aspects of the immune response (44, 116). Identification and characterization of all of these virulence factors is a daunting task but can help researchers explain how these pathogens have evolved to counteract any change in the immune response. Mutations in the *S. aureus* genome have led to a number of strains being resistant to a significant number of newly developed antibiotics, labeling these strains as methicillin-resistant *S. aureus* or MRSA. Because of *S. aureus's* ability to out mutate the development of new antibiotics and vaccines, finding treatment for this bacteria has become a daunting task in recent years. Although a number of genome sites are highly conserved like metabolism, strain by strain differences have been seen in amino acid/nucleotide biosynthesis, virulence factors, enzymes, non-coding RNA, transcription factors, etc. which makes treating this bacteria more difficult. The highly variable regions of genome were likely acquired through genomic islands horizontal integration through DNA recombination (141). These variable regions likely carry genes for virulence properties and antibiotic resistance, which aids in the pathogenesis of the bacteria, and the combination of these acquired gene blocks can be directly linked to the manifestation of *S. aureus* disease in humans (141, 142).

MRSA strains N315 and Mu50 were the first *S. aureus* genomes to be completely sequence in order to compare and study their antibiotic resistance and virulence (143). This led

to the whole genome sequencing of a number of other strains, and specifically, strain Newman was isolated and sequenced in 1952 from a human infection (141, 144). This strain has been particularly useful in animal models to mimic the effects of disease states due to its potent virulent phenotypes. In comparison to the Mu50, which we have elucidated a number virulent factor mechanism, strain Newman is very similar in its genetic makeup. Both have similar sequence length (2.88 Mb), protein coding regions (~2700), and tRNAs (~60), but their main differences lie in the number of insertion sequences, 12 for strain Newman and 23 for strain Mu50 (141).

In the context of this manuscript, we wanted to compare the strain-by-strain differences in the extracellular adherence protein (Eap), a virulence factor secreted during infection. Both contain the genetic makeup to produce Eap, as well as the two structurally related homologs, EapH1 and EapH2. Genetic analysis of the produces released by these two strains reveals that Eap from Mu50 contains four domains while Eap from Newman contains five domains. Previous work has shown that Eap from strain Mu50 is a potent inhibitor of the classical (CP) and lectin (CP) pathways of complement through its direct competitive inhibition of C2 binding to C4b and formation of the CP/LP C3-proconvertase (40). Additionally, only two of the domains, Eap3 and Eap4, are critical for binding to C4b and the inhibitory effects on the complement cascade (40). Through a genetic and structural approach, we want to examine the differences in the makeup of the proteins and the mechanistic ability of the Eap-Newman protein to act on the CP and LP.

Since the discovery of Eap, there has been numerous publications stating that Eap binds to extracellular matrix proteins like fibrinogen, fibronectin, vitronectin, prothrombin, etc. so we also want to examine the mechanistic understanding of this binding and the differences in binding between the Mu50 and Newman proteins (100, 145). In addition, Eap has been shown to

be a potent inhibitor of the neutrophil serine proteases elastase, cathepsin G, and proteinase 3, but an understanding of the structural differences in the two strains is beyond the scope of this manuscript (75, 76). With this wide-range of potential binding partners, the effects of this protein on the virulence of *S. aureus* is critical and genetic loci encoding this protein are found in >98% of all examined strains (145). Because of this, we screened a library of small-chain variable fragment (scFv) antibodies for specific binders of Eap34. We identified one antibody that specifically binds to this protein and characterized the domain interaction as well as a possible anti-microbial mechanism against *S. aureus* survival.

Results

Pairwise identity between Eap from strain Mu50 and Eap from strain Newman identifies an unexpected homology and new domain – Using the BLAST program, each single EAP domain from strain Mu50 was compared against each single EAP domain from strain Newman in a pairwise manner, as well as compared to structurally related homologs, EapH1, EapH2, EapH1-N, EapH2-N and SAV1937. These BLAST values were plotted as a percentage of sequence similarities between the Mu50 domains and the Newman domains (**Fig. 5-1**). From this

PAIRWISE IDENTITY BETWEEN EAP-MU50 AND EAP-NEWMAN (BLAST Two Sequences)

	Eap1	Eap2	Eap3	Eap4	SAV1937	EapH1	EapH2	Eap1N	Eap2N	Eap3N	Eap4N	Eap5N	EapH1_N	EapH2_N
Eap1	*													
Eap2	83	*												
Eap3	49	52	*											
Eap4	57	63	59	*										
SAV1937	31	37	32	34	*									
EapH1	32	37	26	35	36	*								
EapH2	43	48	35	45	36	48	*							
Eap1N	84	96	52	62	31	33	43	*						
Eap2N	83	99	52	64	37	36	47	86	*					
Eap3N	49	52	100	58	32	26	35	52	52	*				
Eap4N	53	55	56	61	28	37	40	52	55	55	*			
Eap5N	57	63	59	100	34	35	45	62	64	59	62	*		
EapH1_N	33	38	26	35	22	95	48	34	38	26	37	35	*	
EapH2_N	43	48	34	45	36	49	100	43	48	34	39	45	48	*

Figure 5-1. The Pairwise Identity Between Eap-Mu50 and Eap-Newman through BLAST Sequence Comparison. Single EAP domains from Mu50 and Newman were BLASTed against one another and the pairwise sequence similarities were shown as a percentage. The *green* color shows the high percentage of sequence conservation between Eap2-Mu50 with Eap1/Eap2-Newman, Eap3-Mu50 with Eap3-Newman, and Eap4-Mu50 with Eap5-Newman. The *orange* color highlights the Eap4-Newman domain that does not show sequence similarities to any of the Eap-Mu50 domains. The *blue* color shows the comparison between EapH1/H2-Mu50 with EapH1/H2-Newman.

pairwise comparison, we can see that EapH1 and EapH2 from strain Mu50 and Newman are almost identical at 95% and 100%, respectively. In addition, the comparison between Eap3 and

Eap4 from Mu50 are 100% identical to Eap3 and Eap5 from Newman, respectively. The interesting difference in the sequence besides the addition of a fourth domain to strain Newman that shows no sequence similarities to any other EAP domain, is the Eap1 and Eap2 Newman domains are identical to the Eap2 domain of Mu50. Adding this data together and putting it in sequence with respect to the Mu50 EAP domains, we have Eap Mu50, 1-2-3-4, and Eap Newman, 2-2-3-4N-4. The main difference between the two is Eap Newman has a non-similar fourth domain and an extra Eap2 domain with no Eap1 domain.

Staphylococcus aureus strain Mu50 Eap proteins bind with a similar affinity to strain Newman proteins – Although there is a difference in the number of domains and the domain orientation with respect to the Eap proteins from both strains, we wanted to know if the addition of a fifth domain made a difference in the affinity for complement C4b. Using an AlphaScreen similar to previous work as well as generating a signal using myc-tagged EapFL-N and Eap344-N, we were able to directly compete out the interactions with untagged EapFL, Eap34, EapFL-N, and Eap345-N (**Figs. 5-2A, B, C, and D**). Comparison of the direct K_D values shows that EapFL and EapFL-Newman bind with similar affinities, 1.969 x $10^{-}7$ M and 3.743 x 10^{-7} M, respectively. A major difference is in the comparison the K_D values between Eap34 and Eap345-N, 5.858 x 10^{-7} M and 1.607 x 10^{-7} M, respectively, which is a 3.6-fold increase in affinity with the addition of the new fourth domain. This indicates that a change from four domains to five domains does not make a difference because there is not additional space for a fifth domain to interact on C4b, and the first and second domains are not required for binding and inhibition, but addition of the new fourth domain increases the affinity of the Newman protein. This could be based merely on electrostatic interactions between Eap and C4b, which would mean the three-domain (Eap345) protein is more electrostatically positive than the two-domain (Eap34) form.

Additionally, the Eap4-Newman protein by itself shows no difference in affinity for C4b than the Eap3 and Eap4 proteins of Mu50 (*data not shown*).

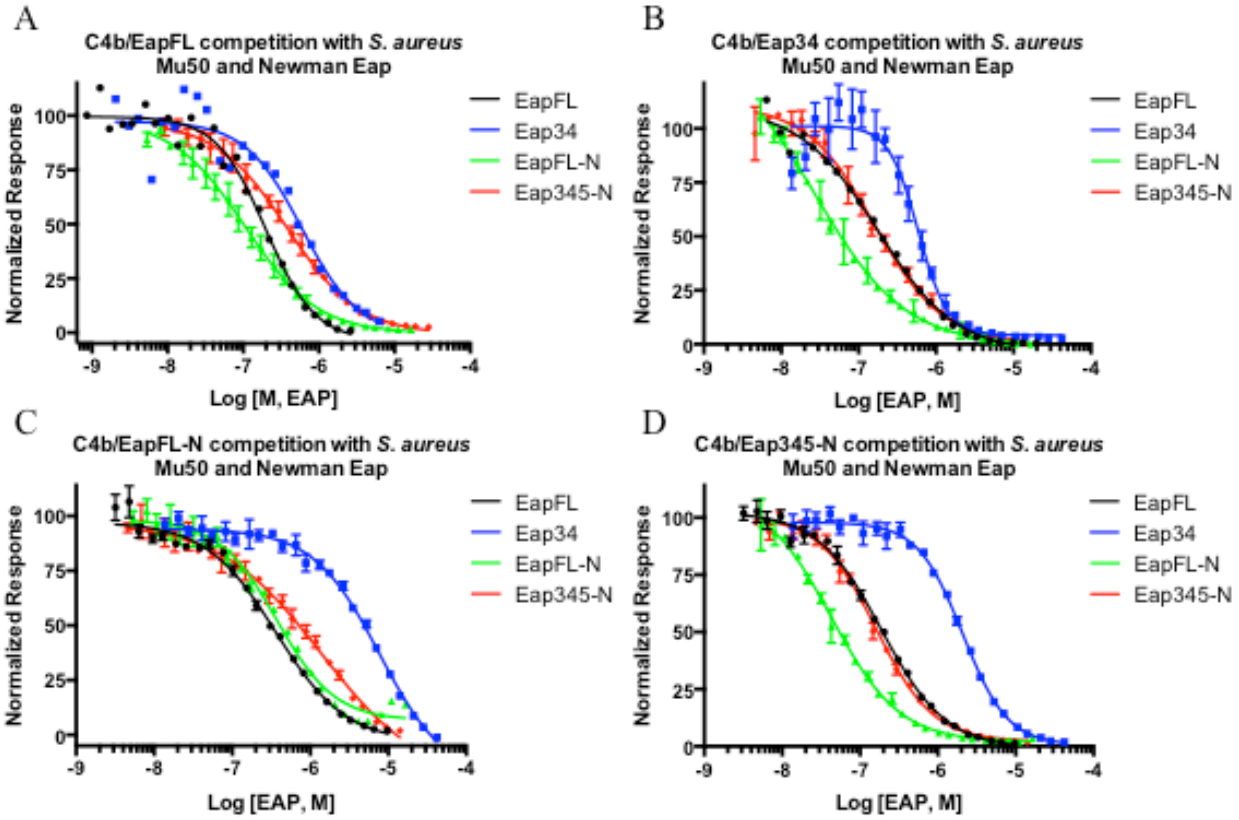

Figure 5-2. Eap Proteins from Strain Mu50 and Strain Newman Contain a C4b-binding Site. (A-D) The ability of untagged EapFL, Eap34, EapFL-N, and Eap345-N to compete the AlphaScreen signal generated by myc-tagged Eap (listed above) and C4b-biotin was assessed over a logarithmic dilution series. Data here are the average of three independent experiments and the error bars indicate +/- SD. Legend is inset.

Addition of a fifth domain to Eap Newman increases the complement inhibitory activity of the protein when compared to the four domain Eap Mu50 protein – We have shown that the difference in affinity between the Mu50 and Newman Eap proteins is minor with the addition of a fifth domain. Using an ELISA based approach; we wanted to compare the difference in complement inhibitory activity between the two strains. Activation of complement was done through the lectin pathway and complement activity was tested through the deposition of C3b and C5b-9 (**Figs. 5-3A, B**). Similar to the binding affinity for C4b, we see that the full-length proteins from Mu50 and Newman inhibit complement activity with similar IC_{50} values, 7.105 x 10^{-8} M (C3b)/7.493 x 10^{-8} M (C5b-9) and 8.890 x 10^{-8} M (C3b)/8.049 x 10^{-8} M (C5b-9),

respectively. Once again, the main difference was with the Eap34 and Eap345 proteins, with IC_{50} values of 2.271 x 10^{-7} M (C3b)/1.630 x 10^{-7} M (C5b-9) and 4.580 x 10^{-8} M (C3b)/4.498 x 10^{-8} M (C5b-9), respectively, corresponding to a 3.6- and 5-fold difference in complement inhibitory activity. Interestingly, the Eap345 protein from strain Newman was the best inhibitor of complement activity even compared to the full-length proteins.

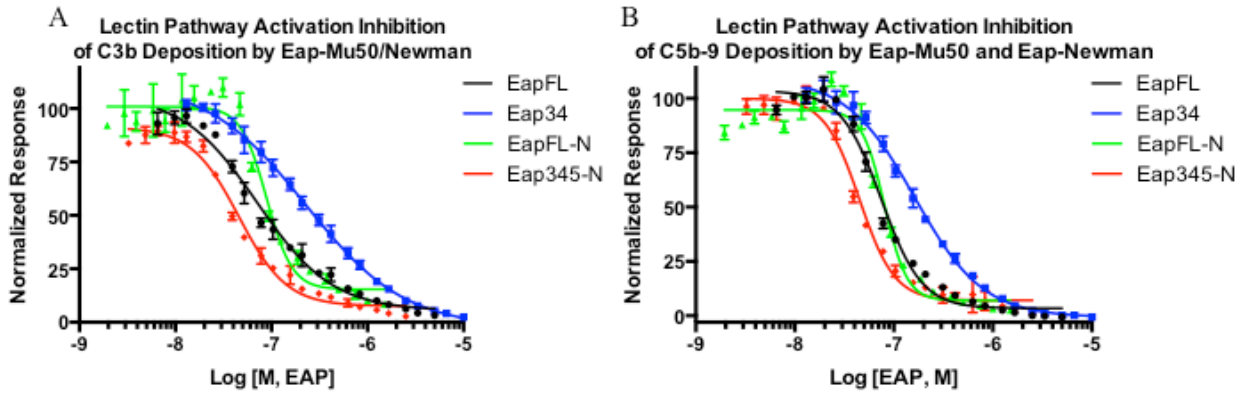

Figure 5-3. Eap from Strains Mu50 and Newman Inhibit the Lectin Pathway of Complement. Lectin pathway complement activity was assessed over a logarithmic dilution series of various Eap-Mu50 and Eap-Newman proteins. 1% (v/v) NHS was used as a source of complement components, and each assay point was repeated in triplicate prior to fitting each series to a dose-response curve. Legends are inset. (A/B) Lectin pathway activity in the presence of EapFL, Eap34, EapFL-N, and Eap345-N was assed by ELISA specific for either C3b (*left*) or C5b-9 (*right*) deposition.

Eap from strains Mu50 and Newman bind directly to an additional target protein, fibrinogen – Although previous research on Eap has been shown to bind extracellular matrix proteins, no direct evidence of this binding has been shown. Using an ELISA-based approach by coating the surface of the plate with Fibrinogen, we see that the Eap proteins bind in a concentration dependent manner to the surface, with SCIN-A as a negative control showing zero binding (**Fig. 5-4**). Interestingly, Eap proteins from strain Newman bind with greater strength to the fibrinogen-coated surface than Mu50 Eap proteins, specifically a 2.5 to 5-fold increase in

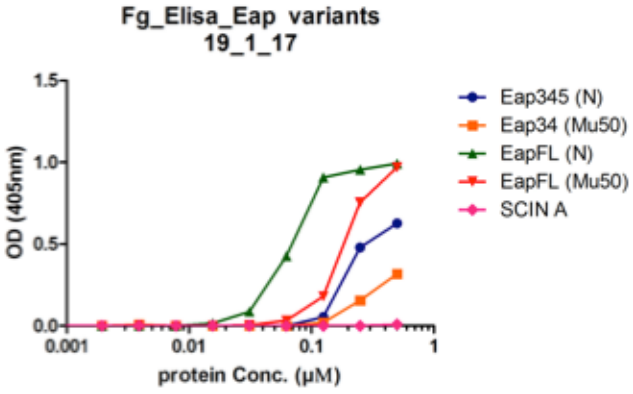

Figure 5-4. Eap proteins from strain Mu50 and Newman bind directly to a fibrinogen-coated ELISA surface. The ability of Eap EapFL, Eap34, EapFL-N, Eap345-N, and SCIN-A (negative control) to bind directly to fibrinogen was assessed over a logarithmic dilution series. Legend is inset. Data collected from Dimitris C. Mastellos lab.

binding when comparing the Newman strain to the Mu50 strain.

Identification of a small-chain variable fragment (B1scFv) antibody that binds directly to Eap34 – Through the use of a phage-display approach to test for a library of scFv antibodies that bind directly to Eap, we have identified the B1scFv that binds specifically to the Mu50 version of the Eap34 protein (**Fig. 5-5A**). After identification, recombinant expression, and purification, the next step was to characterize the specificity of binding to Eap34 and which domain is specifically interacting with the B1scFv. Using a surface plasmon resonance approach, we coupled Eap34, Eap3, and Eap4 to the surface of the chip by amine coupling. A dose-response curve was done by injecting the B1scFv at various concentrations from 1.95 nM to 1000 nM, and fit using a kinetic model (**Figs. 5-5B, C, and D**). This data indicates that the B1scFv binds to Eap34 and specifically, Eap4 with K_D values of 5.2 nM and 7.6 nM, respectively, but shows no interaction with Eap3.

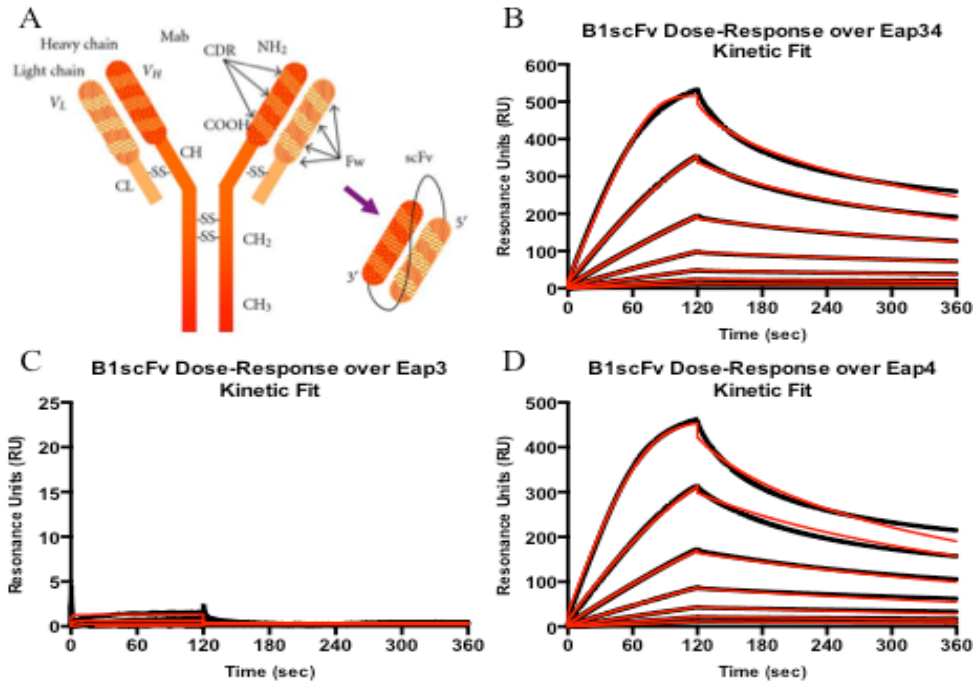

Figure 5-5. B1scFv Binds Directly to Eap34 on a surface plasmon resonance surface. (A) Model representation of a small-chain variable fragment in comparison to an immunoglobulin (IgG). SPR chip surface conjugated with Eap34, Eap3, and Eap4 through amine coupling, and the B1scFv antibody was injected directly over each surface and fit using a kinetic model. (B-C) B1scFv binds directly to Eap34 and Eap4, but not Eap3 in a dose-dependent manner. *Black* line represents relative response from each concentration in RU and *red* line represents the kinetic fit.

B1scFv shows anti-microbial properties toward the killing of S. aureus – After identification and characterization of the B1scFv antibody as a tight and specific binder to Eap34, and Eap4, we wanted to test whether this had any activity towards the complement inhibitory effects of Eap. First, using an AlphaScreen with signal generated through myc-tagged EapFL and Eap34 and C4b-biotin, we were able to partially compete out the signal with the B1scFv, obtaining IC_{50} values for competition with EapFL and Eap34 of 3 μM and 10 μM, respectively (**Fig. 5-6A**). Because this is ~600 to 1000-fold weaker than the binding affinity of the B1scFv for Eap34, it would indicate that the antibody just partially overlaps the binding region for C4b. To test this hypothesis another way, we set up an SPR competition experiment, coupling Eap34 to the surface and injecting C4b alone, B1scFv alone, and a both proteins together (**Fig. 5-6B**). Using this method, and comparing the injection of C4b+B1scFv to the theoretical curve (curve calculated by the addition of the injections of C4b alone and B1scFv alone), we can see that they completely overlap, indicating that there is just an additive effect to injecting both proteins over the surface and showing no competition for the binding of Eap34.

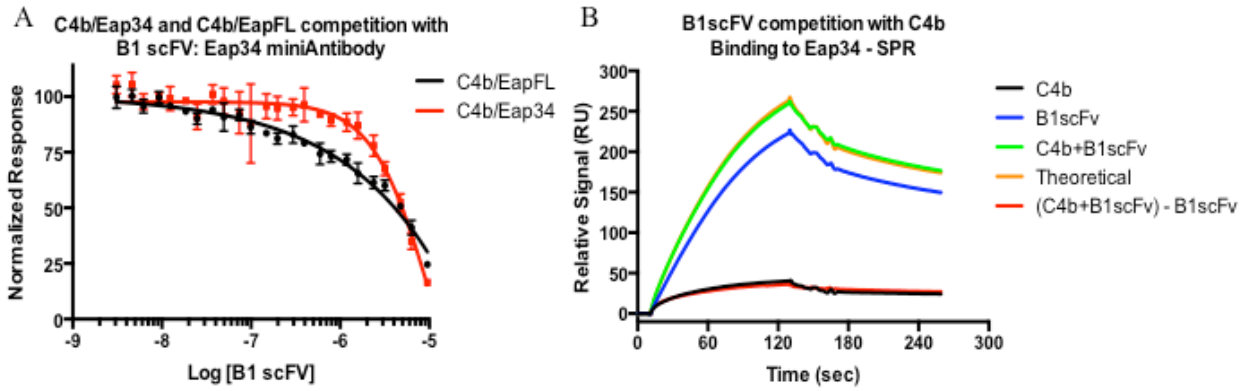

Figure 5-6. B1scFv binds to Eap34 and partially overlaps the binding site for C4b. (A) The ability of untagged B1scFv to compete the AlphaScreen signal generated by myc-EapFL/Eap34 and C4b-biotin was assessed over a logarithmic dilution series, error bars represent +/- SD of three independent experiments. (B) The ability of B1scFv to block binding of C4b to an SPR surface coupled with Eap34. Legend is inset.

Although we did not see any competition for Eap binding to its target, Eap34, we wanted to test if this antibody had any secondary effects on the anti-complement activity of Eap. Using a similar ELISA assay described above, but activation through the classical pathway, we added 1

μM Eap to 2% normal human serum to get a basal level of complement inhibition through the deposition of C3b. Then we performed subsequent experiments, keeping the Eap concentration constant, and adding increasing amounts of the B1scFv antibody, we saw a significant decrease in complement inhibition in a dose-dependent manner (**Fig. 5-7A**).

The next step was to use this hypothesis to see if the addition of the antibody reduced the survival of *S. aureus* in a whole blood killing assay based on its decrease in complement inhibitory activity. Interestingly, addition of the antibody at increasing concentrations showed significant anti-microbial effects by less survival of *S. aureus* in comparison the addition of just Eap (**Fig. 5-7B**). In comparison to the above data, the antibody having anti-microbial effects on the survival of *S. aureus* is similar to the effects that we saw in the complement-based assays, meaning the antibody must be affecting Eap's ability to block the classical and lectin pathways of complement.

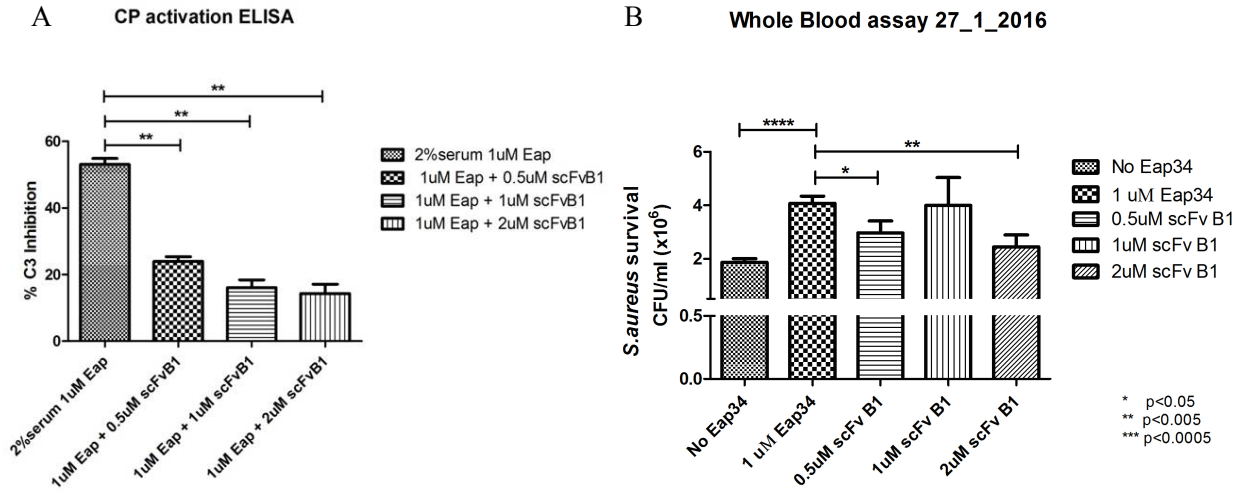

Figure 5-7. B1scFv antibody shows antimicrobial effects through complement activity and survival of *S. aureus*. Classical pathway complement activity was assessed through a series of B1scFv concentrations, keeping the Eap concentration constant. 2% (v/v) NHS was used as a source of complement components, and each assay point was repeated in triplicate. A) Classical pathway activity in the presence of 1 μM Eap, and 1 μM Eap with the addition of increasing concentrations of B1scFv (0.5 μM to 2 μM). (B) The ability of *S. aureus* to survive in a whole blood killing assay with the addition of 1 μM Eap34 and varying concentrations of B1scFv (0.5 μM to 2 μM), in triplicate. Legends are inset. Data collected from Dimitris C. Mastellos lab.

Discussion

Strain-by-strain variations in *Staphylococcus aureus* has allowed it to out mutate and develop resistance to numerous antibiotics and therapeutics. In addition to developing drug resistance, co-evolution alongside humans has forced it to mutate and genetically recombine with other pathogens to develop new mechanisms to counteract the onslaught of phagocytic responses from the immune system. A major factor in *S. aureus's* ability to counteract the immune system is the release of virulence factors that are designed to specifically block and inhibit different aspects of the immune response as well as allow it to go undetected and lay dormant inside the body. Identifying the different proteins and mechanisms that inhibit the immune response is the first step in understanding the pathogenesis of the bacteria.

One of these virulence factors, the extracellular adherence protein (Eap), was discovered in a strain of *S. aureus* in the early 1990'. Since its discovery, numerous manuscripts have reported on the large range of host-derived ligands thought to interact with Eap (99, 100, 109, 120-122). The majority of the proteins thought to be ligands for Eap are extracellular matrix proteins like fibrinogen, fibronectin, collagen, etc., and ICAM-1. Recently, we discovered that Eap binds with nanomolar affinity to the complement protein C4b, which is the key connection between the classical and lectin pathways (40). In addition, Eap has been shown to be a potent inhibitor of the neutrophil serine proteases (NSPs) elastase, cathepsin G, and proteinase 3 (75, 76). The four domain Eap protein studied for its interactions with C4b and NSPs is secreted from *S. aureus* strain Mu50, although strain-specific differences exist due to the presence of four, five or six domain isoforms (145). Repeats in the Mu50 strain share 40-80% sequence identity with one another, and ~25-50% identity with the structurally related *S. aureus* homologs, EapH1 and EapH2, which only consist of a single domain (1).

A direct comparison of the Eap protein released b *S. aureus* strain Newman contains five repeat domains as opposed to the four repeat domains of Eap from strain Mu50. Using the sequences of the secreted proteins from each strain, we compared each single domain of the Mu50 protein with each single domain of the Newman protein using the BLAST program (**Fig. 5-1**). The two proteins show some similarities, specifically with the EapH1 and EapH2 homologs, with over 95% sequence identity. In addition, the third domain and fourth domain of Mu50 match 100% to the third domain and fifth domain of Newman, respectively. Two interesting changes have evolved across strains; the Eap-Newman protein shows no sequence similarity to Eap1 of Mu50, meaning that it contains two domains that show sequence similarities to Eap2 of Mu50. In addition, the fourth domain of Eap-Newman shows no sequence similarities with any other domain, meaning that it is a new, uncharacterized domain.

With the addition of a fifth domain, we hypothesized that this would increase the binding affinity for C4b, based on the combinatorial effects of having an extra domain with similar affinity to the other single EAP domains as well as an added electrostatic interaction making the Eap-Newman protein more positively charged. What we found was surprising because we were able to show using AlphaScreens that the full-length proteins from Mu50 and Newman show no significant difference in binding affinity for C4b (**Figs. 5-2A, B, C, and D**). This suggests that the binding site on C4b can only fit a set number of domains and the fifth domain must not have direct interactions with the complement protein. Similar to the hypothesized effects, addition of a third domain to the Newman variant (Eap345) led to a ~4-fold increase in affinity when compared to the two domain variant of strain Mu50 (Eap34). This is not surprising because the affinity of the Eap4-N protein (*data not shown*) is comparable to Eap3 and Eap4 of Mu50,

similar to the effects that we would see when we add Eap2 onto the Mu50 variant (Eap234) (*data not shown*).

Comparison of the full-length and variant proteins from each strain based on their complement activity should yield similar results to their binding affinities. Activation of the lectin pathway through an ELISA-based approach, we can see that the full-length proteins show similar IC_{50} values, ~8 x 10^{-8} M, but interestingly, the Eap345-N variant shows an increased IC_{50} value when compared to the full-length proteins as well as Eap34 (**Figs. 5-3A, B**). These results suggest that the inhibitory activity of these proteins is based on their steric ability to block the interaction between C4b and C2. Because Eap34 has been shown to share similar effects with the full-length protein, an added domain allows it to block more of the C2 binding site, leading to an increase in affinity as well as an increase in complement inhibitory activity. The same could be said about the full-length Newman protein but the data suggests that the binding site on C4b can only occupy a set number of domains so addition of a fifth domain doesn't change its affinity or inhibitory activity.

As mentioned earlier, Eap has been shown to have multiple host-derived ligands, but understanding the mechanism of these interactions has been elusive. Using an ELISA-based approach, coating the surface with fibrinogen, we were able to show that Eap from strain Mu50 and Newman interact specifically with fibrinogen in a dose-dependent manner (**Fig. 5-4**). Similar to what was seen for binding C4b, the affinity for fibrinogen is directly proportional to the number of domains in the protein, with EapFL-N binding with the highest affinity and Eap34 binding with the lowest. Although the reason for Eap binding to fibrinogen is unknown, we can speculate based on other bacteria and another virulence factor secreted by *S. aureus*, the extracellular fibrinogen binding protein (Efb).

The Efb family of proteins also contains the extracellular complement protein (Ecb) and Ehp. This family shares a similar mechanism; they bind to the C3d domain of complement C3, initiating an allosteric mechanism that modifies the solution conformation of C3, blocking cleavage and formation of C3b (61-64). Additionally, Efb is able to bind multiple components, the C-terminus of the protein binds C3/C3b, described above, and the N-terminus interacts with fibrinogen. This interaction attracts fibrinogen to opsonized surface of the *S. aureus* cell, generating a "capsule"-like shield around the bacteria, blocking advanced opsonization by C3b and detection by phagocytic receptors (65). Our data suggest that Eap shares a similar mechanism to that of Efb, but on the classical and lectin pathway C4b, rather than on C3b of the alternative pathway. In addition, previous research has shown that Eap causes agglutination of the *S. aureus* bacteria because it's able to rebind the surface of the cell (146). This can be attributed to a phosphatase on the bacterial surface, which Eap has shown to have strong affinity (99, 146). Together, this would suggest that in addition to Eap binding opsonized C4b and inhibiting complement, it's also able to attract fibrinogen to the surface when bound to C4b and when rebound to the *S. aureus* cell, forming the coat similar to that of Efb.

Because of the abundance of Eap proteins found in *S. aureus* strains, we screened Eap34 (the critical domains required for C4b binding and complement inhibition (40)) through a library of small-chain variable fragment (scFv) (**Fig. 5-5A**) antibodies and identified the B1scFv as a specific binder. Through surface plasmon resonance characterization, we were able to show that the B1scFv binds in a dose-dependent manner to Eap34, and specifically Eap4 with K_D = ~5-10 nM, but not to Eap3 (**Figs. 5-5B, C, and D**). Although this antibody bound specifically to the crucial Eap domains, we wanted to test for its effect on the complement inhibitory properties of Eap. Using an AlphaScreen approach, we were able to show that the B1scFv competes out the

interaction between Eap/Eap34 and C4b, although the IC_{50} value is ~700-fold weaker than the K_D, indicating that the antibody only moderately overlaps the Eap/C4b binding site (**Fig. 5-6A**). Testing this through a surface plasmon resonance competition-based method, we have shown that the B1scFv does not compete out the interaction of C4b for Eap34 on the conjugated surface when compared to the theoretical curve (addition of C4b injection curve + B1scFv injection curve) (**Fig. 5-6B**). These data suggests that the B1scFv shows very little overlap between the C4b and Eap binding site.

Although the competition-based data does not suggest any type of anti-Eap activity, we wanted to test for B1scFv's activity in a complement-based approach. Interestingly, an ELISA-based approach of classical pathway activity shows that addition of the B1scFv along with a constant concentration of Eap shows an increase in complement activity in a dose-dependent manner when compared to Eap alone, through a decrease in % C3 inhibition (**Fig. 5-7A**). To see if this translates to the survival of *S. aureus*, we tested this in a whole blood assay. Addition of Eap34 to the assay significantly increases the survival of *S. aureus* in comparison to the control (**Fig. 5-7B**). Addition of the B1scFv decreased the level of *S. aureus* survival in a dose-dependent manner (0.5-2 μM). Together, these results suggest that the B1scFv shows anti-microbial activity towards *S. aureus* through binding to Eap and slightly blocking the interaction to C4b in addition to an unknown mechanism. The IC_{50} value of the B1scFv blocking Eap from binding to C4b doesn't directly correlate with the effect that the antibody has on complement activity and *S. aureus* survival, suggestion a second anti-microbial mechanism. Further studies will delve into the precise mechanism of fibrinogen binding and further characterization of the anti-microbial effects of the B1scFv.

Experimental Procedures

Native and Recombinant Proteins – Human serum proteins C4, C4b, C1s, C4b-binding protein (C4BP), and Factor I were obtained in purified form from Complement Technologies (Tyler, TX). Site-specific biotinylation of C4b was carried out using a previously described method (40). All recombinant *S. aureus* proteins were overexpressed and purified according to previously described methods (88).

The B1scFv antibody was overexpressed in *E. coli*, centrifuged at 6500 rcf, 4°C for 15 minutes, the supernatant removed, and the pellet re-suspended in denaturing buffer [6 M Guanidine-HCl, 100 mM Tris (pH 8.0), 10 mM Imidazole) for 45 minutes at RT. The re-suspended pellet was centrifuged at 27000 rcf, 4°C for 35 minutes and the supernatant run over a Ni-NTA column under denaturing conditions [20mM NaPi (pH 6.5), 0.5 M NaCl, 10 mM Imidazole, 8 M Urea). Antibody was eluted with 20mM NaPi (pH 6.5), 0.5 M NaCl, 0.2 M Imidazole, 8 M Urea. The eluted, denatured B1scFv subjected to a three-step dialysis refold. Step one, overnight in 2 L of 100 mM Tris (pH 8.6), 20 mM Glycine, 1 mM EDTA, 1 mM L-Cysteine, 2.5 M Urea; step two, 5 hours in 2 L of Phosphate Buffered Saline (pH 7.4); step three, overnight in 2 L of Native Binding Buffer (pH 8.0) with addition of 2-mercaptoethanol and TEV protease. Digested B1scFv purified over a 5 mL Hi Trap Chelating HP column. The flow through was run through a final purification step over a HiLoad 26/600 Superdex 75 pg GFC column (GE Healthcare Life Sciences).

AlphaScreen-binding assays - An AlphaScreen competition-based binding assay was performed using a previously published protocol (40, 59). In short, C4b/EapFL, C4b/Eap34, C4b/EapFL-Newman, and C4b/Eap345-Newman competition based assays were done using a total volume of 25 μL, in a buffer composed of HBS (pH 7.4), 0.1% (w/v) BSA, 0.01% (v/v)

Triton-X 100. Each component was added to the final concentrations: 50 nM myc-Eap, 5 nM C4b biotin, 20 μg/μL anti-c-myc AlphaScreen acceptor beads, and 20 μg/μL AlphaScreen donor beads. A two-fold dilution series was prepared for each unlabeled competitor protein and allowed to equilibrate with myc-Eap and C4b biotin for 1 h. Following this, the acceptor beads were added, incubated for 1 h, and then the donor beads were added and incubated for an additional 0.5 h. Reactions were then transferred to ½-Area 96-well plates and measured using an EnSpire multimode plate reader (Perkin Elmer Life Sciences). Data analysis and curve fitting were carried out as previously described (59).

Activity of the Lectin Pathway of Complement on an Artificial Surface – Functional activity of the lectin pathway (LP) was determined using a previously described method (40, 92). In short, 96-well polystyrene high bind microplates (Corning Life Sciences) were coated overnight to specifically activate the LP (coated with 20 μg/ml *Saccharomyces cerevisiae* mannan [Sigma-Aldrich]). Plates were blocked with 1% (w/v) BSA, in PBS (pH 7.4) with 0.05% (v/v) Tween 20 for 1 h at 37 °C. In order to obtain IC_{50} values for each inhibitor, a two-fold dilution series was done by diluting the protein 1:1 in LP buffer [50 mM HEPES (pH 7.5), 140 mM NaCl, 0.1% (w/v) Gelatin, 0.1% (w/v) BSA, 2mM $CaCl_2$, 0.5 mM $MgCl_2$, 1% (v/v) Serum (Pooled Complement Human Serum, Innovative Research Inc.)] before direct application to the coated, blocked ELISA plate and incubated for 1 h at 37 °C. Deposited C3b and C5b-9 were detected with 0.333 μg/mL C3d Antibody (003-05): sc-58928 and 0.2 μg/mL C5b-9 (aE11): sc-58935 (Santa Cruz Biotechnology, Inc.), respectively, diluted in PBS (pH 7.4), 0.1% (w/v) BSA, 0.05% (v/v) Tween-20 and incubated at RT for 0.5 h. Finally, the Goat anti-Mouse IgG, IgM (H+L) Cross Absorbed Secondary Antibody, HRP conjugate (Thermo Scientific) was diluted to 1.6 μg/mL in equivalent dilution buffer and added to each well for 0.5 h at RT. HRP-labeled Abs

were detected with 50 μL of 1-Step Ultra TMB-ELISA (Thermo Scientific), the reaction was stopped by the addition of an equal volume of 2 M H_2SO_4, and the absorbance at 450 nm was measured using a $VERSA_{MAX}$ microplate reader. Data were fit to a four-parameter (variable slope) dose-response – inhibition curve software (GraphPad, La Jolla, CA).

Surface plasmon resonance experiments – B1scFv experiments were done by immobilization of Eap34 (700 RU), Eap3 (600 RU), and Eap4 (630 RU) to a CMD-200m sensor chip (Xantec). Dose-response curves were run on a Biacore T200 (GE Healthcare) instrument using HBS-T (pH 7.4) at a flow rate of 20 uL min^{-1} at 25°C. B1scFv was injected for 2 min followed by a 4 min dissociation, and the surface was regenerated by a 10 s injection of 0.2 M Glycine (pH 2.2). BIAevaluation software (GE Healthcare) was used to perform kinetic analyses using a 1:1 Langmuir model of interaction. Similarly, a C4b competition experiment was done using the conditions above with the addition of 5 mM $NiCl_2$ in the running buffer. 200 nM C4b and 100 nM B1scFv were injected separately for 2 min with a 2 min dissociation to establish basal levels of each protein. C4b and B1scFv were then injected together and the basal B1scFv response was subtracted out and the remaining C4b response was compared to the basal C4b response. Regeneration was done using multiple 10 s pulses of 0.2 M Glycine (pH 2.2) until baseline was reached. The theoretical curve was calculated by adding the responses from C4b and B1scFv injected separately.

Acknowledgements

This work was supported by the American Heart Association Midwest Affiliate Pre-doctoral Research Fellowship 15PRE25750013 to J.L.W. and by National Institutes of Health (NIH) Grants AI111203 and AI113552 to B.V.G. We thank Dr. Dimitris C. Mastellos for identifying the B1scFv and cell-based assays done with this antibody.

Chapter 6 - Conclusion

Throughout this dissertation and research, we have drawn many new and interesting conclusions about the extracellular adherence protein (Eap) secreted from *Staphylococcus aureus* and its effects on the complement system upon infection and initial challenge by the immune system. Using a blood-based method of complement activation and a library of secreted *S. aureus* proteins, Eap was discovered to be a potent inhibitor of downstream complement activity when screened next to numerous *S. aureus* virulence factors. Although it was discovered to inhibit complement activity, the mechanism of action was still unknown.

Chapter 2 of this dissertation focused on understanding the mechanism of action on the complement cascade. Using an ELISA-based approach, where we can activate specific complement pathways and test for deposition of downstream proteins, we were able to show that Eap inhibited deposition of C5b-9 (membrane-attack-complex) and C3b (initial step in alternative (AP) pathway activation) but not C4b (initial step in classical and lectin pathway activation) when the ELISA was activated through the classical (CP) and lectin (LP) pathways. This concluded that Eap's activity must be upstream of the AP but downstream of the CP and LP, which mean it's focused towards formation of the CP/LP C3-convertase. Using a size-exclusion chromatography approach, we showed that Eap interacts directly with C4b through a peak shift corresponding to an increase in mass when the proteins are injected over the column together, and confirmation of both proteins in the peak was done using SDS-PAGE. Surface plasmon resonance (SPR) and AlphaScreen methods allowed us to determine the binding affinities of the full-length Eap protein, as well as each of the domain-deleted variants.

Now that we have Eap's binding partner, we looked to understand the actual mechanism of inhibition of the CP and LP. Initial formation of the C3 pro-convertase involves complement

C2 binding directly to C4b deposited on the surface. Using competition-based methods from AlphaScreens and SPR, we were able to show that Eap competes directly with C2 for binding to C4b, and the binding affinity of Eap for C4b is ~3-fold higher than that for C2 binding to C4b. This concludes that the mechanism of action is Eap directly inhibiting the initial interaction of C2 for C4b and blocks formation of the CP/LP C3 pro-convertase, leading to no downstream complement activity.

With the mechanism understood, chapter 3 begins with trying to understand the structural basis for Eap's interaction with C4b and the inhibitory effects on the complement cascade. Expanding on the ELISA and AlphaScreen approaches, we were able to conclude that the third and fourth domains of Eap are critical for its interaction with C4b and complement inhibitory effects. Although a co-crystal structure of Eap34 bound to C4b would have been ideal, the crystals we were able to grow didn't diffract with high enough quality to determine a structure. Because of this, we used a suite of other structural methods to answer these questions, starting with zero-length crosslinking plus mass spectrometry of Eap34 and C4b. Cross-linking the two proteins and running them out over SDS-PAGE under reducing conditions, Western blotting, and staining with an antibody specific for Eap, we were able to see that it's interacting with the α-chain of C4b. In addition, we noticed a change in electrophoretic mobility of the γ-chain of C4b over time during the crosslinking reaction with Eap34. Although it didn't show another band through staining with anti-Eap, we were able to in-gel digest the final band and confirm that Eap34 and C4b γ-chain were both present.

The γ-chain of C4b is critical for its interaction with C2 because of the metal-ion-dependent adhesion site (MIDAS) located in the C345c domain. Coordination of a divalent metal cation (Mg^{2+}) with the von Willebrand factor (vWF) domain of C2 is the initial reaction for C2

binding to C4b and forming the CP/LP C3 pro-convertase. Fortunately, we were able to recombinantly express the C345c domain of the γ-chain and showed that it binds directly to Eap/Eap34 using SPR, as well as compete with C4b for binding to Eap/Eap34. Because of the low affinity of C345c binding directly to Eap34 (~50-fold weaker than Eap34 binding to C4b), we concluded that only a single domain of Eap34 must have been interacting with the C345c domain, confirming that the other domain must be binding to a site on the α-chain of C4b. Together, this data concludes that Eap, specifically Eap34, binding to C4b is overlapping the MIDAS site and inhibiting the initial interaction between C2 and C4b through direct competition for a similar binding site.

The other goal of chapter 3 was to understand the important regions on Eap34 that are necessary for binding to C4b and subsequent complement inhibition. Taking advantage of the numerous surface exposed lysine residues on Eap34, we were able to use a technique that specifically acetylates solvent exposed lysine residues. Upon binding to C4b, certain lysine residues will be covered up and not exposed to solvent, protecting them from acetylation. After separation by SDS-PAGE, in-gel digestion with chymotrypsin, and peptide analysis by MALDI-TOF mass spectrometry, we identified seven lysine residues (3 on Eap3 and 4 on Eap4) that showed a decrease in acetylation upon binding to C4b. Confirmation of these residues was done through site-directed mutagenesis of these residues at either alanine or glutamate. Once mutated, these proteins showed a decrease in binding affinity, as well as a decrease in complement inhibitory activity, confirming that these lysine residues must be critical for Eap34 interacting with C4b.

X-ray crystallography and small-angle X-ray scattering have been very advantageous in understanding the structure of full-length Eap and the single domains of Eap. Unfortunately, we

were unable to obtain a structure of the fourth domain of Eap using these techniques. This required an alternative approach, solution-based nuclear magnetic resonance (NMR). Double-labeling Eap4 with ^{15}N and ^{13}C, we were able to collect triple resonance NMR spectra in order to identify the backbone sequence from the 2D, ^{15}N-HSQC. Once we identified the sequence links between the HSQC peaks, we were able to use the RosettaCS program to obtain a model structure of Eap4 by addition of the known structures of Eap1, Eap2, and Eap3. This confirmed that the overall structure of Eap4 (shown in chapter 4) is very similar to the other three domains but also shows sequence specificity in its ability to bind C4b as concluded from chapters 2 and 3.

Although the final chapter is still in its infancy, we were able to draw some conclusions from the data that we've obtained so far. The basis for chapter 5 is a structural and functional comparison of the extracellular adherence protein from *S. aureus* strain Mu50 vs. strain Newman. Interestingly, strain Newman, the overall more virulent strain, contains an Eap protein that consists of five domains as opposed to the four-domain Mu50 protein. Using AlphaScreen and ELISA-based approaches, we were able to identify the binding affinities and IC_{50} values of complement activity to compare with the Mu50 data. An interesting conclusion from these experiments was that the binding affinities between the Newman and Mu50 proteins were very similar, but the inhibitory effects of the Newman protein (C3b and C5b-9 deposition) were more potent than the Mu50 proteins. Without the comparison of a crystal structure between both proteins bound to C4b, we concluded that the difference in complement inhibition comes from the sterics of another domain being bound to C4b. The Newman protein must be able to block more of the binding site of C2 on C4b and subsequently become a more potent inhibitor of the classical and lectin pathways.

The second section to chapter 5 is comprised of Eap-Mu50 and Eap-Newman's ability to bind directly to fibrinogen in an ELISA-based assay. Although we do not have conclusive evidence as to why this interaction takes place, this draws comparisons to another *S. aureus* virulence factor, Efb. Similar to Efb, Eap is able to bind to a complement protein, C4b, and bind to fibrinogen. Efb is able to bind to C3b and inhibit the alternative pathway of complement in addition to binding fibrinogen. The basis for this mechanism is that Efb binds to C3b coated on the *S. aureus* cell surface and then binds fibrinogen and coats the surface of the cell with fibrinogen, adding to its ability to block multiple aspects of the immune system. Its possibly that Eap shares a similar mechanism but with the classical and lectin pathways of complement, but more data and further analysis of this interaction will be needed to confirm these conclusions.

A final element to chapter 5 was the identification and characterization of a small-chain variable fragment (scFv) antibody, specific for Eap34. Screening through a large library of antibodies, we identified an scFv antibody that bound with high affinity to Eap34. Using SPR, we were able to show that the high affinity interaction between Eap34 and scFv was specific for the fourth domain of Eap34 only. Through multiple competition-based approaches, we determined that the scFv only partially overlaps the binding site between Eap and C4b. Because of this, we hypothesized that this antibody might show an effect on Eap's ability to inhibit the CP and LP, and interestingly, we saw that the addition of the scFv to the ELISA assays made Eap/Eap34 a less potent inhibitor of complement activity. Additionally, this concluded that the scFv partially overlaps the C4b binding site on Eap because we see significant anti-microbial effects on complement activity when compared to Eap alone.

Further analysis of the scFv showed the antibody has anti-microbial properties towards the survival of *S. aureus* in a whole blood assay. Although we do not have supporting data to

understand the anti-microbial properties of the scFv, we have hypothesized that the antibody, in addition to partially overlapping Eap's complement binding site, is blocking the interaction between Eap and one of its other extracellular binding partners, possibly fibrinogen or the neutrophil serine protease, elastase, cathepsin G, and proteinase 3, allowing the immune response to overcome the inhibitory properties of Eap.

References

1. Geisbrecht, B.V., Hamaoka, B.Y., Perman, B., Zemla, A., and Leahy, D.J. (2005) The crystal structures of EAP domains from Staphylococcus aureus reveal an unexpected homology to bacterial superantigens. *J.Biol.Chem.* **280,** 17243-17250

2. Hammel, M., Nemecek, D., Keightley, J.A., Thomas, G.J.,Jr, and Geisbrecht, B.V. (2007) The Staphylococcus aureus extracellular adherence protein (Eap) adopts an elongated but structured conformation in solution. *Protein Sci.* **16,** 2605-2617

3. Victora, G.D., and Nussenzweig, M.C. (2012) Germinal centers. *Annu.Rev.Immunol.* **30,** 429-457

4. Gatto, D., and Brink, R. (2010) The germinal center reaction. *J.Allergy Clin.Immunol.* **126,** 898-907; quiz 908-9

5. Lanzavecchia, A., and Sallusto, F. (2000) Dynamics of T lymphocyte responses: intermediates, effectors, and memory cells. *Science.* **290,** 92-97

6. Sallusto, F., Mackay, C.R., and Lanzavecchia, A. (2000) The role of chemokine receptors in primary, effector, and memory immune responses. *Annu.Rev.Immunol.* **18,** 593-620

7. Akbar, A.N., Terry, L., Timms, A., Beverley, P.C., and Janossy, G. (1988) Loss of CD45R and gain of UCHL1 reactivity is a feature of primed T cells. *J.Immunol.* **140,** 2171-2178

8. Gutcher, I., and Becher, B. (2007) APC-derived cytokines and T cell polarization in autoimmune inflammation. *J.Clin.Invest.* **117,** 1119-1127

9. Hivroz, C., Chemin, K., Tourret, M., and Bohineust, A. (2012) Crosstalk between T lymphocytes and dendritic cells. *Crit.Rev.Immunol.* **32,** 139-155

10. Abbas, A.K., Benoist, C., Bluestone, J.A., Campbell, D.J., Ghosh, S., Hori, S., Jiang, S., Kuchroo, V.K., Mathis, D., Roncarolo, M.G., Rudensky, A., Sakaguchi, S., Shevach, E.M., Vignali, D.A., and Ziegler, S.F. (2013) Regulatory T cells: recommendations to simplify the nomenclature. *Nat.Immunol.* **14,** 307-308

11. Singh, B., Schwartz, J.A., Sandrock, C., Bellemore, S.M., and Nikoopour, E. (2013) Modulation of autoimmune diseases by interleukin (IL)-17 producing regulatory T helper (Th17) cells. *Indian J.Med.Res.* **138,** 591-594

12. Serriari, N.E., Eoche, M., Lamotte, L., Lion, J., Fumery, M., Marcelo, P., Chatelain, D., Barre, A., Nguyen-Khac, E., Lantz, O., Dupas, J.L., and Treiner, E. (2014) Innate mucosal-associated invariant T (MAIT) cells are activated in inflammatory bowel diseases. *Clin.Exp.Immunol.* **176,** 266-274

13. Barnum, S.R. (2016) Complement: A primer for the coming therapeutic revolution. *Pharmacol.Ther.*

14. Anas, A.A., Wiersinga, W.J., de Vos, A.F., and van der Poll, T. (2010) Recent insights into the pathogenesis of bacterial sepsis. *Neth.J.Med.* **68,** 147-152

15. de Jong, H.K., van der Poll, T., and Wiersinga, W.J. (2010) The systemic pro-inflammatory response in sepsis. *J.Innate Immun.* **2,** 422-430

16. Wiersinga, W.J., and van der Poll, T. (2010) Sepsis: new insights into its pathogenesis and treatment. *Ned.Tijdschr.Geneeskd.* **154,** A1130

17. Peitsch, M.C., and Tschopp, J. (1991) Assembly of macromolecular pores by immune defense systems. *Curr.Opin.Cell Biol.* **3,** 710-716

18. Hadders, M.A., Bubeck, D., Roversi, P., Hakobyan, S., Forneris, F., Morgan, B.P., Pangburn, M.K., Llorca, O., Lea, S.M., and Gros, P. (2012) Assembly and regulation of the membrane attack complex based on structures of C5b6 and sC5b9. *Cell.Rep.* **1,** 200-207

19. Laarman, A., Milder, F., van Strijp, J., and Rooijakkers, S. (2010) Complement inhibition by gram-positive pathogens: molecular mechanisms and therapeutic implications. *J.Mol.Med.(Berl).* **88,** 115-120

20. Booth, N.A., Campbell, R.D., Smith, M.A., and Fothergill, J.E. (1979) The isolation and characterization of bovine C4a, an activation fragment of the fourth component of complement. *Biochem.J.* **183,** 573-578

21. Gennaro, R., Pozzan, T., and Romeo, D. (1984) Monitoring of cytosolic free Ca2+ in C5a-stimulated neutrophils: loss of receptor-modulated Ca2+ stores and Ca2+ uptake in granule-free cytoplasts. *Proc.Natl.Acad.Sci.U.S.A.* **81,** 1416-1420

22. Tonnesen, M.G., Smedly, L.A., and Henson, P.M. (1984) Neutrophil-endothelial cell interactions. Modulation of neutrophil adhesiveness induced by complement fragments C5a and C5a des arg and formyl-methionyl-leucyl-phenylalanine in vitro. *J.Clin.Invest.* **74,** 1581-1592

23. Gennaro, R., Simonic, T., Negri, A., Mottola, C., Secchi, C., Ronchi, S., and Romeo, D. (1986) C5a fragment of bovine complement. Purification, bioassays, amino-acid sequence and other structural studies. *Eur.J.Biochem.* **155,** 77-86

24. Gros, P., Milder, F.J., and Janssen, B.J. (2008) Complement driven by conformational changes. *Nat.Rev.Immunol.* **8,** 48-58

25. Khera, R., and Das, N. (2009) Complement Receptor 1: disease associations and therapeutic implications. *Mol.Immunol.* **46,** 761-772

26. Riley-Vargas, R.C., Gill, D.B., Kemper, C., Liszewski, M.K., and Atkinson, J.P. (2004) CD46: expanding beyond complement regulation. *Trends Immunol.* **25,** 496-503

27. Lachmann, P.J., and Muller-Eberhard, H.J. (1968) The demonstration in human serum of "conglutinogen-activating factor" and its effect on the third component of complement. *J.Immunol.* **100,** 691-698

28. Wu, J., Wu, Y.Q., Ricklin, D., Janssen, B.J., Lambris, J.D., and Gros, P. (2009) Structure of complement fragment C3b-factor H and implications for host protection by complement regulators. *Nat.Immunol.* **10,** 728-733

29. Brodbeck, W.G., Kuttner-Kondo, L., Mold, C., and Medof, M.E. (2000) Structure/function studies of human decay-accelerating factor. *Immunology.* **101,** 104-111

30. Cicardi, M., Bergamaschini, L., Cugno, M., Beretta, A., Zingale, L.C., Colombo, M., and Agostoni, A. (1998) Pathogenetic and clinical aspects of C1 inhibitor deficiency. *Immunobiology.* **199,** 366-376

31. Davis, A.E.,3rd (2004) Biological effects of C1 inhibitor. *Drug News.Perspect.* **17,** 439-446

32. Cicardi, M., Zingale, L., Zanichelli, A., Pappalardo, E., and Cicardi, B. (2005) C1 inhibitor: molecular and clinical aspects. *Springer Semin.Immunopathol.* **27,** 286-298

33. Hirt-Minkowski, P., Dickenmann, M., and Schifferli, J.A. (2010) Atypical hemolytic uremic syndrome: update on the complement system and what is new. *Nephron Clin.Pract.* **114,** c219-35

34. Leffler, J., Bengtsson, A.A., and Blom, A.M. (2014) The complement system in systemic lupus erythematosus: an update. *Ann.Rheum.Dis.* **73,** 1601-1606

35. Sjoholm, A.G., Jonsson, G., Braconier, J.H., Sturfelt, G., and Truedsson, L. (2006) Complement deficiency and disease: an update. *Mol.Immunol.* **43,** 78-85

36. Anonymous (1984) Classics in infectious diseases. "On abscesses". Alexander Ogston (1844-1929). *Rev.Infect.Dis.* **6,** 122-128

37. Kluytmans, J., van Belkum, A., and Verbrugh, H. (1997) Nasal carriage of Staphylococcus aureus: epidemiology, underlying mechanisms, and associated risks. *Clin.Microbiol.Rev.* **10,** 505-520

38. Graham, P.L.,3rd, Lin, S.X., and Larson, E.L. (2006) A U.S. population-based survey of Staphylococcus aureus colonization. *Ann.Intern.Med.* **144,** 318-325

39. Drago, L., De Vecchi, E., Nicola, L., and Gismondo, M.R. (2007) In vitro evaluation of antibiotics' combinations for empirical therapy of suspected methicillin resistant Staphylococcus aureus severe respiratory infections. *BMC Infect.Dis.* **7,** 111

40. Woehl, J.L., Stapels, D.A., Garcia, B.L., Ramyar, K.X., Keightley, A., Ruyken, M., Syriga, M., Sfyroera, G., Weber, A.B., Zolkiewski, M., Ricklin, D., Lambris, J.D., Rooijakkers, S.H., and Geisbrecht, B.V. (2014) The extracellular adherence protein from Staphylococcus aureus inhibits the classical and lectin pathways of complement by blocking formation of the C3 proconvertase. *J.Immunol.* **193,** 6161-6171

41. Woehl, J.L., Takahashi, D., Herrera, A.I., Geisbrecht, B.V., and Prakash, O. (2016) (1)H, (15)N, and (13)C resonance assignments of Staphylococcus aureus extracellular adherence protein domain 4. *Biomol.NMR Assign.* **10,** 301-305

42. Garcia, B.L., Zwarthoff, S.A., Rooijakkers, S.H., and Geisbrecht, B.V. (2016) Novel Evasion Mechanisms of the Classical Complement Pathway. *J.Immunol.* **197,** 2051-2060

43. Kang, M., Ko, Y.P., Liang, X., Ross, C.L., Liu, Q., Murray, B.E., and Hook, M. (2013) Collagen-binding microbial surface components recognizing adhesive matrix molecule (MSCRAMM) of Gram-positive bacteria inhibit complement activation via the classical pathway. *J.Biol.Chem.* **288,** 20520-20531

44. Foster, T.J., Geoghegan, J.A., Ganesh, V.K., and Hook, M. (2014) Adhesion, invasion and evasion: the many functions of the surface proteins of Staphylococcus aureus. *Nat.Rev.Microbiol.* **12,** 49-62

45. Xu, Y., Liang, X., Chen, Y., Koehler, T.M., and Hook, M. (2004) Identification and biochemical characterization of two novel collagen binding MSCRAMMs of Bacillus anthracis. *J.Biol.Chem.* **279,** 51760-51768

46. Sillanpaa, J., Nallapareddy, S.R., Qin, X., Singh, K.V., Muzny, D.M., Kovar, C.L., Nazareth, L.V., Gibbs, R.A., Ferraro, M.J., Steckelberg, J.M., Weinstock, G.M., and Murray, B.E. (2009) A collagen-binding adhesin, Acb, and ten other putative MSCRAMM and pilus family proteins of Streptococcus gallolyticus subsp. gallolyticus (Streptococcus bovis Group, biotype I). *J.Bacteriol.* **191,** 6643-6653

47. Kreikemeyer, B., Nakata, M., Oehmcke, S., Gschwendtner, C., Normann, J., and Podbielski, A. (2005) Streptococcus pyogenes collagen type I-binding Cpa surface protein. Expression profile, binding characteristics, biological functions, and potential clinical impact. *J.Biol.Chem.* **280,** 33228-33239

48. Patti, J.M., and Hook, M. (1994) Microbial adhesins recognizing extracellular matrix macromolecules. *Curr.Opin.Cell Biol.* **6,** 752-758

49. Krishnan, V., and Narayana, S.V. (2011) Crystallography of gram-positive bacterial adhesins. *Adv.Exp.Med.Biol.* **715,** 175-195

50. Patti, J.M., Allen, B.L., McGavin, M.J., and Hook, M. (1994) MSCRAMM-mediated adherence of microorganisms to host tissues. *Annu.Rev.Microbiol.* **48,** 585-617

51. MacKichan, J.K., Gerns, H.L., Chen, Y.T., Zhang, P., and Koehler, J.E. (2008) A SacB mutagenesis strategy reveals that the Bartonella quintana variably expressed outer membrane proteins are required for bloodstream infection of the host. *Infect.Immun.* **76,** 788-795

52. Wagner, C., Khan, A.S., Kamphausen, T., Schmausser, B., Unal, C., Lorenz, U., Fischer, G., Hacker, J., and Steinert, M. (2007) Collagen binding protein Mip enables Legionella pneumophila to transmigrate through a barrier of NCI-H292 lung epithelial cells and extracellular matrix. *Cell.Microbiol.* **9,** 450-462

53. Fink, D.L., Green, B.A., and St Geme, J.W.,3rd (2002) The Haemophilus influenzae Hap autotransporter binds to fibronectin, laminin, and collagen IV. *Infect.Immun.* **70,** 4902-4907

54. Rooijakkers, S.H., Milder, F.J., Bardoel, B.W., Ruyken, M., van Strijp, J.A., and Gros, P. (2007) Staphylococcal complement inhibitor: structure and active sites. *J.Immunol.* **179,** 2989-2998

55. Garcia, B.L., Tzekou, A., Ramyar, K.X., McWhorter, W.J., Ricklin, D., Lambris, J.D., and Geisbrecht, B.V. (2009) Crystallization of human complement component C3b in the presence of a staphylococcal complement-inhibitor protein (SCIN). *Acta Crystallogr.Sect.F.Struct.Biol.Cryst.Commun.* **65,** 482-485

56. Rooijakkers, S.H., Wu, J., Ruyken, M., van Domselaar, R., Planken, K.L., Tzekou, A., Ricklin, D., Lambris, J.D., Janssen, B.J., van Strijp, J.A., and Gros, P. (2009) Structural and functional implications of the alternative complement pathway C3 convertase stabilized by a staphylococcal inhibitor. *Nat.Immunol.* **10,** 721-727

57. Garcia, B.L., Ramyar, K.X., Tzekou, A., Ricklin, D., McWhorter, W.J., Lambris, J.D., and Geisbrecht, B.V. (2010) Molecular basis for complement recognition and inhibition determined by crystallographic studies of the staphylococcal complement inhibitor (SCIN) bound to C3c and C3b. *J.Mol.Biol.* **402,** 17-29

58. Garcia, B.L., Ramyar, K.X., Ricklin, D., Lambris, J.D., and Geisbrecht, B.V. (2012) Advances in understanding the structure, function, and mechanism of the SCIN and Efb families of Staphylococcal immune evasion proteins. *Adv.Exp.Med.Biol.* **946,** 113-133

59. Garcia, B.L., Summers, B.J., Lin, Z., Ramyar, K.X., Ricklin, D., Kamath, D.V., Fu, Z.Q., Lambris, J.D., and Geisbrecht, B.V. (2012) Diversity in the C3b [corrected] contact residues and tertiary structures of the staphylococcal complement inhibitor (SCIN) protein family. *J.Biol.Chem.* **287,** 628-640

60. Garcia, B.L., Summers, B.J., Ramyar, K.X., Tzekou, A., Lin, Z., Ricklin, D., Lambris, J.D., Laity, J.H., and Geisbrecht, B.V. (2013) A structurally dynamic N-terminal helix is a key functional determinant in staphylococcal complement inhibitor (SCIN) proteins. *J.Biol.Chem.* **288,** 2870-2881

61. Hammel, M., Sfyroera, G., Pyrpassopoulos, S., Ricklin, D., Ramyar, K.X., Pop, M., Jin, Z., Lambris, J.D., and Geisbrecht, B.V. (2007) Characterization of Ehp, a secreted complement inhibitory protein from Staphylococcus aureus. *J.Biol.Chem.* **282,** 30051-30061

62. Hammel, M., Sfyroera, G., Ricklin, D., Magotti, P., Lambris, J.D., and Geisbrecht, B.V. (2007) A structural basis for complement inhibition by Staphylococcus aureus. *Nat.Immunol.* **8,** 430-437

63. Chen, H., Schuster, M.C., Sfyroera, G., Geisbrecht, B.V., and Lambris, J.D. (2008) Solution insights into the structure of the Efb/C3 complement inhibitory complex as revealed by lysine acetylation and mass spectrometry. *J.Am.Soc.Mass Spectrom.* **19,** 55-65

64. Chen, H., Ricklin, D., Hammel, M., Garcia, B.L., McWhorter, W.J., Sfyroera, G., Wu, Y.Q., Tzekou, A., Li, S., Geisbrecht, B.V., Woods, V.L.,Jr, and Lambris, J.D. (2010) Allosteric inhibition of complement function by a staphylococcal immune evasion protein. *Proc.Natl.Acad.Sci.U.S.A.* **107,** 17621-17626

65. Ko, Y.P., Kuipers, A., Freitag, C.M., Jongerius, I., Medina, E., van Rooijen, W.J., Spaan, A.N., van Kessel, K.P., Hook, M., and Rooijakkers, S.H. (2013) Phagocytosis escape by a Staphylococcus aureus protein that connects complement and coagulation proteins at the bacterial surface. *PLoS Pathog.* **9,** e1003816

66. Laursen, N.S., Gordon, N., Hermans, S., Lorenz, N., Jackson, N., Wines, B., Spillner, E., Christensen, J.B., Jensen, M., Fredslund, F., Bjerre, M., Sottrup-Jensen, L., Fraser, J.D., and Andersen, G.R. (2010) Structural basis for inhibition of complement C5 by the SSL7 protein from Staphylococcus aureus. *Proc.Natl.Acad.Sci.U.S.A.* **107,** 3681-3686

67. Bestebroer, J., Aerts, P.C., Rooijakkers, S.H., Pandey, M.K., Kohl, J., van Strijp, J.A., and de Haas, C.J. (2010) Functional basis for complement evasion by staphylococcal superantigen-like 7. *Cell.Microbiol.* **12,** 1506-1516

68. Rosenzweig, R., and Kay, L.E. (2016) Solution NMR Spectroscopy Provides an Avenue for the Study of Functionally Dynamic Molecular Machines: The Example of Protein Disaggregation. *J.Am.Chem.Soc.* **138,** 1466-1477

69. Mittermaier, A., and Kay, L.E. (2006) New tools provide new insights in NMR studies of protein dynamics. *Science.* **312,** 224-228

70. Ishima, R., and Torchia, D.A. (2000) Protein dynamics from NMR. *Nat.Struct.Biol.* **7,** 740-743

71. Palmer, A.G.,3rd, Kroenke, C.D., and Loria, J.P. (2001) Nuclear magnetic resonance methods for quantifying microsecond-to-millisecond motions in biological macromolecules. *Methods Enzymol.* **339,** 204-238

72. Sekhar, A., and Kay, L.E. (2013) NMR paves the way for atomic level descriptions of sparsely populated, transiently formed biomolecular conformers. *Proc.Natl.Acad.Sci.U.S.A.* **110,** 12867-12874

73. Anthis, N.J., and Clore, G.M. (2015) Visualizing transient dark states by NMR spectroscopy. *Q.Rev.Biophys.* **48,** 35-116

74. Nikolova, E.N., Kim, E., Wise, A.A., O'Brien, P.J., Andricioaei, I., and Al-Hashimi, H.M. (2011) Transient Hoogsteen base pairs in canonical duplex DNA. *Nature.* **470,** 498-502

75. Stapels, D.A., Ramyar, K.X., Bischoff, M., von Kockritz-Blickwede, M., Milder, F.J., Ruyken, M., Eisenbeis, J., McWhorter, W.J., Herrmann, M., van Kessel, K.P., Geisbrecht, B.V., and Rooijakkers, S.H. (2014) Staphylococcus aureus secretes a unique class of neutrophil serine protease inhibitors. *Proc.Natl.Acad.Sci.U.S.A.* **111,** 13187-13192

76. Stapels, D.A., Geisbrecht, B.V., and Rooijakkers, S.H. (2015) Neutrophil serine proteases in antibacterial defense. *Curr.Opin.Microbiol.* **23,** 42-48

77. Summers, B.J., Garcia, B.L., Woehl, J.L., Ramyar, K.X., Yao, X., and Geisbrecht, B.V. (2015) Identification of peptidic inhibitors of the alternative complement pathway based on Staphylococcus aureus SCIN proteins. *Mol.Immunol.* **67,** 193-205

78. Huston, J.S., Levinson, D., Mudgett-Hunter, M., Tai, M.S., Novotny, J., Margolies, M.N., Ridge, R.J., Bruccoleri, R.E., Haber, E., and Crea, R. (1988) Protein engineering of antibody binding sites: recovery of specific activity in an anti-digoxin single-chain Fv analogue produced in Escherichia coli. *Proc.Natl.Acad.Sci.U.S.A.* **85,** 5879-5883

79. Colwill, K., Renewable Protein Binder Working Group, and Graslund, S. (2011) A roadmap to generate renewable protein binders to the human proteome. *Nat.Methods.* **8,** 551-558

80. Nollau, P. (2011) Generating high-quality protein binders: a large screening effort pays off. *Nat.Methods.* **8,** 545-546

81. Ricklin, D., Hajishengallis, G., Yang, K., and Lambris, J.D. (2010) Complement: a key system for immune surveillance and homeostasis. *Nat.Immunol.* **11,** 785-797

82. Harboe, M., Ulvund, G., Vien, L., Fung, M., and Mollnes, T.E. (2004) The quantitative role of alternative pathway amplification in classical pathway induced terminal complement activation. *Clin.Exp.Immunol.* **138,** 439-446

83. Lambris, J.D., Ricklin, D., and Geisbrecht, B.V. (2008) Complement evasion by human pathogens. *Nat.Rev.Microbiol.* **6,** 132-142

84. Zecconi, A., and Scali, F. (2013) Staphylococcus aureus virulence factors in evasion from innate immune defenses in human and animal diseases. *Immunol.Lett.* **150,** 12-22

85. Rooijakkers, S.H., Ruyken, M., Roos, A., Daha, M.R., Presanis, J.S., Sim, R.B., van Wamel, W.J., van Kessel, K.P., and van Strijp, J.A. (2005) Immune evasion by a staphylococcal complement inhibitor that acts on C3 convertases. *Nat.Immunol.* **6,** 920-927

86. Jongerius, I., Kohl, J., Pandey, M.K., Ruyken, M., van Kessel, K.P., van Strijp, J.A., and Rooijakkers, S.H. (2007) Staphylococcal complement evasion by various convertase-blocking molecules. *J.Exp.Med.* **204,** 2461-2471

87. Bouyain, S., and Watkins, D.J. (2010) The protein tyrosine phosphatases PTPRZ and PTPRG bind to distinct members of the contactin family of neural recognition molecules. *Proc.Natl.Acad.Sci.U.S.A.* **107,** 2443-2448

88. Geisbrecht, B.V., Bouyain, S., and Pop, M. (2006) An optimized system for expression and purification of secreted bacterial proteins. *Protein Expr.Purif.* **46,** 23-32

89. Xie, C., Alcaide, P., Geisbrecht, B.V., Schneider, D., Herrmann, M., Preissner, K.T., Luscinskas, F.W., and Chavakis, T. (2006) Suppression of experimental autoimmune encephalomyelitis by extracellular adherence protein of Staphylococcus aureus. *J.Exp.Med.* **203,** 985-994

90. Berends, E.T., Dekkers, J.F., Nijland, R., Kuipers, A., Soppe, J.A., van Strijp, J.A., and Rooijakkers, S.H. (2013) Distinct localization of the complement C5b-9 complex on Gram-positive bacteria. *Cell.Microbiol.* **15,** 1955-1968

91. Prat, C., Bestebroer, J., de Haas, C.J., van Strijp, J.A., and van Kessel, K.P. (2006) A new staphylococcal anti-inflammatory protein that antagonizes the formyl peptide receptor-like 1. *J.Immunol.* **177,** 8017-8026

92. Roos, A., Bouwman, L.H., Munoz, J., Zuiverloon, T., Faber-Krol, M.C., Fallaux-van den Houten, F.C., Klar-Mohamad, N., Hack, C.E., Tilanus, M.G., and Daha, M.R. (2003) Functional characterization of the lectin pathway of complement in human serum. *Mol.Immunol.* **39,** 655-668

93. Pang, Y.Y., Schwartz, J., Thoendel, M., Ackermann, L.W., Horswill, A.R., and Nauseef, W.M. (2010) agr-Dependent interactions of Staphylococcus aureus USA300 with human polymorphonuclear neutrophils. *J.Innate Immun.* **2,** 546-559

94. Lu, T., Porter, A.R., Kennedy, A.D., Kobayashi, S.D., and DeLeo, F.R. (2014) Phagocytosis and killing of Staphylococcus aureus by human neutrophils. *J.Innate Immun.* **6,** 639-649

95. Ricklin, D., Tzekou, A., Garcia, B.L., Hammel, M., McWhorter, W.J., Sfyroera, G., Wu, Y.Q., Holers, V.M., Herbert, A.P., Barlow, P.N., Geisbrecht, B.V., and Lambris, J.D. (2009) A molecular insight into complement evasion by the staphylococcal complement inhibitor protein family. *J.Immunol.* **183,** 2565-2574

96. Keightley, J.A., Shang, L., and Kinter, M. (2004) Proteomic analysis of oxidative stress-resistant cells: a specific role for aldose reductase overexpression in cytoprotection. *Mol.Cell.Proteomics.* **3,** 167-175

97. Girish, V., and Vijayalakshmi, A. (2004) Affordable image analysis using NIH Image/ImageJ. *Indian J.Cancer.* **41,** 47

98. Hussain, M., Becker, K., von Eiff, C., Peters, G., and Herrmann, M. (2001) Analogs of Eap protein are conserved and prevalent in clinical Staphylococcus aureus isolates. *Clin.Diagn.Lab.Immunol.* **8,** 1271-1276

99. Flock, M., and Flock, J.I. (2001) Rebinding of extracellular adherence protein Eap to Staphylococcus aureus can occur through a surface-bound neutral phosphatase. *J.Bacteriol.* **183,** 3999-4003

100. Palma, M., Haggar, A., and Flock, J.I. (1999) Adherence of Staphylococcus aureus is enhanced by an endogenous secreted protein with broad binding activity. *J.Bacteriol.* **181,** 2840-2845

101. Kerr, M.A., and Parkes, C. (1984) The effects of iodine and thiol-blocking reagents on complement component C2 and on the assembly of the classical-pathway C3 convertase. *Biochem.J.* **219,** 391-399

102. Milder, F.J., Raaijmakers, H.C., Vandeputte, M.D., Schouten, A., Huizinga, E.G., Romijn, R.A., Hemrika, W., Roos, A., Daha, M.R., and Gros, P. (2006) Structure of complement component C2A: implications for convertase formation and substrate binding. *Structure.* **14,** 1587-1597

103. Kerr, M.A. (1980) The human complement system: assembly of the classical pathway C3 convertase. *Biochem.J.* **189,** 173-181

104. Blom, A.M., Villoutreix, B.O., and Dahlback, B. (2004) Complement inhibitor C4b-binding protein-friend or foe in the innate immune system?. *Mol.Immunol.* **40,** 1333-1346

105. Papageorgiou, A.C., and Acharya, K.R. (2000) Microbial superantigens: from structure to function. *Trends Microbiol.* **8,** 369-375

106. Blom, A.M., Hallstrom, T., and Riesbeck, K. (2009) Complement evasion strategies of pathogens-acquisition of inhibitors and beyond. *Mol.Immunol.* **46,** 2808-2817

107. Sharp, J.A., and Cunnion, K.M. (2011) Disruption of the alternative pathway convertase occurs at the staphylococcal surface via the acquisition of factor H by Staphylococcus aureus. *Mol.Immunol.* **48,** 683-690

108. Hair, P.S., Wagner, S.M., Friederich, P.T., Drake, R.R., Nyalwidhe, J.O., and Cunnion, K.M. (2012) Complement regulator C4BP binds to Staphylococcus aureus and decreases opsonization. *Mol.Immunol.* **50,** 253-261

109. Chavakis, T., Hussain, M., Kanse, S.M., Peters, G., Bretzel, R.G., Flock, J.I., Herrmann, M., and Preissner, K.T. (2002) Staphylococcus aureus extracellular adherence protein serves as anti-inflammatory factor by inhibiting the recruitment of host leukocytes. *Nat.Med.* **8,** 687-693

110. Lee, L.Y., Miyamoto, Y.J., McIntyre, B.W., Hook, M., McCrea, K.W., McDevitt, D., and Brown, E.L. (2002) The Staphylococcus aureus Map protein is an immunomodulator that interferes with T cell-mediated responses. *J.Clin.Invest.* **110,** 1461-1471

111. Joost, I., Jacob, S., Utermohlen, O., Schubert, U., Patti, J.M., Ong, M.F., Gross, J., Justinger, C., Renno, J.H., Preissner, K.T., Bischoff, M., and Herrmann, M. (2011) Antibody response to the extracellular adherence protein (Eap) of Staphylococcus aureus in healthy and infected individuals. *FEMS Immunol.Med.Microbiol.* **62,** 23-31

112. Amulic, B., Cazalet, C., Hayes, G.L., Metzler, K.D., and Zychlinsky, A. (2012) Neutrophil function: from mechanisms to disease. *Annu.Rev.Immunol.* **30,** 459-489

113. Ricklin, D., and Lambris, J.D. (2013) Complement in immune and inflammatory disorders: therapeutic interventions. *J.Immunol.* **190,** 3839-3847

114. Ricklin, D., and Lambris, J.D. (2013) Complement in immune and inflammatory disorders: pathophysiological mechanisms. *J.Immunol.* **190,** 3831-3838

115. Ricklin, D., and Lambris, J.D. (2013) Progress and trends in complement therapeutics. *Adv.Exp.Med.Biol.* **735,** 1-22

116. Thammavongsa, V., Kim, H.K., Missiakas, D., and Schneewind, O. (2015) Staphylococcal manipulation of host immune responses. *Nat.Rev.Microbiol.* **13,** 529-543

117. Mortensen, S., Jensen, J.K., and Andersen, G.R. (2016) Solution Structures of Complement C2 and Its C4 Complexes Propose Pathway-specific Mechanisms for Control and Activation of the Complement Proconvertases. *J.Biol.Chem.* **291,** 16494-16507

118. Grabarek, Z., and Gergely, J. (1990) Zero-length crosslinking procedure with the use of active esters. *Anal.Biochem.* **185,** 131-135

119. Pietrocola, G., Rindi, S., Rosini, R., Buccato, S., Speziale, P., and Margarit, I. (2016) The Group B Streptococcus-Secreted Protein CIP Interacts with C4, Preventing C3b Deposition via the Lectin and Classical Complement Pathways. *J.Immunol.* **196,** 385-394

120. McGavin, M.H., Krajewska-Pietrasik, D., Ryden, C., and Hook, M. (1993) Identification of a Staphylococcus aureus extracellular matrix-binding protein with broad specificity. *Infect.Immun.* **61,** 2479-2485

121. Boden, M.K., and Flock, J.I. (1992) Evidence for three different fibrinogen-binding proteins with unique properties from Staphylococcus aureus strain Newman. *Microb.Pathog.* **12,** 289-298

122. Kreikemeyer, B., McDevitt, D., and Podbielski, A. (2002) The role of the map protein in Staphylococcus aureus matrix protein and eukaryotic cell adherence. *Int.J.Med.Microbiol.* **292,** 283-295

123. Mortensen, S., Kidmose, R.T., Petersen, S.V., Szilagyi, A., Prohaszka, Z., and Andersen, G.R. (2015) Structural Basis for the Function of Complement Component C4 within the Classical and Lectin Pathways of Complement. *J.Immunol.* **194,** 5488-5496

124. Forneris, F., Ricklin, D., Wu, J., Tzekou, A., Wallace, R.S., Lambris, J.D., and Gros, P. (2010) Structures of C3b in complex with factors B and D give insight into complement convertase formation. *Science.* **330,** 1816-1820

125. Fishelson, Z., and Muller-Eberhard, H.J. (1982) C3 convertase of human complement: enhanced formation and stability of the enzyme generated with nickel instead of magnesium. *J.Immunol.* **129,** 2603-2607

126. Villiers, M.B., Thielens, N.M., and Colomb, M.G. (1985) Soluble C3 proconvertase and convertase of the classical pathway of human complement. Conditions of stabilization in vitro. *Biochem.J.* **226,** 429-436

127. Comeau, S.R., Gatchell, D.W., Vajda, S., and Camacho, C.J. (2004) ClusPro: an automated docking and discrimination method for the prediction of protein complexes. *Bioinformatics.* **20,** 45-50

128. Comeau, S.R., Gatchell, D.W., Vajda, S., and Camacho, C.J. (2004) ClusPro: a fully automated algorithm for protein-protein docking. *Nucleic Acids Res.* **32,** W96-9

129. Krishnan, V., Xu, Y., Macon, K., Volanakis, J.E., and Narayana, S.V. (2009) The structure of C2b, a fragment of complement component C2 produced during C3 convertase formation. *Acta Crystallogr.D Biol.Crystallogr.* **65,** 266-274

130. Horiuchi, T., Macon, K.J., Engler, J.A., and Volanakis, J.E. (1991) Site-directed mutagenesis of the region around Cys-241 of complement component C2. Evidence for a C4b binding site. *J.Immunol.* **147,** 584-589

131. Krishnan, V., Xu, Y., Macon, K., Volanakis, J.E., and Narayana, S.V. (2007) The crystal structure of C2a, the catalytic fragment of classical pathway C3 and C5 convertase of human complement. *J.Mol.Biol.* **367,** 224-233

132. Boucher, H., Miller, L.G., and Razonable, R.R. (2010) Serious infections caused by methicillin-resistant Staphylococcus aureus. *Clin.Infect.Dis.* **51 Suppl 2,** S183-97

133. Nimmo, G.R. (2012) USA300 abroad: global spread of a virulent strain of community-associated methicillin-resistant Staphylococcus aureus. *Clin.Microbiol.Infect.* **18,** 725-734

134. Thurlow, L.R., Joshi, G.S., and Richardson, A.R. (2012) Virulence strategies of the dominant USA300 lineage of community-associated methicillin-resistant Staphylococcus aureus (CA-MRSA). *FEMS Immunol.Med.Microbiol.* **65,** 5-22

135. Serruto, D., Rappuoli, R., Scarselli, M., Gros, P., and van Strijp, J.A. (2010) Molecular mechanisms of complement evasion: learning from staphylococci and meningococci. *Nat.Rev.Microbiol.* **8,** 393-399

136. Delaglio, F., Grzesiek, S., Vuister, G.W., Zhu, G., Pfeifer, J., and Bax, A. (1995) NMRPipe: a multidimensional spectral processing system based on UNIX pipes. *J.Biomol.NMR.* **6,** 277-293

137. Serrano, P., Pedrini, B., Mohanty, B., Geralt, M., Herrmann, T., and Wuthrich, K. (2012) The J-UNIO protocol for automated protein structure determination by NMR in solution. *J.Biomol.NMR.* **53,** 341-354

138. Shen, Y., Delaglio, F., Cornilescu, G., and Bax, A. (2009) TALOS+: a hybrid method for predicting protein backbone torsion angles from NMR chemical shifts. *J.Biomol.NMR.* **44,** 213-223

139. Shen, Y., Lange, O., Delaglio, F., Rossi, P., Aramini, J.M., Liu, G., Eletsky, A., Wu, Y., Singarapu, K.K., Lemak, A., Ignatchenko, A., Arrowsmith, C.H., Szyperski, T., Montelione, G.T., Baker, D., and Bax, A. (2008) Consistent blind protein structure generation from NMR chemical shift data. *Proc.Natl.Acad.Sci.U.S.A.* **105,** 4685-4690

140. Shen, Y., Vernon, R., Baker, D., and Bax, A. (2009) De novo protein structure generation from incomplete chemical shift assignments. *J.Biomol.NMR.* **43,** 63-78

141. Baba, T., Bae, T., Schneewind, O., Takeuchi, F., and Hiramatsu, K. (2008) Genome sequence of Staphylococcus aureus strain Newman and comparative analysis of staphylococcal genomes: polymorphism and evolution of two major pathogenicity islands. *J.Bacteriol.* **190,** 300-310

142. Baba, T., Takeuchi, F., Kuroda, M., Yuzawa, H., Aoki, K., Oguchi, A., Nagai, Y., Iwama, N., Asano, K., Naimi, T., Kuroda, H., Cui, L., Yamamoto, K., and Hiramatsu, K. (2002) Genome and virulence determinants of high virulence community-acquired MRSA. *Lancet.* **359,** 1819-1827

143. Kuroda, M., Ohta, T., Uchiyama, I., Baba, T., Yuzawa, H., Kobayashi, I., Cui, L., Oguchi, A., Aoki, K., Nagai, Y., Lian, J., Ito, T., Kanamori, M., Matsumaru, H., Maruyama, A., Murakami, H., Hosoyama, A., Mizutani-Ui, Y., Takahashi, N.K., Sawano, T., Inoue, R., Kaito, C., Sekimizu, K., Hirakawa, H., Kuhara, S., Goto, S., Yabuzaki, J., Kanehisa, M., Yamashita, A., Oshima, K., Furuya, K., Yoshino, C., Shiba, T., Hattori, M., Ogasawara, N., Hayashi, H., and Hiramatsu, K. (2001) Whole genome sequencing of meticillin-resistant Staphylococcus aureus. *Lancet.* **357,** 1225-1240

144. DUTHIE, E.S., and LORENZ, L.L. (1952) Staphylococcal coagulase; mode of action and antigenicity. *J.Gen.Microbiol.* **6,** 95-107

145. Harraghy, N., Hussain, M., Haggar, A., Chavakis, T., Sinha, B., Herrmann, M., and Flock, J.I. (2003) The adhesive and immunomodulating properties of the multifunctional Staphylococcus aureus protein Eap. *Microbiology.* **149,** 2701-2707

146. Haggar, A., Hussain, M., Lonnies, H., Herrmann, M., Norrby-Teglund, A., and Flock, J.I. (2003) Extracellular adherence protein from Staphylococcus aureus enhances internalization into eukaryotic cells. *Infect.Immun.* **71,** 2310-2317